UNIVERSITY OF CALIFORNIA
Los Angeles

Quantitative Approaches for Studying the Effects of Stressors in the Growth of Living Organisms

A dissertation submitted in partial satisfaction
of the requirements for the degree
Doctor of Philosophy in Biomathematics

by

Mauricio Cruz Loya

2022

ABSTRACT OF THE DISSERTATION

Quantitative Approaches for Studying the Effects of
Stressors in the Growth of Living Organisms

by

Mauricio Cruz Loya
Doctor of Philosophy in Biomathematics
University of California, Los Angeles, 2022
Professor Van M. Savage, Chair

Living organisms encounter multiple stressors that reduce their growth. These include physical stressors, like changes in temperature and pressure, and chemical stressors such as poisons or antibiotics. This dissertation presents various mathematical and computational approaches to the study of the effects of stressors in living organisms, with a focus on antibiotic and temperature interactions. The first chapter of this dissertation consists of introductory material presenting the background needed to understand the contents of the later chapters. Chapters 2 through 4 consist of projects done in collaboration with the Pamela Yeh lab at UCLA, where we focus on combining quantitative approaches with experimental data to explore the interactions between the effects of antibiotics and temperature in the growth of bacteria. In the second chapter, we find groups of antibiotics that damage bacteria in a similar way to either high or low temperatures through network clustering methods. In the third chapter, we develop a flexible mathematical model with biologically interpretable parameters for describing temperature response curves. In the fourth chapter, we then apply this model to study the temperature dependence of *E. coli* growth under the presence of

antibiotics, applying a Bayesian approach to infer the model parameters. We find that heat-similar and cold-similar antibiotic groups tend to shift the optimal temperature for growth in opposite directions, suggesting a similar damage hypothesis, where growth is reduced more sharply at temperatures where the antibiotic and temperature-induced damage to the bacteria overlap. Finally, in the fifth chapter we present work on a mathematical model for the evolution of stress responses, and show results regarding the favorability of evolving stress responses to stressors that primarily affect either the growth rate or death rate of a living organism. The mathematical techniques relevant to this dissertation span network theory, Bayesian statistics, and mathematical modeling. The biological impact of this work lies in an increased understanding of how overlap in the physiological damage caused by different stressors influences their joint effects in the growth of living organisms and the emergence of cross-sensitivity and cross-resistance, as well as a theoretical framework to explore the tradeoffs in the evolution of stress responses.

The dissertation of Mauricio Cruz Loya is approved.

Marcus L. Roper

Marc A. Suchard

Pamela J. Yeh

Van M. Savage, Committee Chair

University of California, Los Angeles

2022

To my mother . . .

for an example of getting an education

against seemingly insurmountable odds.

To my father . . .

for sparking my curiosity about the world.

TABLE OF CONTENTS

LIST OF FIGURES

LIST OF TABLES

ACKNOWLEDGMENTS

The research presented here was funded by UC-MEXUS and CONACYT (the Mexican Council for Science and Technology), and financial support from the UCLA Biomathematics program and Graduate Division.

First, I would like to thank my advisor Van Savage. His support, advice and mentorship during graduate school has been invaluable to my development as a scientist. I've made it this far in no small part due to his support, and I very much appreciate his willingness to give me the freedom to explore research directions and approaches that I find interesting. Very special thanks also go to Pamela Yeh, who has essentially been a second advisor throughout my time as a graduate student at UCLA. Being able to collaborate closely with her lab group, in a way that went much further than only sharing data, has been an invaluable experience that would have been difficult to obtain anywhere else. Additionally, I want to thank my doctoral committee members Marc Suchard and Marcus Roper for their thoughtful comments and discussion, as well as their excellent classroom instruction.

I am also grateful to Tina Manzhu Kang and Natalie Lozano-Huntelman, my main experimental collaborators for the projects that comprise the first and third chapters of this dissertation. This work would have been impossible without them and I greatly appreciated being able to discuss experimental details with them. My labmates Alex Brummer, Paheli Desai-Chowdry, Jason Lin and Elif Tekin provided some great conversations about science and were always willing to lend a helping hand, for which I am incredibly grateful as well.

Next, I want to thank my fellow biomath students, past and present. I enjoyed playing board games with Lindsay Riley, Timothy Stutz, and Christian Mason (although I seldom won). I also have good memories of going for swipes with Benjamin Chu and Alfonso Landeros, making cider with Gabe Hassler and great conversations with Bhaven Mistry, Paheli Desai-Chowdry, Alfonso Landeros and Rachel Mester.

I also want to thank Emily Fitch and David Tomita for their support with all the logistics

that are needed to navigate graduate school. Emily in particular has saved me from various mishaps, both self-inflicted and otherwise, an uncountable number of times.

Lastly, I want to thank my family and especially my mother Josefina. I sincerely hope that I can make her proud, and I hope that my graduation may bring her some joy that might make up to some extent for being away from home for so long.

VITA

2015 B.S. (Basic Biomedical Research), National Autonomous University of Mexico.

2016 M.S. (Biomathematics), University of California, Los Angeles.

2021 Teaching Assistant, Computational and Systems Biology Interdepartmental Program, UCLA. Taught sections of CaSB 150M (Mathematical and Computational Modeling of Biological Systems) under direction of Van Savage.

2021 Teaching Assistant, Life Sciences Department, UCLA. Taught sections of LS 30A (Mathematics for Life Scientists) under direction of Jukka Keranen.

2022 Tutor, Undergraduate Research Center, UCLA. Taught problem-solving workshops as support for students from underrepresented backgrounds in the LS 30A and 30B (Mathematics for Life Scientists) series under direction of Brent Corbin.

PUBLICATIONS

Tekin, E., White, C., Kang, T.M., Singh, N., Cruz-Loya M., Damoiseaux R., Savage, V.M., Yeh, P.J. *Prevalence and patterns of higher-order drug interactions in Escherichia coli.* npj Syst Biol Appl 4, 31 (2018).

Cruz-Loya, M., Kang, T.M., Lozano, N.A., Watanabe R., Tekin E., Damoiseaux R., Savage, V.M., Yeh, P.J. *Stressor interaction networks suggest antibiotic resistance co-opted from*

stress responses to temperature. ISME J 13, 12–23 (2019).

Rodríguez-Verdugo, A., Lozano-Huntelman, N.A., Cruz-Loya, M., Savage, V.M., Yeh, P.J. *Compounding Effects of Climate Warming and Antibiotic Resistance.* iScience 23, 4 (2020).

Tekin, E., Diamant, E.S., Cruz-Loya, M., Enriquez, V., Singh, N., Savage, V.M., Yeh, P.J. *Using a newly introduced framework to measure ecological stressor interactions.* Ecology Letters 23, 9 (2020).

Lozano-Huntelman, N.A., Zhou, A., Tekin, E., Cruz-Loya, M., Østman, B., Boyd, S., Savage, V.M., Yeh, P.J. *Hidden suppressive interactions are common in higher-order drug combinations.* iScience 24, 4 (2021).

Cruz-Loya, M., Tekin, E., Kang, T.M., Cardona, N., Lozano-Huntelman, N.A., Rodríguez-Verdugo, A., Savage, V.M., Yeh, P.J. *Antibiotics Shift the Temperature Response Curve of Escherichia coli Growth.* mSystems 6, 4 (2021).

CHAPTER 1

Introduction

Living organisms encounter stressors in their environment that have detrimental effects on their fitness. In order to improve their survival and reproductive success under these conditions, organisms have developed *stress responses*, changes in their physiology and gene expression profile that reduce the negative impacts of a stressor to themselves [Boo06, CZJ20, CHK20, GYK18, Wen97].

Environmental stressors can be biocidal, primarily killing living organisms, or biostatic, primarily slowing down their rate of growth or reproduction [ASC19, BSP13, PS04]. However, in either case, stressors ultimately harm living organisms by damaging some aspect of their physiology. Because of this, stressors that are apparently very different may have some degree of overlap in terms of the physiological processes harmed. This may be the reason that some stress responses have protective effects against multiple kinds of stress [PKM16, BMG11, Poo12a] and that evolution of resistance to a stressor can sometimes result in cross-resistance to a different stressor [DMQ13, Św16, VMS92].

Stressors to bacteria come in many different forms, including antibiotics [CUB14, KDH07], changes in temperature [Gil95], variations in salt concentration or pH [CH91], or a lack of nutrients [SC10]. The cellular stress responses that are used by bacteria to deal with these stressors range from specific subcellular mechanisms such as efflux pumps that pump out toxic compounds [Lev92, PPC97] and outer membrane porins that regulate osmolarity [BW06] to more global modulation that includes dormancy or quiescence under nutrient limitation [KK93].

The contents of this dissertation focuses on understanding how different stressors interact in affecting the population growth of living organisms, and how evolution of resistance to one stressor affects resistance or sensitivity to other stressors. To study these questions, we combine various quantitative approaches with experimental data. In particular, we study how the mechanisms of damage of antibiotics and temperature overlap in the bacterium *Escherichia coli*, and how these overlaps can inform our understanding of the evolution of antibiotic resistance. The projects presented here were done in close collaboration with the Pamela Yeh lab at UCLA.

In the next section of this introduction, we present some background on the main stressors that are the subject of study in this dissertation: antibiotics and temperature. We also introduce some of the approaches that have been previously used to study these stressors, which we build upon on this work. We then conclude this introduction by outlining the contents of this dissertation and presenting it in context of this background material.

1.1 Antibiotics

An antibiotic is a chemical substance that can either kill or slow the growth of bacteria. Many antibiotics are naturally produced by microbes. Because of this, most antibiotics are believed to have arisen as part of an arms race between competing microorganisms. However, it is not necessarily true that all antibiotics are chemical weapons in their natural environments. It has been proposed that the primary role of some antibiotics in nature is to function as chemical signals for communicating with other species, or that they may simply be byproducts of metabolism that happen to be toxic to other microbes. [HTW19, Mlo09, Mar08, DTP08].

There are multiple classes of antibiotics, which damage the physiology of bacterial cells through different *mechanisms of action*. For example, beta-lactam antibiotics prevent the synthesis of the bacterial cell wall [CUB14]. This compromises the integrity of the bacterial

Antibiotic class	Main mechanism of action	Ref
Aminoglycosides	Misfolded proteins due to introduced translational errors.	[MGT99, GGB13]
Beta-lactams	Inhibition of cell-wall synthesis.	[CUB14]
Fluoroquinolones	Changes in DNA supercoiling.	[HTW19]
Macrolides	Inhibition of protein synthesis (50S ribosomal subunit).	[HTW19]
Tetracyclines	Inhibition of protein synthesis (30S ribosomal subunit).	[CR01]
Nitrofurans	DNA damage and impaired DNA synthesis.	[HTW19]

Table 1.1: Mechanisms of action of some common classes of antibiotics.

cell, making it more vulnerable to changes in osmotic pressure. In contrast, other antibiotics, like tetracyclines and macrolides inhibit protein synthesis by binding the ribosome, slowing down bacterial growth and metabolism [HTW19, CR01]. The mechanisms of action of common classes of antibiotics are summarized in Table 1.1.

The first resistance mechanisms to the damaging effects of antibiotics likely arose nearly as early as the emergence of antibiotics themselves [DKK11, Mar08]. However, the discovery of antibiotics by humans and their subsequent widespread use in healthcare and agriculture has led to a dramatic increase in the frequency of antibiotic resistant bacteria in the last century [Ven15], threatening the continued effectiveness of antibiotic therapy.

Antibiotics and other antimicrobial compounds have been shown to activate various stress responses in bacteria. In particular, stress responses to nutrient limitation, reactive oxygen and nitrogen species, membrane damage, elevated temperature and ribosome disruption have been linked to protective effects to antimicrobial compounds [Poo12a]. This suggests that existing stress responses that originally evolved to deal with other stressors may have been co-opted to deal with antibiotic stress, especially when the antibiotic damages bacterial physiology in a similar way as the stressor.

1.1.1 Antibiotic interactions

Due to their use as therapeutic agents to treat bacterial infections and the widespread emergence of antibiotic resistance [Ven15], clinicians are interested in finding antibiotics that are especially effective when used in combination. Antibiotics are considered *synergistic* if they work especially well in combination, reducing the growth of bacteria more than expected given the individual effects of the drugs. In contrast, antibiotics are considered *antagonistic* when growth is reduced less than expected given the individual effects of the antibiotics.

To determine whether a pair of antibiotics is interacting in a synergistic or antagonistic manner it is first necessary to determine what the expected effect in a baseline case of non-interacting antibiotics. Various frameworks have been developed to deal with this problem [GBP95]. The most used ones in practice are Loewe additivity [LM26] and Bliss independence [Bli39]. Both the Loewe additivity and the Bliss independence frameworks are based on comparing the observed growth when two antibiotics are present to a null model that corresponds to the expected growth that assume the antibiotics are non-interacting. However, these frameworks differ on what this null model is, or in other words, on how to define non-interacting antibiotics.

Loewe additivity

The framework by Loewe is based on the assumption that an antibiotic cannot be synergistic or antagonistic with itself [LM26]. Thus, in this framework, two antibiotics are considered non-interacting when a dose of one antibiotic can always be substituted by a dose of a second antibiotic. Under these assumptions, it can be derived that two non-interacting antibiotics x and y should follow the so-called *isobole* equation

$$1 = \frac{c_x}{c_x^*} + \frac{c_y}{c_y^*}$$

where c_x and c_y are the concentrations of x and y respectively, and c_x^* and c_y^* are the concentrations of x and y (when the antibiotics are used individually) that are needed to

obtain the same effect in growth as a combination of both antibiotics present simultaneously with concentrations c_x, c_y [BYH16, LDH18].

Bliss independence

A different, non-compatible, framework for defining antibiotic interactions, which is the one we use in this work, is the Bliss independence framework [Bli39]. This framework considers two antibiotics as non-interacting if they have independent effects on growth.

The Bliss independence framework is based on comparing growth proportions when antibiotics are present simultaneously with the growth proportion when they are present individually. The relative growth under a fixed dose of an antibiotic x is defined as $w_x = \frac{g_x}{g_\phi}$, where g_x is the growth of a bacterial culture under a fixed dose of antibiotic x and g_ϕ is the growth of the culture in the absence of antibiotics.

Under the Bliss independence criterion [Bli39], fixed doses of two non-interacting antibiotics x and y are assumed to follow the equation

$$w_{xy} = w_x w_y \tag{1.1}$$

where w_x and w_y are the proportion of growth when antibiotics x and y are present individually and $w_{xy} = \frac{g_{xy}}{g_\phi}$ the proportion of growth when both antibiotics are present simultaneously (relative to when antibiotics are absent).

Interactions between antibiotics under the Bliss independence framework are defined with the equation

$$\varepsilon_{xy} = w_{xy} - w_x w_y \tag{1.2}$$

which quantifies the deviation from the Bliss independence null model of Equation 1.1. For historical reasons, non-interacting antibiotics are often called additive in the literature. Because of this, it is common to refer to this measure as the *deviation from additivity* despite the effects being multiplicative.

The sign of Equation 1.2 determines whether antibiotics x and y are synergistic or antagonistic. When $\varepsilon_{xy} < 0$, the observed growth proportion w_{wy} is less than the expected growth under Bliss independence $w_x w_y$. Thus $\varepsilon_{xy} < 0$ corresponds to a synergistic interaction. A similar argument shows that $\varepsilon_{xy} > 0$ corresponds to an antagonistic interaction between the antibiotics.

The deviation from Bliss independence is very similar to the concept of epistasis in population genetics [Phi08], where the effects of gene mutations are assumed to have multiplicative effects in the absence of an interaction. In fact, the equation for an epistatic effect is identical to Equation 1.2, if we interpret w_x, w_y and w_{xy} as the fitness effects of gene mutations x and y individually and in combination instead of the effects of antibiotics.

Antibiotic interaction networks

Interactions based on Bliss independence have been used to define antibiotic interaction networks, where nodes represent antibiotics and the edges represent whether the antibiotics are synergistic or antagonistic. To measure these networks, all the pairwise interactions ε_{xy} of a set of antibiotics must be determined by measuring the growth of bacterial cultures under unstressed conditions, under fixed doses of all single antibiotics and under all possible pairs of antibiotics present simultaneously.

Antibiotic interaction networks have an interesting property: antibiotics with the same mechanism of action tend have similar interactions with other antibiotics in the network. This property can be used to infer groups of antibiotics with the same mechanism of action by finding groups of antibiotics that interact similarly with other antibiotics through network clustering methods [YTK06].

In this way, it is possible to infer the likely mechanism of action of an antibiotic of unknown function based only on growth measurements under single drugs and pairs of drugs. To do this, an antibiotic interaction network can be constructed containing both the an-

tibiotic of unknown function and antibiotics of known mechanism of action. Clustering this interaction network will yield groups of antibiotics with shared mechanisms of action. The likely mechanism of action of the antibiotic of unknown function can then be inferred through the mechanism of action of the other members of its cluster, provided that other antibiotics with the same mechanism of action exist in the network.

Rescaling of Bliss independence interaction effects

In order to find groups of antibiotics that interact in a similar way in an antibiotic interaction network, we need to quantify the similarity (or dissimilarity) of interactions between two antibiotics. However, in practice, the raw interaction values ε_{xy} can be difficult to compare directly across different antibiotic combinations since they can have widely different magnitudes. For example, consider the following two cases:

1. $w_x = w_y = 0.7$, $w_{xy} = 0.45$
2. $w_x = w_y = 0.1$, $w_{xy} = 0$

For the first case $\varepsilon_{xy} = -0.04$ and for the second $\varepsilon_{xy} = -0.01$. However, arguably, the first case is much closer to additivity than the second, despite the smaller magnitude of the interaction. In fact, the second case cannot be any more synergistic, since it is impossible to have less than zero growth.

To make the interactions comparable across different overall growths, they are rescaled as follows before clustering:

$$\tilde{\varepsilon}_{xy} = \tilde{\varepsilon}(w_x, w_y, w_{xy}) = \begin{cases} \frac{w_{xy} - w_x w_y}{|0 - w_x w_y|} & w_{xy} \leq w_x w_y \text{ (synergy)} \\ \frac{w_{xy} - w_x w_y}{|\min(w_x, w_y) - w_x w_y|} & w_x w_y < w_{xy} \leq \min(w_x, w_y) \text{ (ant. buffering)} \\ 1 + \frac{w_{xy} - \min(w_x, w_y)}{|1 - \min(w_x, w_y)|} & w_{xy} > \min(w_x, w_y) \text{ (ant. suppression)} \end{cases} \tag{1.3}$$

The main idea behind this rescaling, introduced in [YTK06], is to make the interaction values comparable in magnitude by scaling them relative to some special cases of interest.

For synergistic interactions, the interactions are scaled relative to the lethal case ($w_{xy} = 0$), which is the strongest possible synergy, so that after rescaling synergistic interactions are in the interval $[-1, 0)$. Antagonistic interactions can be subdivided in two cases. In *antagonistic buffering* the observed growth under a combination is less than expected, but the antibiotics in combination are still more effective than the best single antibiotic. In this case, the interactions are scaled relative to $\min(w_x, w_y)$, the growth observed with the best single antibiotic, so that the rescaled interactions are in the interval $(0, 1]$. *Antagonistic suppression* is a stronger version of antagonism in which the combination is less effective than the best single antibiotic. In this case the interaction values are rescaled so that they are (almost always) in the interval $(1, 2]$. This is done by making a rescaled interaction of 2 correspond to the case where the growth is the same as the unstressed growth ($w_{xy} = 1$). The interactions can (very rarely) take values greater than 2, in cases when the antibiotic combination results in more bacterial growth than in the absence of antibiotic.

After rescaling, these interactions are now comparable across different antibiotics. These rescaled interactions can be used to quantify the similarity of the interactions of antibiotics x and y with the rest of the antibiotics in the network in order to find groups of antibiotics with similar interactions and thus similar mechanisms of action. Details on how to cluster antibiotic interaction networks using these rescaled interactions are covered in the Methods section in Chapter 2 of this dissertation.

.

1.2 Temperature stress

Living organisms have been exposed to changes in temperature since life first evolved [BL02, BL04]. As such, adaptations to better survive changes in temperature must have arisen

very early in the evolution of life. Phylogenetic evidence from ribosomal RNA sequences places the emergence of hyperthermophiles, organisms that specialize in living under high temperatures, near the root of the tree of life [SL04, Ste06]. Thus, mechanisms to better survive under temperature stress must constitute some of the oldest adaptations in nature. In contrast, antibiotics are thought to have first arisen more recently in evolutionary history, between 2 billion and 40 million years ago [DKK11].

In contrast to antibiotics, that usually have well-defined molecular targets and have effects in specific molecular pathways, temperature stress can have detrimental effects in a wide variety of cellular functions. The main mechanism responsible for the death of living organisms at high temperatures is believed to be protein unfolding and aggregation. However, high temperatures have also been linked to other effects in the cell, such as changes in membrane fluidity and DNA damage [RHB10, De 99, NLG06].

The heat-shock response is the main stress response that helps living organisms deal with the damaging effects of high temperature at a cellular level. The heat-shock response is present and highly conserved across all domains of life [S10, De 99, Lin86, RHB10]. This suggests resistance mechanisms to high temperature stress arose very early in the evolution of life, and that temperature is a pervasive stressor to living organisms that constantly mantains a strong selective pressure in the evolution of living organisms.

Low temperature stress has also been linked to many damaging effects in the cells of living organisms. These include a decrease in protein translation, decreased protein stability, changes in metabolism, decreased membrane fluidity and changes in DNA supercoiling [JI94, Yam99, GD84, MKO97]. The cold-shock response is the main stress response that helps living organisms deal with the damaging effects of low temperatures [Yam99, PAI99, JI94, BN14, PI04]. Interestingly, the cold shock response is less conserved than the heat-shock response.

There is some overlap in the physiological damage caused to bacteria when exposed to some classes of antibiotics and temperature stress. For example, one of the main effects of high temperatures in the cell is causing proteins to unfold and aggregate. Aminoglycosides

are antibiotics that introduce errors in protein translation, thereby producing misfolded proteins that aggregate, which is a similar kind of damage [MGT99]. The existence of these overlaps raises the question of whether resistance mechanisms against temperature stress could also help deal with some kinds of antibiotic stress.

There is some evidence that this may be the case, at least for aminoglycosides. In particular, molecular chaperones, which are proteins that aid the correct folding of proteins and participate in the heat-shock stress response, have previously been shown to be activated in response to aminoglycosides [CGW10] and to increase bacterial survival when activated [GGB13]. Some classes of antibiotics that bind the ribosome have been observed to induce a similar protein expression profile to either heat stress (in the case of aminoglycosides) or cold stress (in the case of other protein synthesis inhibitors) [VN90] in bacteria.

1.2.1 Temperature response curves

Temperature fluctuations in the environment affect the ability of living organisms to survive, and cause changes in the rates of physiological processes. At various temporal scales, these temperature fluctuations can be driven by day-night cycles, changes in weather conditions and seasonal effects. These changes affect the evolution of biological and ecological traits [CR54, HK89, LG87, FSS16, Som10, OMS08, Ben80, SGB04, Ali70, ACU17]. Since organisms vary in their ability to function and survive at different temperatures, temperature fluctuations can be an important factor in the evolution of species and communities [HK89, PYB16, Par06, BRI02, BH16, Ang09, ABG06].

Understanding how the growth and other physiological processes of living organisms thus has important implications for evolutionary biology and projecting the effects of climate change in biodiversity. Because of this, ecologists are interested in measuring how the growth of living organisms depends on temperature, and how this dependence changes across individuals and species [DPS11, FGS97, MCE17, SGB04].

In order to perform these studies, measurements of the growth of living organisms (or some other measurable quantity used as a proxy) are taken at different temperatures. A mathematical model of the temperature response is then fit to the data to extract useful quantities such as the optimal growth temperature and temperature niche (defined as the range of temperatures where growth exceeds some threshold) for the organism in question. Various mathematical models, both descriptive and mechanistic have been developed for fitting the temperature dependence of the growth of living organisms [BPL99, LHJ95, SD77, ROR05, SG10, SGS11, YKM95].

Based on the shapes of most empirically determined TRCs, these models typically assume a temperature response curve have a single maximum value for growth corresponding to an optimal growth temperature, as shown in Figure 1.1. As the temperature changes away from the optimum in either direction, growth decreases, with an especially steep decline at higher temperatures.

While most models for TRCs assume this right skewed shape with a single optimal temperature that maximizes growth, they differ on other ways. For instance, some models assume the existence of a maximum and minimum temperature for growth. Outside of this range of temperatures, growth is assumed to be exactly zero. In contrast, other models assume growth remains positive, only going to zero in the limits when temperature goes to $\pm\infty$.

1.3 Dissertation outline

We finish this introductory chapter with an outline of the contents of the work presented in this dissertation. In doing so, we also put this work in context of the material presented in this introduction.

In Chapter 2, we introduce stressor interaction networks (SINs) as a novel generalization of antibiotic interaction networks. In a stressor interaction network, nodes can be any stressor

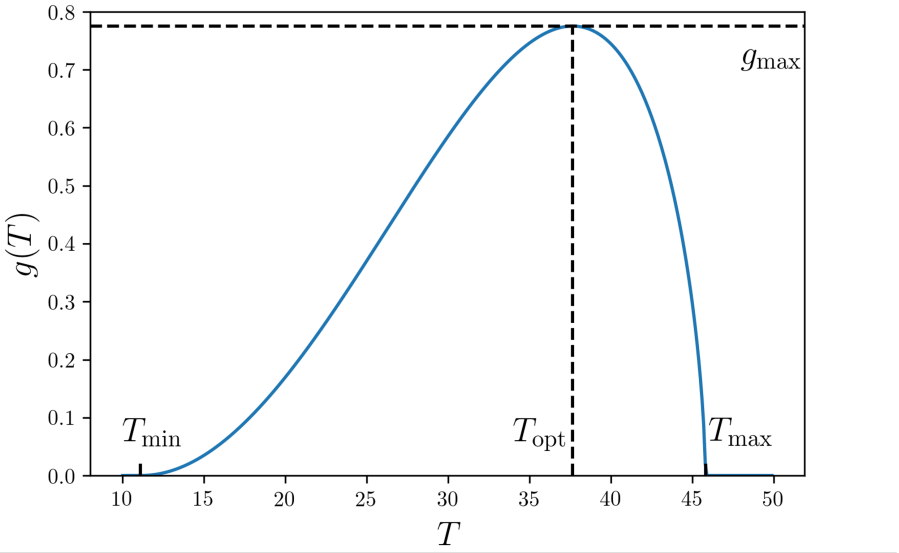

Figure 1.1: *Schematic of a typical temperature response curve.* A temperature response curve (TRC) describes how a trait g of a living organism (typically growth or some physiological process) varies with temperature T. Models for TRCs are used to infer quantities of interest from experimental data, such as the optimal temperature T_{opt} for the trait g, the maximum value of the trait $g_{\max}$, and a temperature breadth, representing a range of temperatures in which the trait g exceeds a certain value. Here, we represent the temperature breadth as the values for which $g > 0$, corresponding to the range between the minimum and maximum temperatures for the trait ($T_{\min}$, $T_{\max}$). However, another common choice in applications is to consider the temperatures under which g is over half of its maximum value, especially in models where the trait is only assumed to go to zero at $\pm\infty$.

that reduces the growth of a living organism, and mixed kinds of stressors can for a part of the same network. As before, interactions between stressors are based on the Bliss independence framework. We then apply this extended framework to find groups of antibiotics and non-optimal growth temperatures (corresponding to either heat stress or cold stress) that interact with other stressors in a similar way. In doing so, we identify specific classes of antibiotics with similar physiological effects to either high or low temperature stress.

We also find that the antibiotic resistance profile of bacterial strains evolved under high temperature stress is modified despite the bacteria not having been exposed to the antibiotics. These high-temperature adapted bacterial strains become more sensitive to specific classes of antibiotics that have similar physiological effects to cold temperature, and more resistant to antibiotics similar to high temperature. This indicates a tradeoff between stress responses to cold and hot temperature stress, and that the acquisition of cross-sensitivity or cross-resistance to other stressors is influenced by the similarity of the physiological effects of stressors. Taken together, our results suggest that living organisms have likely co-opted previously existing stress responses to ancient stressors (like temperature) to deal with different kinds of stress that damage similar cellular components (like some antibiotic classes).

In Chapter 3, we develop a model for describing the temperature response curves (TRCs) of living organisms. This model is based on the Briere model–one of the most popular models for TRCs in applications–but our model differs in crucial ways. First, unlike the original Briere model, the modified Briere model proposed here can be used to describe the TRCs of living organisms that can grow below freezing temperatures. Second, the model presented here is able to describe TRCs with many different shapes, including symmetric and left-skewed TRCs. These cases are typically assumed not to happen often in practice, but we found them to occur frequently in our data for TRCs in the presence of antibiotics. Lastly, the model is parametrized in terms of quantities of interest to ecologists and other biologists.

In Chapter 4, we use the model developed in the third chapter to explore how bacterial temperature response curves (TRCs), which describe the growth of bacteria as a function of temperature, are modified by antibiotics and antibiotic combinations. The flexibility of our model allows us to fit data of TRCs under multiple antibiotic backgrounds, which we found to have a much wider variety of shapes than a typical right-skewed TRC, as shown in Figure 1.1. We infer the parameters of this model through a nonlinear regression using a Bayesian approach. The main results here are that the optimal temperature of growth often changes in the presence of antibiotics, while the temperature range of half-maximum growth

decreases. Interestingly, the direction of the observed optimal temperature shifts depends on whether the antibiotic is similar to low or high temperature, as determined in the work described in Chapter 2.

Finally, in Chapter 5, we develop a mathematical model to explore the tradeoffs in the evolution of stress responses based on evolutionary game theory and present some preliminary results. Based on this model, stress responses to biocidal stressors (i.e stressors that kill living organisms) are predicted to be more likely to arise than stress responses to biostatic stressors (i.e. stressors that slow down population growth without killing the organism).

CHAPTER 2

Stressor interaction networks suggest antibiotic resistance co-opted from stress responses to temperature

Note: The contents of this chapter is based on an article published in The ISME Journal [CKL19].

Environmental factors like temperature, pressure, and pH partly shaped the evolution of life. As life progressed, new stressors (e.g., poisons and antibiotics) arose as part of an arms race among organisms. In this chapter, we ask if cells co-opted existing mechanisms to respond to new stressors, or whether new responses evolved *de novo*. To explore this question, we use a network-clustering approach based purely on phenotypic growth measurements and interactions among the effects of stressors on population growth. This method is applied to two types of stressors—temperature and antibiotics-to discover the extent to which their cellular responses overlap in *Escherichia coli*. Our clustering reveals that responses to low and high temperatures are clearly separated, and each is grouped with responses to antibiotics that have similar effects to cold or heat, respectively. As further support, we use a library of transcriptional fluorescent reporters to confirm heat-shock and cold-shock genes are induced by antibiotics. We also show strains evolved at high temperatures are more sensitive to antibiotics that mimic the effects of cold. Taken together, our results suggest that temperature stress responses may have been co-opted to deal with antibiotic stress.

2.1 Introduction

Organisms encounter and respond to myriad stressors [HP93, MB02]. Stresses to bacteria can come in many different forms, such as use of antibiotics [CUB14, KDH07], changes in temperature [Gil95], variations in salt concentration or pH [CH91], or a lack of nutrients [SC10]. Cellular responses to these stressors vary but can range from specific subcellular mechanisms such as efflux pumps that pump out toxic compounds [Lev92, PPC97] and outer membrane porins that regulate osmolarity [BW06] to more global modulation that includes dormancy or quiescence under nutrient limitation [KK93].

Temperature and pressure gradients are stressors that living organisms have needed to contend with since life first evolved [BL02, BL04, DOW06, HBB02]. Indeed, phylogenetic evidence based on ribosomal RNA sequences places the emergence of hyperthermophiles near the root of the tree of life [SL04, Ste06], so sensing, responding, and adapting to pressure and temperature must constitute some of the oldest adaptations in nature. The heat-shock response machinery, which is a mechanism for cells to deal with the noxious effects of high temperatures, is present across all domains of life and is highly conserved [S10, De 99, Lin86, RHB10]. In contrast, the first antibiotics are thought to have arisen more recently in evolutionary history, between 2 billion and 40 million years ago [DKK11]. Consequently, it seems likely that adaptive responses to variations in environmental temperature evolved before responses to antibiotics.

It seems possible that some of the mechanisms that confer resistance to variations in temperature have been co-opted to deal with antibiotic stress as well, especially since temperature and drugs harm many of the same cellular components. For instance, high temperatures and antibiotics (e.g., macrolides and aminoglycosides) both affect protein synthesis and folding [MPR14, VRH10]. In addition to functional overlap, there are compelling reasons for cells to evolve a relatively small suite of stress responses to multiple types of stressors. Developing a novel stress response requires investment in terms of genetic material (i.e.,

information), protein production, time to evolve, and energy to support simultaneous responses. Thus, it is inefficient for a cell or organism to evolve an independent response for every single stressor it encounters. Greater efficiency can be achieved if cells can co-opt similar pathways to respond to different stressors [DMQ13, Św16, VMS92]. A prime example of this evolutionary strategy in bacteria is the alternative sigma factor σ^{S}, which regulates the expression of more than 70 genes that confer resistance against stresses as diverse as temperature change, starvation, pH, and DNA damage [BMG11, GG03, SAB16].

It is natural to ask which response mechanisms evolved first, whether these original responses were co-opted to respond to other stressors, and how much overlap exists among how stressors affect bacteria. It has previously been shown that heat-shock proteins are induced by some antibiotics [CGW10], and that resistance to antibiotics can be temperature-dependent [LHK16]. Furthermore, selection of heat-resistant *Escherichia coli* results in the evolution of resistance to rifampicin, despite the drug being absent during the selection process [RGT13]. Additionally, overexpression of heat-shock proteins increases short-term survival of bacteria exposed to aminoglycosides [GGB13]. Other stress responses, such as those for nutrient starvation and oxidative stress, have also been linked to the emergence of antibiotic resistance [Poo12b].

Despite these intriguing, isolated subcellular studies, we are unaware of any systematic, comprehensive study of these overlaps and co-opting. Typically, the overlap between cellular responses to stress has been studied by isolating subcellular parts and attempting to piece together the information involved to understand stress responses at a whole-cell level. Here, we take a reverse and complementary approach: by studying the effect of perturbations on the whole system, we gain more insights into the mechanisms of its specific parts. It is feasible to accomplish this with network-clustering methods that reveal mechanism of action of antibiotics [SDC05, YTK06]. For these clustering methods, interactions between drugs are inferred based on growth assays of bacteria exposed to antibiotic combinations. Interactions between drugs are typically characterized in one of three ways: additivity (drugs have

independent effects on growth), synergy (the drug combination is more potent for inhibiting growth than expected based on their single effects), or antagonism (the drug combination is less potent than expected based on their single effects) [Bli39]. Networks are then constructed in which edges represent these interactions and nodes represent drugs. Because drugs with similar functional effects in the cell tend to have very similar interactions with other drugs, clustering this network according to interaction profiles (a procedure called monochromatic clustering) has been shown to yield groups of drugs with the same mechanisms of action [YTK06]. The interaction profile of a drug can thus reveal its functional effect in the cell.

In this chapter, the ideas of monochromatic clustering are extended and generalized. We develop and use a clustering method for stressor interaction networks (SINs) to categorize non-drug stressors that affect bacterial growth, and reveal information about the shared effects of temperature and antibiotics on the cell. Comprehensive data on bacterial growth in the presence of each stressor separately, and when pairs of stressors are present simultaneously are used to determine interactions between stressors and construct a SIN. Groups of antibiotics that have similar physiological effects to low- and high-temperature stress are then found by grouping stressors that interact similarly with other stressors, as revealed through the SIN clustering analysis. In this way, the overlap between stress responses to temperature and antibiotics is comprehensively analyzed to assess the extent that cellular responses to drugs co-opt and mimic the responses to temperature, an ancient stressor.

By systematically carrying out experiments and performing network-clustering analysis, we determine the overlap between the physiological effects of multiple classes of antibiotics and those of six temperatures, ranging from near normal to extreme, in *E. coli*. Moreover, we confirm that temperature-response genes are involved in responding to antibiotics by measuring genome-wide transcriptional expression with a library of about 1800 strains that contain fusions of green fluorescent protein (GFP) with *E. coli* promoters. Finally, to assess the extent to which adaptation to temperature confers antibiotic resistance, we evaluate the cross-resistance to antibiotics of high-temperature-adapted strains obtained in a previous

study [RGT13]. Our results provide evidence that elements of the low- and high-temperature stress responses may have been co-opted through evolution to combat multiple classes of antibiotics.

2.2 Materials and methods

Bacterial strain

The study used BW25113, a derivative of the F-, λ-, *E. coli* K-12 strain BD792 (CGSC6159) [DW00]. A single colony was inoculated into 2 mL of LB media (10 g/L tryptone, 5 g/L yeast extract, and 10 g/L NaCl) and grown overnight followed by resuspension in 25% glycerol, then aliquoted into 50 μL and frozen at -80°C. Cultures used for daily experiments were started by adding 20 μL of thawed aliquots into 2 mL of LB media. The culture was incubated at 37°C until it reached exponential growth phase and diluted to maintain 10^4 cells per experimental condition.

Compounds and materials

A total of 12 antibiotics were included in the study as representatives of all major drug classes. Gentamycin (GEN), levofloxacin (LVX), tetracycline (TET), tobramycin (TOB), erythromycin (ERY), ampicillin (AMP), clindamycin (CLI), streptomycin (STR), nitrofurantoin (NTR), cefoxitin (FOX), and trimethoprim (TMP), all from Sigma (St. Louis, MO); and ciprofloxacin (CPR) from MP Biomedicals (Santa Ana, CA). Stock solution at 20 mg/mL of each antibiotic was stored in 50 μL aliquot at -20°C and each aliquot was only frozen and thawed once to preserve potency.

Growth experiment

Drug concentrations were selected to partially inhibit bacterial growth (10–50% inhibition) that were first determined by a 12-step concentration series of twofold at each step in 96-well plates (Costar). A 5 mL stock solution of each drug in LB media was made at 10-fold of their respective concentrations (Table 1). For drug pair experiments, 10 L of each component drug was mixed into 96-well plates followed by the addition of 80 μL cell inoculum; while 10 μL of LB media was added in replacement of a second drug for single-drug experiments. Replicate plates were prepared from the same antibiotic stock solution to minimize variation and incubated at 300 r.p.m. in parallel at various temperatures (22°C, 25°C, 30°C, 37°C, 41°C, 44°C, 46°C). OD600 measurements for cell density were taken after 4-h, 8-h, 12-h, and 24-h growth. To examine the drug interaction clustering of *E. coli* in a different external environment, we used LB media without salt, prepared with 10 g/L tryptone, 5 g/L yeast extract.

Relative growth and interactions

The relative growth under stressor x (presence of a drug or a non-optimal temperature) is defined as $w_x = \frac{g_x}{g_\phi}$, where g_x is the growth of the bacterial culture under stressor x and g_ϕ is the growth of the culture at reference state ϕ —the culture at its optimal temperature for growth in the absence of antibiotics (41°C in our study). Under the Bliss Independence criterion [Bli39], an interaction is additive if $w_{xy} = w_x w_y$, where w_{xy} is the relative growth when stressors x and y are both present. The deviation from additivity is defined as $\varepsilon_{xy} = w_{xy} - w_x w_y$. The sign of this quantity determines the interaction type ($\varepsilon_{xy} < 0$ corresponds to synergy and $\varepsilon_{xy} > 0$ to antagonism). The raw ε_{xy} is then rescaled by appropriate reference values to yield a rescaled measure which magnitude can be interpreted as the strength of interaction, as described in the Rescaling of Bliss independence interaction effects section in the Introduction.

Statistics of interaction effects

With the experimental procedure detailed above, four measurements of the OD600 were taken at every time point, each one corresponding to a different experimental replicate, for each stressor, and all possible pairwise combinations. The OD (optical density) values were used as a proxy that is proportional to the absolute growth (g_x, g_y, g_{xy}, g_ϕ). The point estimate $\hat{g}_x$ was chosen to be the sample mean of the four measurements of absolute growth under condition x. The point estimate for each relative growth was taken to be $\hat{w}_x = \frac{\hat{g}_x}{\hat{g}_0}$ and the point estimate for the interaction $\hat{\varepsilon}_{xy} = \tilde{\varepsilon}(\hat{g}_x, \hat{g}_y, \hat{g}_{xy})$ (where $\tilde{\varepsilon}$ refers to the rescaled interaction as a function of the relative growths). A parametric bootstrap approach was used for constructing a 95% confidence interval $(\tilde{\varepsilon}_{2.5}, \tilde{\varepsilon}_{97.5})$ for each interaction, with the assumption that the OD measurements under each condition follow a log-normal distribution.

Network of antibiotic and temperature effects and monochromatic clustering

We constructed an interaction network where nodes represent the stressors (i.e., drugs or temperatures), and colored edges represent non-additive interactions, with the edge color corresponding to interaction type (red for synergy and green for antagonism). The discretized interaction (i.e., color) of an edge is defined to be

$$c(\tilde{\varepsilon}_{2.5}, \tilde{\varepsilon}_{97.5}) = \begin{cases} 1 \text{ (green/antagonism)} & \tilde{\varepsilon}_{2.5} > \tilde{\varepsilon}_{\text{ref}} \\ -1 \text{ (red/synergy)} & \tilde{\varepsilon}_{97.5} < -\tilde{\varepsilon}_{\text{ref}} \\ 0 \text{ (no edge)} & \text{otherwise} \end{cases}$$

where $\tilde{\varepsilon}_{\text{ref}}$=0.2 represents the limit for an interaction to be considered approximately additive.

Monochromatic clustering

The stressors in the interaction network were clustered into monochromatic classes using a modified version of the Prism 2 algorithm [YTK06], which is a variant of hierarchical

clustering. Briefly,

1. Each node (representing a stressor) starts in a different cluster.

2. At every iteration of the algorithm, the pair of clusters (X, Y) that minimizes the penalty
$$F(X,Y) = k_D D(X,Y) + k_S \left(\Delta S(X,Y) + \alpha(1 - p_{XY})\right) \tag{2.1}$$
is merged (for an explanation of this penalty, please see below).

3. Repeat this procedure until a single cluster remains, containing all nodes in the network.

The term $k_D D(X,Y)$ in Equation 2.1 corresponds to the standard cost term in hierarchical clustering. It penalizes merging clusters that are dissimilar to each other in terms of their interactions with other clusters. The *dissimilarity* between nodes x, y is defined as

$$d(x,y) = \frac{1}{N(x,y)} \sum_{z \neq x,y} \left(\frac{\hat{\tilde{\varepsilon}}_{xz} - \hat{\tilde{\varepsilon}}_{yz}}{2} \right)^2 \tag{2.2}$$

where $N(x,y)$ is the number of interactions with other nodes $z \neq x, y$ (i.e., number of $(\tilde{\varepsilon}_{xz}, \tilde{\varepsilon}_{yz})$ pairs) that were measured for both conditions x and y. The mean value of the dissimilarity between all pairs of nodes belonging to clusters (X, Y)

$$D(X,Y) = \frac{1}{n_X \cdot n_Y} \sum_{x \in X, y \in Y} d(x,y)$$

where n_X, n_y are the number of nodes in clusters X and Y, respectively, is taken as a measure of the dissimilarity between clusters. This is another thing that was changed compared to the previous algorithm. The use of the mean distance between the antibiotics (average linkage) as the distance between clusters $D(X,\ Y)$ is less sensitive to outliers than the previous choice of the minimum distance (single-linkage). This term uses the point estimates of the interactions directly (before discretization).

The second term in the penalty $k_S \Delta S(X,Y)$ is based on the information-theoretic concept of entropy, and penalizes non-monochromatic interactions between clusters X and Y. The interaction entropy between two clusters is defined as

$$S(\vec{m}_{X,Y}) = -(m^+_{X,Y} + m^-_{X,Y})(p^+_{X,Y} \log_2 p^+_{X,Y} + p^-_{X,Y} \log_2 p^-_{X,Y})$$

where $m^+_{X,Y}$ and $m^-_{X,Y}$ are the number of red (synergy) and green (antagonism) edges between clusters X and Y, and $p^+_{X,Y} = \frac{m^+_{XY}}{m^+_{XY}+m^-_{XY}}$, $p^-_{X,Y} = \frac{m^-_{XY}}{m^+_{XY}+m^-_{XY}}$ are the corresponding proportions (we use the vector $\vec{m}_{X,Y} = (m^+_{XY}, m^-_{XY})$ as a shorthand for notational simplicity). Only the entropy of between-clusters interactions is penalized (but not the entropy of interactions where both nodes are part of the same cluster). When a pair of clusters X, Y is merged into cluster $M = X \cup Y$, the entropy of their interactions $S(\vec{m}_{X,Y})$ is thus "hidden" inside the new cluster and no longer penalized. The change in the interaction entropy across all the network upon merging is

$$\begin{aligned}
\Delta S(X,Y) &= S_{\text{gained}} - S_{\text{lost}} \\
&= \sum_{Z \neq X,Y} [S(\vec{m}_{M,Z}) - S(\vec{m}_{X,Z}) - S(\vec{m}_{Y,Z})] - S(\vec{m}_{X,Y}) \\
&= \sum_{Z \neq X,Y} [S(\vec{m}_{X,Z} + \vec{m}_{Y,Z}) - S(\vec{m}_{X,Z}) - S(\vec{m}_{Y,Z})] - S(\vec{m}_{X,Y})
\end{aligned}$$

where S_{gained} is the net change in entropy over all interactions X and Y had with all other clusters, and $S_{lost} = S(\vec{m}_{X,Y})$ is the entropy lost by the newly "hidden" interactions between X and Y. Note that in this formulation we chose to write ΔS with an opposite sign as in [YTK06], to be consistent with the usual convention that positive values mean increases and negative values decreases.

A third ingredient in the algorithm, which is not present in previous versions, is the term $\alpha(1 - p_{XY})$, where p_{XY} is the proportion of shared edges between clusters X, Y and α an arbitrary tuning constant. It is always possible to form monochromatic clusters by simply merging clusters with members which have no, or few, shared edges, but these clusters need

not have similar overall interactions (and thus lack any physiological relevance). This is particularly important in the earlier steps of the algorithm, where most clusters are small, so there is a larger proportion of clusters with missing or unknown edge colors. The purpose of this term is to avoid this problem by penalizing the entropy term so joining clusters with more shared interactions is favored with respect to clusters with few.

In the penalty $F(X, Y)$, each term is multiplied by constants that affect the relative weight of each term. The values of $k_D = 1$, $k_S = 0.1$ were chosen to be the same as in [YTK06]. The third tuning constant, $\alpha = 0.1$, is new to this work, and was chosen to be of roughly the same order of magnitude, but smaller, than the entropy $\Delta S_{XY} \in [0, 1]$, and to give clusters with better separation by mechanism of action in networks with a small number of edges than $\alpha = 0$, which is equivalent to removing the term.

Gene expression profile

The expression of about 1800 genes in *E. coli* was measured using a library with transcriptional fusions of GFP to each promoter [ZBR06]. Strains were maintained in 15% glycerol at 80°C before inoculating and grown overnight in LB medium with 25 μg/mL of kanamycin in 384 well plates. Cultures were then transferred and pinned into 50 of LB medium per well, followed by a 4-h incubation at 37°C to allow growth up to exponential phase. To measure differential expression at high temperature, cultures were moved to 44°C where OD at 595nm and GFP fluorescence (excitation, 480 nm; emission, 535 nm) were measured every 2 h for 20 h using a programmable robotic system (Thermo Cytomat). For expression profile with antibiotic treatment, cultures were pinned into 30 μL of LB medium before 4-h incubation, and another 30 μL of LB medium with the corresponding antibiotic was added into the plates (final concentration: STR at μg/mL and TET at 1 μg/mL). Controls were carried out at 37°C without temperature shift or addition of antibiotics. Antibiotics and control conditions were measured using the same robotic system and timeframe.

Determining over- and under-expressed promoters

The raw OD and GFP fluorescence measurements for each strain in the promoter library were background-corrected and normalized to yield a GFP/OD value that is proportional to the total GFP fluorescence per cell. The median-normalized GFP/OD values were used to calculate log2-fold changes in promoter expression for each experimental condition (44°C, STR, TET) with respect to the control condition (37°C). Four replicates were averaged to yield a final value of the log2-fold change x_{cpt} in gene expression (for each promoter p in experimental condition c at time t).

As a measure of overall similarity between the gene expression profiles of experimental conditions c_1 and c_2, we calculated the mean absolute distance

$$d_{c_1,c_2} = \frac{1}{PT} \sum_{p,t} |x_{c_1pt} - x_{c_1pt}|$$

of the respective log2-fold changes, where P and T are the total number of promoters in the library and measured time points, respectively.

For gene ontology (GO) term analysis, we determined over-expressed (OE) and under-expressed (UE) promoters as compared to control with the robust z-score method, as in ref. [RLH12]. The strains in the promoter library were mapped to GO terms. GO terms of the "biological process" category that are over-represented in the OE and UE sets for each condition were found by ranking the terms using the p-value from Fisher's exact test.

Drug sensitivity profile for heat-adapted strains

We profiled the antibiotic sensitivity of 10 high-temperature-adapted *E. coli* strains collected and described by Rodríguez-Verdugo et al. [RGT13]. In addition, we compared their sensitivity profiles with their ancestor strain (E. coli B genotype REL1206). Growth after 24-h was measured through OD for each strain exposed to each of 12 drugs under an 11-step concentration series with twofold increase per step. Three replicates of these measurements were

obtained using the same methodology as described in the Growth experiment section. IC50 values and their associated credible intervals were determined by fitting a five-parameter logistic model to the growth curve for each strain.

This model, which allows for asymmetric dose-response curves, is given by the equation

$$g(c) = g_{\min} + (g_{\max} - g_{\min}) \left[1 - \left(\frac{1}{1 + \left(\frac{c_b}{c}\right)^n} \right)^s \right] \tag{2.3}$$

where $g(c)$ is the growth as a function of the drug concentration c. The drug concentration at which 50% of growth is obtained is called the IC50, and is typically used as a summary of the susceptibility of a bacterial strain to an antibiotic. Some simple algebra manipulating Equation 2.3 shows that

$$\text{IC50} = \frac{c_b}{(2^{\frac{1}{s}} - 1)^{\frac{1}{n}}}$$

Inference of model parameters

The model was fit with a Bayesian procedure, by first extending it to a statistical model. It is important to make the distinction between the observed data values and the underlying parameters of the model. In statistics, model parameters are typically given Greek letter notation and observed values Roman letters, but this convention is somewhat inconvenient when dealing with deterministic models, which use Roman letters throughout. To avoid confusion, we will use the same Roman letters for parameters that come from the deterministic model, and only use Greek letters for extra parameters that are needed for the statistical model (e.g. variances).

Let $\mathcal{P} = \{g_{\min}, g_{\max}, c_b, n, s\}$ be the parameters of the logistic model and y_{ci} be the i-th replicate of the OD measurement at drug concentration c. We fit a model of the form

$$y_{ci} | \mathcal{P}, \sigma_y(c) \sim \text{Gamma}(\mu = g(c),\, \sigma = \sigma_y(c))$$
$$\sigma_y(c) | \mathcal{P}, \sigma_{\min}, \beta = \sigma_{\min} + \beta \left[g(c) - g_{\min} \right]$$

where $g(c)$ is given by Equation 2.3.

The model for the standard deviation was motivated by the observation that the growth measurements tend to have low variance when there is essentially no growth (at high concentrations), and that the variance increases as the OD increases. A linear form was chosen for simplicity.

We used the following priors:

$$\begin{aligned}
\text{IC50} &\sim \text{Uniform}(0,\ 500) \\
\Delta g &\sim \text{Uniform}(0,\ 1) \\
g_{\min} &\sim \text{Gamma}(\mu = 0.05, \sigma = 0.02) \\
\ln n &\sim \text{Normal}(0,\ 1.5) \\
\ln s &\sim \text{Normal}(0,\ 1.5) \\
\sigma_{\min} &\sim \text{Gamma}(\mu{=}0.02, \sigma = 0.02) \\
\beta &\sim \text{Gamma}(\mu = 0.1, \sigma = 0.3)
\end{aligned}$$

(where we reparametrized the model in terms of the logarithm of the constants n and s). To recover the original parameters $\mathcal{P}$, we have that

$$\begin{aligned}
g_{\max} &= g_{\min} + \Delta g \\
n &= \exp(\ln n) \\
s &= \exp(\ln s) \\
c_b &= \text{IC50}(2^{\frac{1}{s}} - 1)^{\frac{1}{n}}
\end{aligned}$$

The motivation for the non-uniform priors is as follows. In the five-parameter logistic model, n determines the steepness of the change in growth as a function of concentration, and s allows for asymmetric curves. When $s = 1$, the curve is symmetric and the model reduces to a Hill equation. When $s = 1$ and $n = 1$, the model reduces to a simple Michaelis-Menten-like form. We chose to use weakly informative priors for n and s as a form of regularization

to keep the values for n and s in a reasonable range (roughly $\frac{1}{20}$ to 20). We chose to give greater prior probability to models where n and s are close to one due to the connection to simpler models. The informative prior for $\sigma_{\min}$ represents that we expect bacterial growth to be essentially zero at very high antibiotic concentrations, and the variance to consist mostly of measurement error for OD, which is typically below 0.02 in OD units.

Model fitting

For each antibiotic and strain, the model above was fit to the data using NUTS (the no-u-turn sampler), a variant of Hamiltonian Monte Carlo, as implemented in the Python library PyMC3 [SWF16]. Three chains were run for 5000 iterations, after an initial 1500 samples were used for tuning. The output samples from the posterior distribution were used to construct a mean estimate and a 95% credible interval for the IC50 for each antibiotic and strain. For a few strain-antibiotic combinations, the NUTS chain did not converge (as evaluated by $\hat{R} > 1.2$) or had a low number of effective samples ($n_{\text{eff}} < 500$). These estimates were considered unreliable and were removed from the plots and analysis.

2.3 Results

To find groups of stressors (i.e., antibiotics and/or temperatures) that have similar effects on *E. coli* physiology, we first evaluate the interactions—synergy, additivity, or antagonism—between each pair of antibiotics, and between each antibiotic and a range of growth temperatures (22°C, 25°C, 30°C, 37°C, 44°C, 46°C) (Figure 2.1a, b). The maximum growth in the absence of antibiotic was observed at 41°C: this optimum growth temperature was chosen as the unstressed reference state for evaluating the relative growth in the presence of each stressor. We evaluate the interactions based on the 24-h growth of *E. coli* after exposure to the corresponding stressors. We then construct a SIN (Figure 2.1c) where nodes represent the stressors and colored edges represent interaction type (discretized based on a

Compound	Abbreviation	Class/cellular target	Dose
Ampicillin	AMP	Cell wall synthesis inhibitor	1.2
Cefoxitin	FOX	Cell wall synthesis inhibitor	1.2
Levofloxacin	LVX	Fluoroquinolone, DNA gyrase inhibitor	0.01
Ciprofloxacin	CPR	Fluoroquinolone, DNA gyrase inhibitor	0.005
Nitrofurantoin	NTR	DNA damaging, multiple mechanisms	2
Trimethoprim	TMP	Folic acid synthesis inhibitor	0.1
Tobramycin	TOB	Aminoglycoside	1.5
Gentamycin	GEN	Aminoglycoside	1
Streptomycin	STR	Aminoglycoside	2
Clindamycin	CLI	Protein synthesis inhibitor, 50S	40
Erythromycin	ERY	Protein synthesis inhibitor, 50S	50
Tetracycline	TET	Protein synthesis inhibitor, 30S	0.25

Table 2.1: Antibiotics and doses used for the antibiotic-temperature SIN clustering experiments. Doses are in μg/mL.

hypothesis test, see Methods). The resulting network is clustered to find monochromatically interacting groups, which correspond to similar interaction profiles, using our modified Prism 2 algorithm (Figure 2.1d, see Methods for details of the algorithm). These groups consist of drugs/temperatures that have similar overall interactions with other stressors, regardless of their interaction type. Consistent with overlap in the mechanism of action of specific drugs and the physiological effect of non-optimal temperatures, we find that the evaluated temperatures cluster with antibiotics in the following three groups (Figure 2.2): (1) all temperatures lower than the temperature for peak growth cluster together, along with the fluoroquinolones (LVX, CPR), which are DNA gyrase inhibitors, and with the 30S protein synthesis inhibitor tetracycline (TET); (2) the temperature 44°C clusters with the DNA-damaging drug nitrofurantoin (NTR) and with trimethoprim (TMP), an inhibitor of the folic acid biosynthesis pathway that is responsible for generating an essential DNA precursor; (3) the highest evaluated temperature, 46°C, clusters with the aminoglycosides (GEN, STR, TOB), antibiotics that affect protein translation proofreading [MGT99]. We thus conclude that monochromatic clustering successfully separated the antibiotics according to their mechanism of action and/or grouped with temperatures that have similar physiological effects.

Patterns in antibiotic and temperature interactions

We find that the distribution of the interactions between all pairs of stressors at 24-h growth is trimodal (Figure 2.3a), with peaks that correspond to synergy ($\tilde{\varepsilon} = -1$), additivity ($\tilde{\varepsilon} \approx 0$), and antagonism ($\tilde{\varepsilon} \approx 1$), similar to previous work [YTK06]. Ampicillin (AMP) and the aminoglycosides (GEN, STR, TOB) are mostly antagonistic with temperatures lower than the optimum (41°C), and synergistic or additive with higher temperatures (Figure 2.3b). Erythromycin and clindamycin (ERY, CLI) exhibit the opposite pattern: they are mostly synergistic with lower temperatures and antagonistic with temperatures near the optimum or higher, with the exception of 44°C. All interactions were calculated using the

mean growth under each condition (see Methods). Using median values yields similar results. The distribution of interactions changes with different choices of growth measurement time points (Figure 2.4). The 24-h time point was chosen for the analysis since the effects on growth and interactions of many of the stressors are not apparent at earlier time points.

Gene expression dynamics after exposure to antibiotics and high temperatures

Next, we explore the molecular mechanisms involved in the response to antibiotics by evaluating genome-wide transcriptional dynamics after exposure to high temperature (44°C) and two representative drugs that clustered with temperatures: TET (22–37°C, cold cluster) and STR (46°C cluster). To do this, we measure fold changes in gene expression compared to a control condition (37°C) with a library of *E. coli* strains containing GFP fused to more than 1800 promoters [ZBR06]. Consistent with the drug-temperature clusters, we find that the overall gene expression at 44°C is more similar to the response to STR than to TET (Figure 2.5a).

Changes in antibiotic sensitivity for heat-adapted *E. coli* strains

Our above experiments evaluate the overlap between the existing responses of wild-type *E. coli* to antibiotics and temperature. It is also of interest to evaluate if there is cross-resistance between temperature-adapted strains and antibiotics. Previously, Rodríguez-Verdugo et al. [RGT13] adapted an *E. coli* strain for over 2000 generations at 42.2°C and showed the heat-adapted strains acquired resistance to rifampicin. The resistance phenotype was mapped to mutations in the *rpoB* gene [RGT13]. We profile 10 of the heat-adapted strains, their ancestor strain, and 3 different *rpoB* mutants exposed to the antibiotics used in the clustering experiment. As predicted from our clustering analysis, most heat-adapted strains are as or more resistant to antibiotics (NTR and TMP) that mimic the effects of high temperatures (44°C) (Figure 2.6a, b). Resistance to aminoglycosides (which clustered with 46°C, a much

higher temperature to the one the heat-adapted strains were evolved on) was higher in some temperature-adapted strains and lower in others. Moreover, compared with the ancestor strain, most heat-adapted strains are more sensitive to antibiotics that mimic the effects of cold temperatures such as protein synthesis inhibitors (CLI, ERY, TET) (Figure 2.6a, b, Figure 2.7). These results are based on changes in IC50, the antibiotic concentration that results in 50% growth.

Intriguingly, the same patterns were not observed for the *rpoB* mutants exposed to some drugs (e.g., for ERY, CLI). These mutants were not adapted at high temperature, suggesting that there are additional adaptive mutations in the heat-adapted strains besides *rpoB*.

Multidimensional scaling as an alternative to clustering to validate temperature-drug similarity

We used a modified version of the Prism2 algorithm for finding the temperature-drug clusters because similar methods have been used in previous work to cluster antibiotic interaction networks [YTK06]. However, this methodology has some limitations. One issue is that it assumes that a stressor belongs only to a single cluster. This is likely a good approximation for stressors like antibiotics that tend to have specific and well-defined molecular targets in the cell. However, this single cluster assumption may not be true for other stressors like temperature that can harm many cellular functions simultaneously.

To address these limitations and validate our temperature-antibiotic groups, we use multidimensional scaling (MDS) as an alternative method for finding stressors (antibiotics and temperatures) with similar interactions. Notably, multidimensional scaling does not assume the stressors belong to a single cluster or require choosing any arbitrary constants. In multidimensional scaling, the node positions are embedded in the plane so that the distance between nodes approximates the dissimilarity in interactions (Equation 2.2) as closely as possible.

We find that the results of both analyses are mostly in agreement. In fact, the temperature-antibiotic clusters that we obtained with the Prism2 algorithm can be found in contiguous regions of the plane when performing multidimensional scaling (Figure 2.8). As such, both methods agree in terms of the broad patterns of similarity between certain antibiotic classes and temperature. Particularly, MDS maps the aminoglycosides (GEN, STR, TOB) nearby the highest temperature measured 46°C, NTR and TMP near 44°C , and LVX, CPR, TET near low temperatures, mirroring the clusters we obtain with the Prism2 algorithm.

However, relaxing the single cluster assumption shows more detail: for example we can see that the lowest temperatures $22°C, 25°C$ measured are similar to both the antibiotics in the cold group and the macrolides ERY, CLI, who are protein synthesis inhibitors which would be expected to be similar to low temperatures. However, the macrolides seem to be similar only to these very lowest temperatures, but not to mild cold (30°C) or some of the other members of the cold cluster (LVX, CPR, TET). This is likely the reason they did not cluster in the cold group in the Prism algorithm clusters.

2.4 Discussion

In this chapter of the dissertation, we cluster interactions among drugs and temperatures to infer that there are shared physiological responses of *E. coli* to these stressors. Our SIN analysis suggests that the stress responses to low temperatures overlap with those of antibiotics that affect DNA gyrase and a 30S protein synthesis inhibitor. In addition, the stress responses to high temperatures overlap with those of drugs that affect protein translation proofreading and drugs that damage DNA. Due to this overlap, we conclude that cellular responses to temperature stress have likely been evolutionarily co-opted to also respond to many classes of antibiotic stress. Because pressure and pH are also ancient stressors, we expect that responses to them may have also been co-opted to deal with antibiotic stress. Our approach provides a powerful basis for asking similar questions about other environmental,

chemical, or physical stressors that affect the population growth of an organism.

We show that monochromatic clustering successfully separates antibiotics and temperatures into groups that have similar effects on bacterial physiology. First, all temperatures (22°C, 25°C, 30°C, 37°C) lower than the optimum (41°C, which results in the highest growth) cluster with antibiotics that either affect the early stages of protein synthesis (TET prevents the association of aminoacyl tRNAs with the ribosome [CR01]) or are DNA gyrase inhibitors (LVX, CPR). This is consistent with the known effects of low temperature. One of the main effects of cold shock is translational block, which is thought to most likely occur at the translation initiation step [Yam99]. Some previous reports have also shown that cold-shock induces the expression of DNA gyrase and a transient increase of negative supercoiling of DNA in *E. coli* [Yam99, GD84, MKO97]. Second, the highest evaluated temperature (46°C) clusters with the aminoglycosides, antibiotics that affect protein translation proofreading [MGT99]. This leads to misfolding and aggregation of defective proteins that mimic the well-known effects of high temperatures on protein stability and folding [RHB10]. Finally, 44°C clusters separately from 46°C, with antibiotics that either damage nucleic acids or inhibit their synthesis. This intriguing finding suggests the main physiological effect of this temperature (compared to 41°C) could be due to effects on nucleic acids. This connection to nucleic acids is suggestive given that the heat-shock protein Hsp70 enhances repair of UV-induced DNA damage [NLG06]. We speculate that this specific temperature clustering separately from the aminoglycosides may be due to the heat-shock response being able to partially combat protein unfolding at 44°C, but not 46°C.

An important feature of the monochromatic clustering framework is that it implicitly assumes each node (i.e., stressor) in the SIN belongs to a single cluster. This single cluster assumption is likely a good approximation for antibiotics as they tend to bind to specific cellular targets. However, physical or environmental stressors, such as temperature, can affect many cellular processes simultaneously. Because of this, the clusters in our study correspond to consensus effects: these are informative summaries of the dominant effects of

the environmental stressor, but could miss secondary effects that are not shared with the other members of the cluster. Further theoretical and computational work could focus on relaxing the single cluster assumption of monochromatic clustering to allow temperatures to be grouped with multiple, potentially dissimilar classes of antibiotics. This updated methodology could allow a more nuanced approach, capable of breaking down the effects of an environmental stressor in terms of more targeted perturbations such as antibiotics, chemical inhibitors, or gene deletions that are deleterious to different cellular subsystems.

Indeed, some of the evaluated temperatures do have similar interactions to antibiotics in different clusters (Figure 2.7). Examples are the lowest temperatures evaluated (22°C, 25°C). These temperatures have similar interaction profiles to both the 30S (TET) and 50S (ERY, CLI) protein synthesis inhibitors, while higher temperatures that are still below the optimum (30°C, 37°C) are only similar to the 30S inhibitors. This is reflected in (ERY, CLI) being in a separate cluster from the low temperatures. Interestingly, a previous report has shown cold-shock proteins are induced in response to CLI [VN90]. Multidimensional scaling based on the dissimilarity matrix, which embeds the nodes into the plane in a way where the distances between them approximates the dissimilarity between the nodes, places the macrolides (ERY, CLI) nearby (22°C, 25°C). We thus conclude that most likely the macrolides are similar to cold, but only to the very lowest temperatures measured.

Clinically, the impact of temperature on the effects of antibiotics is also of interest because it suggests some antibiotics could have increased or reduced effectiveness in patients with fever or hypothermia. Previous work has shown there is increased resistance to gentamicin (GEN) in *Francisella tularensis*, *Listeria monocytogenes*, and *Klebsiella pneumoniae* at 26°C when compared to 37°C [LHK16]. This increased resistance seems to be mediated by reduced drug uptake. It has also been reported that streptomycin (STR), tetracycline (TET), ampicillin (AMP), and cefoxitin (FOX) have increased effectiveness at 46°C compared to 37°C in *Pseudomonas aeuriginosa* [BKS99]. Our results are consistent with both reports, as we found: (1) aminoglycosides (GEN, STR, TOB) are mostly synergistic with high tempera-

tures and antagonistic with low temperatures, (2) synergy of beta-lactams (AMP and FOX) with high temperatures, and (3) synergy of TET with 46°C (but, interestingly, with 22°C as well). Some other antibiotics (LVX, NTR, and TMP) also exhibit this curious pattern of being synergistic with both temperature extremes and either additive or slightly antagonistic with less stressful temperatures. Further work is needed to obtain a more detailed understanding of these interaction patterns.

Our transcriptional analysis shows that the overall expression patterns of *E. coli* exposed to high temperature are more similar to those induced by STR than those induced by TET (Figure 2.5a). We find that *cspA* and *cspG*, main cold-shock response regulators in *E. coli*, have increased expression in response to TET, but not STR or high temperature (Figure 2.5b). Other cold-shock regulators (*cspB*, cspI) show decreased expression. It has been shown that cold-shock genes are differentially induced depending on the severity of the cold stress. In particular, cspA expression is induced between 20–30°C, while *cspI* is induced between 10 and 15°C [WYI99]. These gene expression results are in agreement with our drug/temperature clusters, since the low temperature cluster contains temperatures between 22 and 37°C. We find that genes involved in the response to unfolded protein (as determined by gene ontology annotations), which commonly results from heat stress, are overrepresented in the genes induced by STR, a representative antibiotic that clustered with heat (Figure 2.5c). Interestingly, some heat-shock response genes that combat unfolded protein stress (*dnaK*, *dnaJ*, *groE*, *grpE*) have increased expression in response to both STR and TET. However, the main heat-shock response regulator *rpoH* is not over-expressed in response to either antibiotic (in fact, is under-expressed in response to TET). Together, these results suggest heat-shock genes participate in the response to both antibiotics. However, they may be activated in a different way than the canonical heat-shock response.

Our clustering and gene expression results show that multiple antibiotics (particularly aminoglycosides, TET, DNA gyrase inhibitors, and DNA-damaging antibiotics) have similar overall effects in *E. coli* physiology to specific low or high temperatures. This is consistent

with components of the stress response to temperature having been co-opted over evolutionary time to deal with antibiotics that disrupt similar cellular structures or functions to those affected by low- and high-temperature stress. Moreover, we show that this overlap between stress responses can be related to the acquired cross-resistance of temperature-adapted strains to specific groups of antibiotics.

Typically, the overlap between cellular responses to stress has been studied by isolating subcellular parts and attempting to piece together this information to understand stress responses at the whole-cell level. Here, we take a reverse, yet complementary approach: by studying the effect of perturbations on the whole system, we gain more insights into the mechanisms of its specific parts. Importantly, no aspect of this methodology is specific to antibiotics and temperature. Our SIN clustering method can be used to evaluate shared responses among any combination of physical, chemical, and/or biological stressors that affect organismic growth.

In conclusion, we evaluate if the overlap between antibiotic and temperature stress responses is predictive of the cross-resistance of high-temperature-adapted strains to antibiotics (Figure 2.6). We find that high-temperature-adapted strains become more sensitive to protein synthesis inhibitors (CLI, ERY, TET), drugs that either clustered with or are similar to low temperatures. In contrast, the temperature-adapted strains become more resistant to drugs that clustered with 44°C (NTR, TMP), but not necessarily to drugs that cluster with 46°C (GEN, STR, TOB). Overall, these results strongly suggest that seemingly novel drug resistance is conferred to strains via adaptations they acquired while being evolved at extreme temperatures. Specifically, strains adapted to heat (42.2°C) are more resistant to drugs that damage DNA (which cluster with 44°C, a similar temperature), while also being more sensitive to drugs that mimic the effect of cold. However, this pattern is not universal, since the strains do not become more sensitive to fluoroquinolones (LVX, CPR), which also cluster with cold. Interestingly, the *rpoB* mutants do not follow the same antibiotic resistance patterns as the temperature-adapted strains, suggesting there may be more adaptive

mutations to temperature besides *rpoB*.

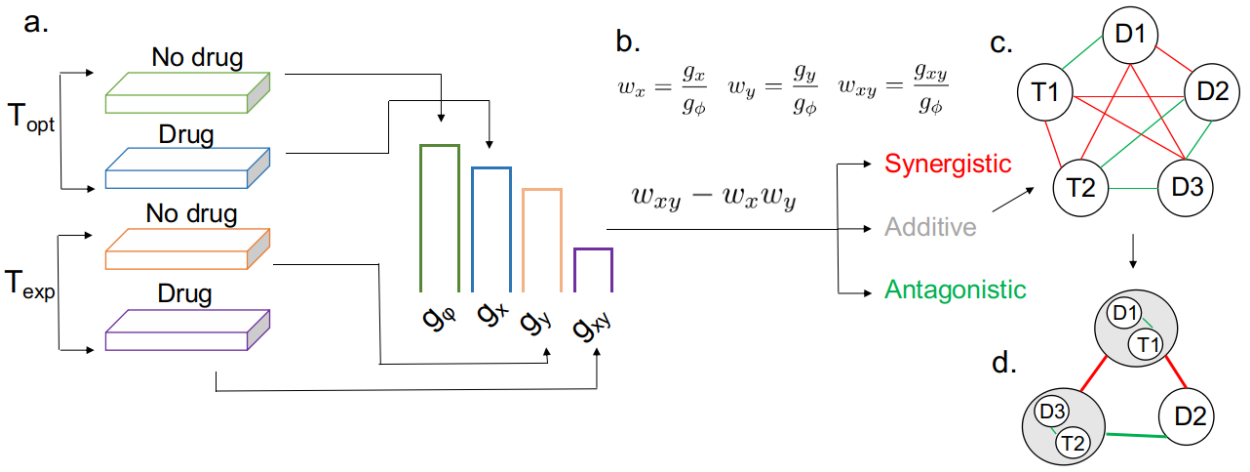

Figure 2.1: *Schematic illustration of the approach taken in this work.* (a) Growth is measured in the following conditions: reference growth g_ϕ at the optimal temperature ($T_{\text{opt}} = 41°\text{C}$) in the absence of drug, g_x at optimal temperature with drug, g_y at experimental temperature T_{exp}, but no drug, and g_{xy} at non-optimal temperature with drug. (b) The growth of each experimental condition is converted to proportions w_x, w_y, w_{xy} by dividing by the reference growth. The difference between w_{xy} (observed growth) and the product of w_x and w_y (expected growth under independence) is then used to classify the interaction between drugs and temperatures into three cases: synergistic (red line), additive (white or not shown), and antagonistic (green line), (c) which can be represented as an interaction network. (d) Drugs and temperatures can then be clustered into a functional class based on the monochromaticity of interactions with a different class. This example shows a drug-temperature interaction, but drug–drug interactions are obtained similarly, by replacing the growth with no drug at T_{exp} with the growth under a second drug at T_{opt}.

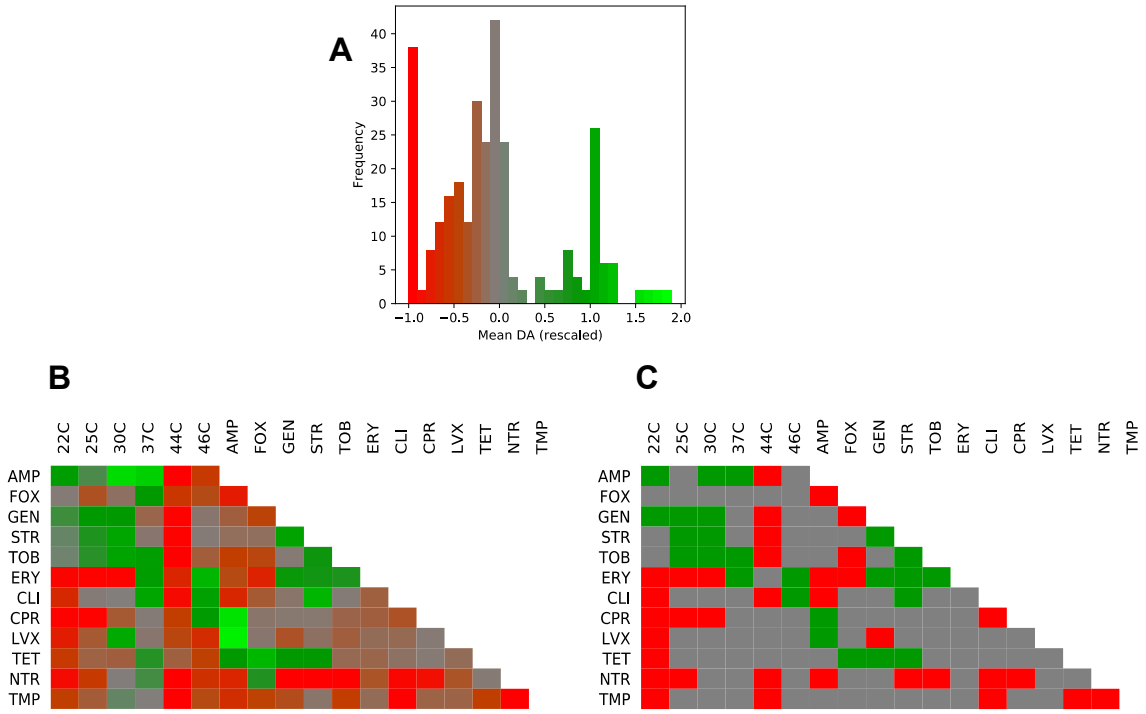

Figure 2.2: *Monochromatic clustering of the interaction network.* (a) Unclustered interaction network. The nodes that correspond to drugs are color-coded by their mechanism of action (Table 2.1 that correspond to temperatures are colored in a gradient from blue (low) to red (high). The edges correspond to discretized interaction type, as in Figure 3c: synergy (red), antagonism (green), additive or unknown (no edge). (b) Network clustered into monochromatic classes by the modified Prism2 algorithm (see Methods).

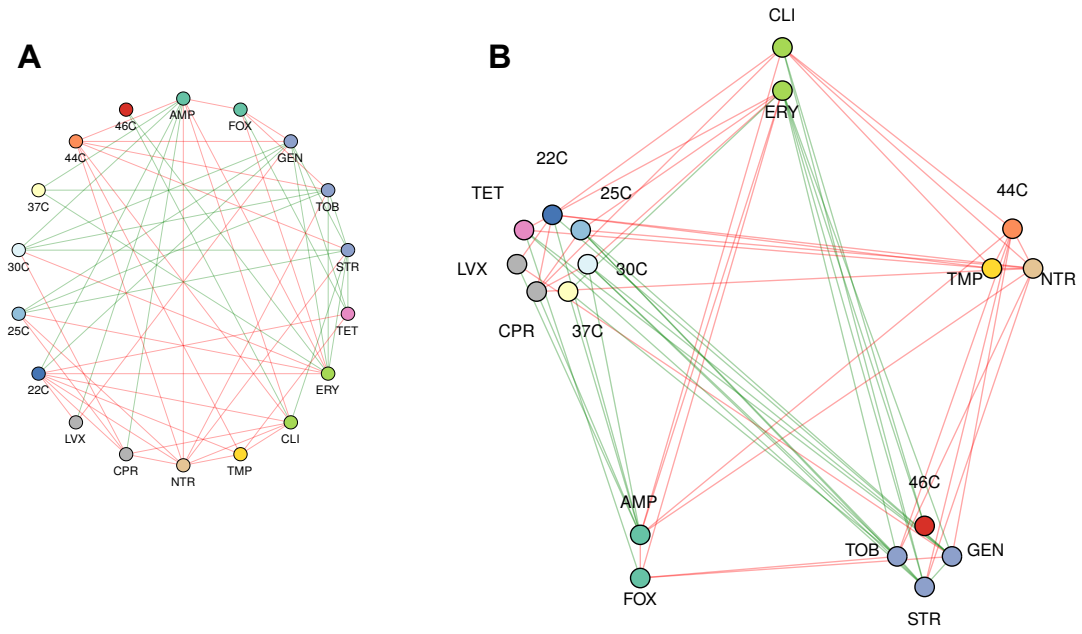

Figure 2.3: *Interaction effects between antibiotics and temperature based on growth after 24-h.* The interaction effect ($\tilde{\varepsilon}$) values are color-coded in a gradient, from synergy (red) to additive (gray) and antagonism (green). (a) Overall distribution of the mean estimated interaction effects across all treatments. The distribution shows three clear peaks, corresponding to strong synergy, additivity, and antagonistic buffering. (b) Matrix heatmap of the mean interaction effects. Antibiotics with the same mechanism of action show similar interaction patterns. (c) Matrix heatmap of the discretized interaction types used for constructing the edges of the interaction network.

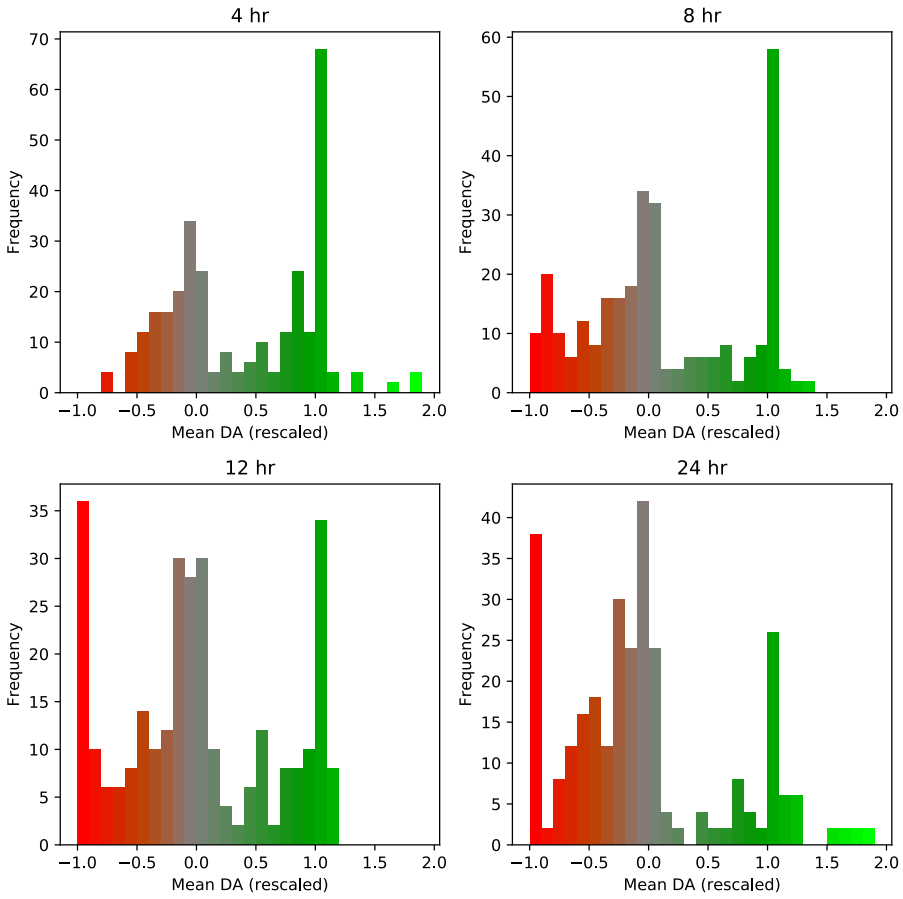

Figure 2.4: *Time-resolved distribution of interaction effects.* The distribution of the mean antibiotic and temperature interaction effects at the four measured timepoints (4, 8, 12 and 24 hr) is shown. At hour 4, synergistic interactions are rare. As time goes by, the antibiotics gradually show their full effects on growth. This results in more synergistic effects being apparent, and an overall shift in the distribution to the left. By hour 24, four modes are clearly visible in the distribution, corresponding to strong antagonism ($\tilde{\varepsilon} \approx -1$), additivity ($\tilde{\varepsilon} \approx 0$), and moderate ($\tilde{\varepsilon} \approx 0.5$) and strong ($\tilde{\varepsilon} \approx 1$) antagonistic buffering.

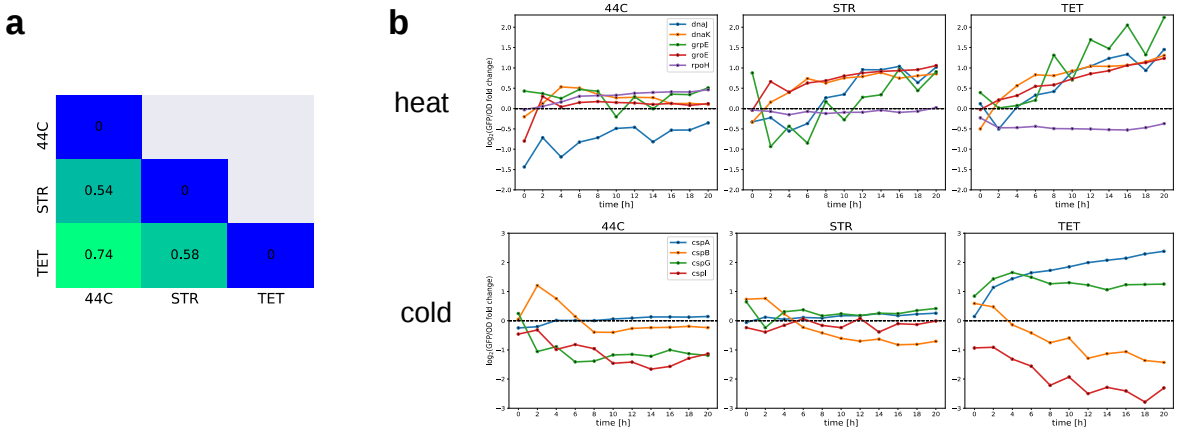

c

Over-Expressed Biological Process GO Terms		
44°C	**STR**	**TET**
pentose catabolic process	chaperone cofactor-dependent protein refolding	glutathione metabolic process
fatty acid beta-oxidation	negative regulation of transcription, DNA-templated	**folic acid-containing compound metabolic process**
bacterial-type flagellum-dependent cell motility	tricarboxylic acid cycle	phospholipid biosynthetic process
carbohydrate transport	positive regulation of transcription, DNA-templated	peptide catabolic process
tetrahydrofolate biosynthetic process	cellular response to sulfate starvation	
extracellular polysaccharide biosynthetic process	translesion synthesis	
	maltodextrin transport	
	cellular response to unfolded protein	
	pyrimidine nucleobase catabolic process	
	folic acid-containing compound metabolic process	
	cellular response to nutrient levels	

Under-Expressed Biological Process GO Terms		
44°C	**STR**	**TET**
deoxyribonucleotide biosynthetic process	purine nucleoside catabolic process	**glutamine biosynthetic process**
positive regulation of transcription, DNA-templated	response to acidic pH	metabolic process
arginine catabolic process	sulfur compound metabolic process	putrescine catabolic process
response to cold	cellular amino acid catabolic process	**nitrogen compound metabolic process**
	L-cysteine catabolic process to pyruvate	transcription, DNA-templated
	glutamine biosynthetic process	
	nitric oxide catabolic process	
	pyrimidine nucleobase catabolic process	
	uracil catabolic process	
	nitrogen utilization	
	putrescine catabolic process	
	nitrogen compound metabolic process	
	carbohydrate metabolic process	

Figure 2.5: *Gene expression of E. coli after exposure to antibiotics and high temperature.* The gene expression response of *E. coli* was evaluated with a library of 1870 fluorescent transcriptional reporters. (a) Mean absolute gene expression distance between experimental conditions. Lower numbers indicate conditions with more similar gene expression profiles. (b) Gene expression of representative heat-shock and cold-shock genes relative to control (37°C) in response to experimental conditions (44°C, STR, TET). (c) Gene ontology terms in the biological process category over-represented in the set of over-expressed and under-expressed genes in each experimental condition relative to control. Terms that are in bold occur in more than one treatment.

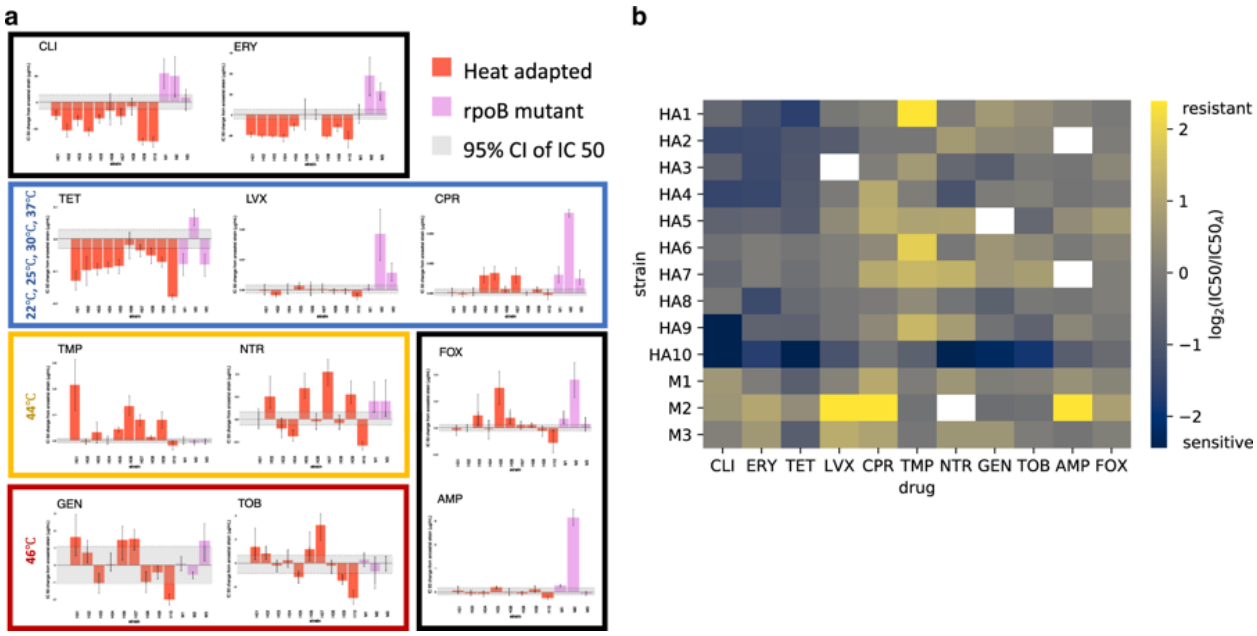

Figure 2.6: *Antibiotic sensitivity of high-temperature-adapted E. coli strains.* (a) Absolute change in the IC50 (g/mL) relative to the ancestral strain. Heat-adapted strains (red), *rpoB* mutant strains (purple). Error bars represent 95% credible intervals (CIs). Gray region represents the 95% CI of ancestral strain. Drugs are grouped according to the clusters of antibiotics and temperature in (Figure 2.2). Conditions where the model fit was poor were removed from the plots. (b) Heatmap of log2 fold changes from the ancestral IC50. Heat-adapted strains are denoted by HA, while rpoB mutant strains are denoted by M. Positive numbers (yellow) indicate increased IC50 (more resistance), while negative numbers (blue) indicate a decreased IC50 (higher sensitivity). Drugs are grouped in the same way as in (a) Missing conditions are shown in white.

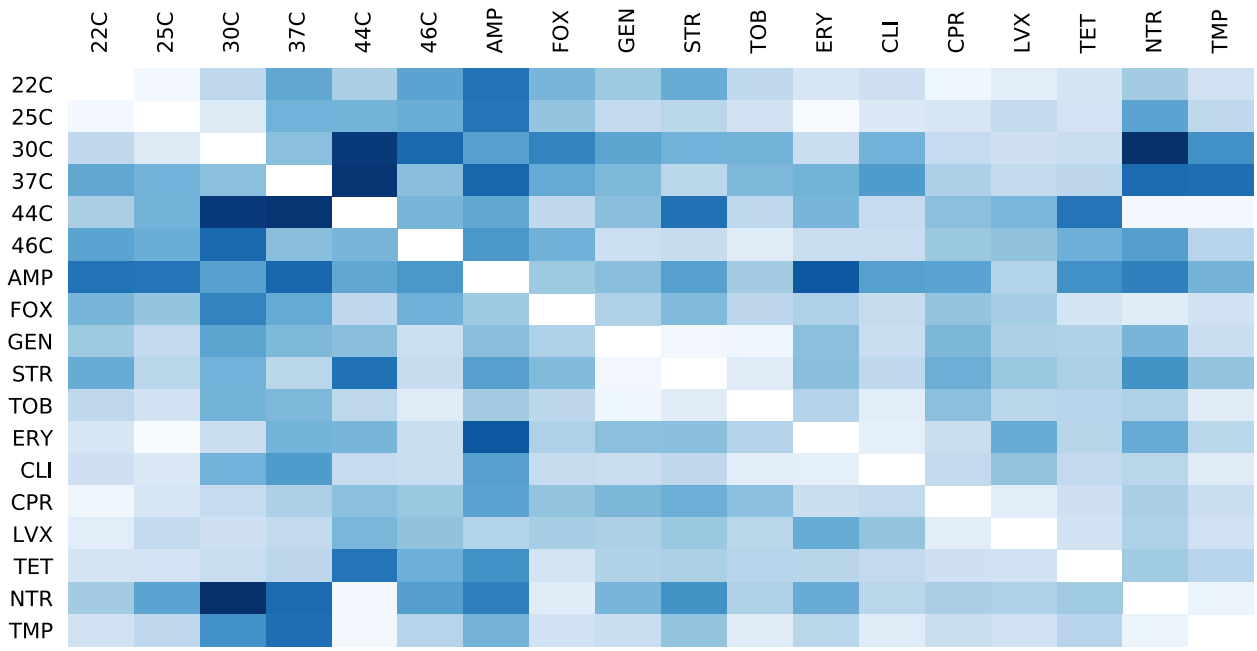

Figure 2.7: *Dissimilarity of interactions.* A heatmap with the dissimilarity between the interactions of each pair of conditions (see Methods) is shown. The dissimilarities are color coded in a gradient from white (more similar) to dark blue (more dissimilar). From these results, it is apparent that temperatures can be similar to multiple classes of antibiotics.

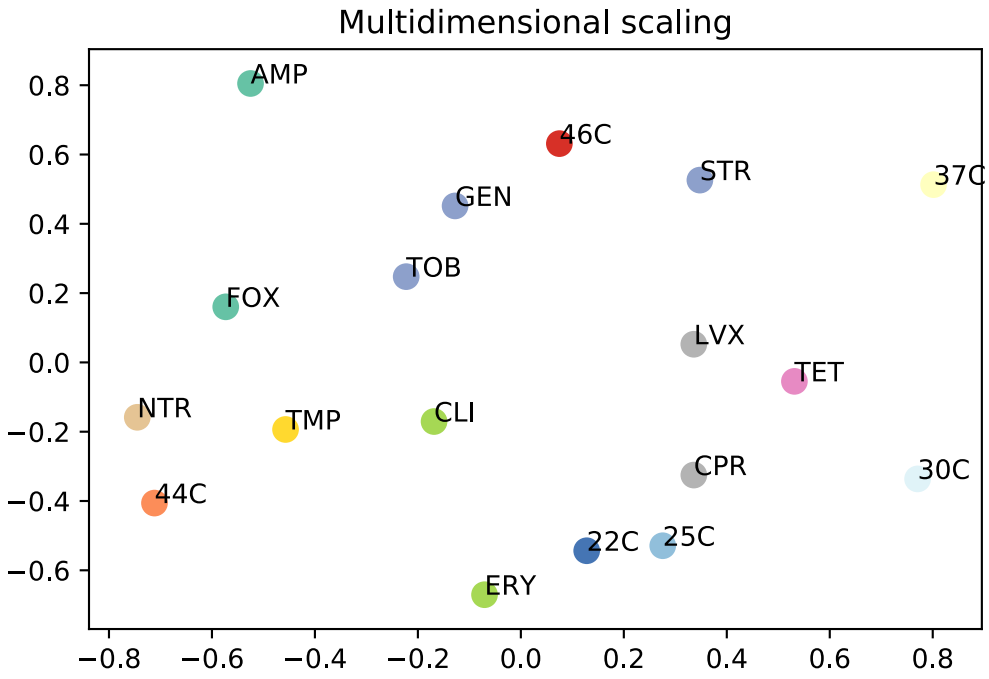

Figure 2.8: *Multidimensional scaling as an alternative to the Prism2 algorithm.* Multidimensional scaling of the dissimilarities (using point estimates for the $\tilde{\varepsilon}_{xy}$). Nodes that are closer together have more similar interactions. The results of this analysis largely agree with the cluster assignments of the Prism2 algorithm (Figure 2.3), with the exception of finding that the macrolides (ERY, CLI) also seem similar to low temperatures.

CHAPTER 3

A flexible model for temperature responses of living organisms with biologically interpretable parameters

In Chapter 2 of this dissertation we studied how single temperatures–either cold or hot relative to the species optimum–impact bacterial growth and how interactions between antibiotics and temperatures can be used to infer groups of temperatures and antibiotics with shared effects in the cell. In this chapter, we now expand to a more comprehensive view by using temperature response curves (TRCs) that model and quantify the overall shape and response of bacterial growth to a range of temperatures. We develop a flexible model for TRCs, based on a generalization of the Briere model, to describe temperature response curves that are parametrized in terms of biological meaningful quantities. This model is applied to the study of temperature response curves in the presence of antibiotics in Chapter 4 of this dissertation.

3.1 Introduction

Understanding how the growth and other physiological processes of living organisms are affected by temperature is a fundamental question in ecology, with important implications for evolutionary biology and projecting the effects of climate change in biodiversity. Because of this, ecologists are interested in measuring how the growth of living organisms depends on temperature, and how this dependence changes across individuals and species depending on factors like body size, geographic distribution, the mean environmental temperature and

its variability [DPS11, FGS97, MCE17, SGB04].

In order to perform these studies, measurements of the growth of living organisms (or some other measurable quantity used as a proxy) are taken at different temperatures. A mathematical model of the temperature response is then fit to the data to extract useful quantities such as the optimal growth temperature and temperature niche (defined as the range of temperatures where growth exceeds some threshold) for the organism in question. Various mathematical models, both descriptive and mechanistic have been developed for fitting the temperature dependence of the growth of living organisms [BPL99, LHJ95, SD77, ROR05, SG10, SGS11, YKM95].

Mechanistic models of temperature response curves

Existing mechanistic models of temperature responses are based on the thermodynamics of protein unfolding [SD77, ROR05]. The general assumption made by these models is that there is a proteic enzyme that catalyzes a chemical reaction that is rate-limiting for the growth or development of the living organism, and that this enzyme is inactivated at high and low temperatures. As an example of a mechanistic model of this kind, consider the Sharpe and Schoolfield model [SD77, SSM81, SG10].

$$r(T) = \frac{\rho \frac{T}{298} \exp\left[\frac{\Delta H_A}{R}\left(\frac{1}{298} - \frac{1}{T}\right)\right]}{1 + \exp\left[\frac{\Delta H_L}{R}\left(\frac{1}{T_L} - \frac{1}{T}\right)\right] + \exp\left[\frac{\Delta H_H}{R}\left(\frac{1}{T_H} - \frac{1}{T}\right)\right]} \tag{3.1}$$

As typical for these kinds of models, the Sharpe-Schoolfield model is parametrized in terms of thermodynamic quantities relating to an average, rate-limiting, or effective chemical reaction that is governing growth. In this case the parameters are the enthalpy of activation of the chemical reaction for growth ΔH_A, the changes in enthalpy due to the inactivation of the enzyme that catalyzes this reaction at low and high temperatures (ΔH_L and ΔH_H), the temperatures of half inactivation of the enzyme (T_L, T_H) and ρ, the growth rate at 25°C.

The strength of these approaches lies in linking protein unfolding, a process that happens at the molecular level, with traits at the level of populations of organisms. However,

given the complexity of living organisms, the assumption that a single chemical reaction is rate-limiting for their growth and further, that this reaction is the same at low and high temperatures, does not seem very realistic. Because of this, the inferred parameters likely correspond to some average between the stability of various different proteins and other molecular components in the cell. Other processes than protein inactivation also occur at extreme temperatures, and may be important contributors to the increased death and reduced growth rate at these temperatures. These issues complicate the interpretation of the thermodynamic parameters inferred from these models when a curve is fitted to empirical data. Moreover, the thermodynamic properties of protein unfolding are rarely an object of interest in ecological applications. Rather, ecologists are interested in the optimal temperature for growth of a living organism, its maximal growth rate and the range of temperatures where its growth or development exceeds a certain threshold. This has led to the development of descriptive models that explicitly contain some of the quantities of interest, and that have less parameters than mechanistic models, a useful property when fitting to limited data.

Descriptive models of temperature response curves

In contrast to mechanistic models for temperature response curves, descriptive models are not based on any underlying physical or chemical theory. Rather, these models aim to provide a function with the right shape to empirically fit temperature response curves in order to infer quantities of interest, such as the optimal temperature for the trait being modeled.

One popular descriptive model for fitting temperature responses in applications is the Briere model [BPL99], originally developed for describing the rate of development of insects. It is given by the equation

$$r(T) = \begin{cases} cT\left(T - T_{\min}\right)\left(T_{\max} - T\right)^{\frac{1}{m}} & T_{\min} \leq T \leq T_{\max} \\ 0 & \text{otherwise} \end{cases} \tag{3.2}$$

This model is parametrized in terms of the minimum and maximum temperatures for growth $T_{\min}$ and $T_{\max}$, where the temperature T is assumed to be in units of degrees Celsius. Typically, a distinction is made between two versions of the Briere model: a) the Briere1 model, in which $m = 2$ is fixed, and b) the Briere2 model where m is a free parameter. The Briere1 model is especially popular in applications due to its parsimony (it has only three parameters), and because of the direct interpretability of $T_{\min}$ and $T_{\max}$ in ecological terms. Another property of the Briere models which is desirable for some applications is that response is exactly zero outside of the interval $(T_{\min}, T_{\max})$, as opposed to approaching zero when $T \to \pm\infty$.

The Briere models remain popular for describing temperature response curves for insect development. However, they have also been used for describing the temperature dependence of various physiological traits in other organisms, such as the growth rates of marine fungi [TRC18] and mosquitoes [MCE17] and the cardiac activity of shrimp [BBL18].

Despite their popularity in applications, there are some shortcomings of the Briere models that need to be carefully considered before their use. First, they make the implicit assumption that $r(0) = 0$. Because of this root at zero, the response cannot be positive below freezing temperatures. This aspect makes them unsuitable to describe temperature responses of organisms where it is possible that $T_{\min} < 0$. There does not seem to be any biological motivation for this implicit assumption, which seems to be an unintended consequence of the functional form chosen for the Briere models.

Another implicit assumption made in the Briere1 model, the most popular in applications, is that the optimal temperature of the response is a deterministic function of the minimum and maximum temperatures. This can be seen from the equation for the optimal temperature that maximizes Equation 3.2, which is

$$T_{\text{opt}} = \frac{2mT_{\max} + (m+1)T_{\min} + \sqrt{4m^2T_{\max}^2 + (m+1)^2T_{\min} - 4m^2T_{\max}T_{\min}}}{4m+2} \tag{3.3}$$

For the Briere1 model, $m = 2$ is fixed. Thus, T_{opt} is completely determined by $T_{\min}$ and $T_{\max}$,

and this dependence is not based on any mechanistic grounds or biological justification. Thus, estimates of the optimal temperature made with this model will be significantly affected by the minimum and maximum temperatures.

Here, we propose to modify the Briere models to address both issues detailed above. We then reparametrize the model in terms of quantities that are biologically interpretable and of interest for ecological applications. Besides the previous discussion, another motivation for developing an alternative is that we were in need of a flexible model to describe temperature responses of bacterial growth in the presence of antibiotics (see the work in Chapter 4). This is because we found that temperature responses under antibiotics show much greater variability in terms of their shapes that were not adequately described by existing models. Our modifications to the Briere model are also partially in order to adequately describe these temperature response curves.

3.2 The modified Briere model

Mathematical framework

We start by modifying the Briere model from Equation 3.2 as follows:

$$r(T) = \begin{cases} c\,(T - T_{\min})^{a}\,(T_{\max} - T)^{b} & T_{\min} \leq T \leq T_{\max} \\ 0 & \text{otherwise} \end{cases} \tag{3.4}$$

In doing this we make two important changes to the Briere model. First, we remove the root at zero which will make the model suitable for organisms that can grow under freezing temperatures. Second, we introduce another exponent a for the first factor to make the model more flexible. We replace the power $\frac{1}{m}$ by a constant b for consistency and notational simplicity. This leads to a flexible model that can describe temperature responses of many different shapes. Similar models have been used to describe the yield of crops as a function of temperature [YKM95]. However, this form of the model contains three arbitrary

mathematical constants a, b, c without a clear biological meaning. To make this model more useful for ecological applications, we reparametrize the model by replacing these arbitrary constants with biologically meaningful quantities.

Optimal temperature for growth

We start by finding the optimal growth temperature. Starting with Equation 3.4, take logarithms, and differentiate to get

$$\frac{d}{dt} \ln r(T) = \frac{a}{T - T_{\min}} - \frac{b}{T_{\max} - T}$$

It follows that

$$T_{\text{opt}} = \alpha T_{\max} + (1 - \alpha) T_{\min} \tag{3.5}$$

where $\alpha = \frac{a}{a+b}$.

The optimal temperature is therefore a convex combination of the minimum and maximum temperatures. The parameter $\alpha \in [0, 1]$ determines the location of the optimal temperature relative to the minimum and maximum, with the extreme cases $\alpha = 0$ and $\alpha = 1$ corresponding to $T_{\text{opt}} = T_{\min}$ and $T_{\text{opt}} = T_{\max}$, respectively. Rearranging Equation 3.5 yields $\alpha = \frac{T_{\text{opt}} - T_{\min}}{T_{\max} - T_{\min}}$, which shows that α can be interpreted as a rescaled (and dimensionless) optimal temperature.

Expressing the model in terms of biologically meaningful parameters

In this section, we reparametrize Equation 3.4 to replace the arbitrary constants a, b, c with parameters that are biologically meaningful and have intuitive effects on the curve. Let $\alpha = \frac{a}{a+b}$ be the dimensionless optimal temperature as defined above, and define $s = a + b$. Then, solving for a, b and substituting into Equation 3.4 yields

$$r(T) = c \left(T - T_{\min}\right)^{\alpha s} \left(T_{\max} - T\right)^{(1-\alpha)s}$$

Now, define the maximum value of the response $r_{\max} = r(T_{\text{opt}})$. Substituting T_{opt} from Equation 3.5 into the expression above and solving for c yields

$$c = \frac{r_{\max}}{[\alpha^{\alpha}(1-\alpha)^{(1-\alpha)}(T_{\max} - T_{\min})]^{s}}$$

Substituting back into the equation to replace c with $r_{\max}$ yields the following form of the modified Briere model, which we term the *biological parametrization* of the model. This can be a convenient parametrization for parameter estimation through Bayesian methods, since the parameter α is constrained to be in the interval $[0, 1]$, making it natural to use a prior probability distribution with support in this interval (see Chapter 4).

$$r(T) = r_{\max}\left[\left(\frac{T - T_{\min}}{\alpha}\right)^{\alpha}\left(\frac{T_{\max} - T}{1-\alpha}\right)^{1-\alpha}\left(\frac{1}{T_{\max} - T_{\min}}\right)\right]^{s} \tag{3.6}$$

An alternative parametrization where the optimal temperature T_{opt} is an explicit parameter in the model can also be constructed by substituting the parameter $\alpha = \frac{T_{\text{opt}} - T_{\min}}{T_{\max} - T_{\min}}$ with the optimal temperature. We expect this form of the model to be most useful for applied ecologists and other applied scientists. This is because it is common to fit TRC models through nonlinear least squares using standard software, which usually provides confidence intervals for the model parameters. Thus, having the optimal temperature in non-dimensionless form as an explicit parameter in the model will allow applied scientists to easily obtain a confidence interval for the optimal temperature, which is typically one of the main quantities of interest, without additional effort.

$$r(T) = r_{\max}\left[\left(\frac{T - T_{\min}}{T_{\text{opt}} - T_{\min}}\right)^{\frac{T_{\text{opt}} - T_{\min}}{T_{\max} - T_{\min}}}\left(\frac{T_{\max} - T}{T_{\max} - T_{\text{opt}}}\right)^{\frac{T_{\max} - T_{\text{opt}}}{T_{\max} - T_{\min}}}\right]^{s} \tag{3.7}$$

Nondimensionalization

In this section, we nondimensionalize the model to find parameters that determine the shape of the temperature curve independent of units and scaling in the T and r axes. We can first

nondimensionalize the response by writing $w(T) = \frac{r(T)}{r_{\max}}$. If the response $r(T)$ corresponds to growth rate (a common case in practice), $w(T)$ represents the relative fitness of the organism at temperature T (compared to the optimal temperature T_{opt}).

Next, we note that our equation for T_{opt} implicitly defines a dimensionless optimal temperature $\alpha = \frac{T_{\text{opt}} - T_{\min}}{T_{\max} - T_{\min}}$. We can define a dimensionless temperature $\tau = \frac{T - T_{\min}}{T_{\max} - T_{\min}}$ in a similar way. Using these definitions, we can write the nondimensionalized response as a function of τ, yielding a dimensionless modified Briere model with only two parameters

$$w(\tau) = \left[\left(\frac{\tau}{\alpha} \right)^{\alpha} \left(\frac{1 - \tau}{1 - \alpha} \right)^{1 - \alpha} \right]^{s} \tag{3.8}$$

where both the maximum attained value and the τ-axis range of nonzero values is always unity.

The remaining parameters in the nondimensionalized model are those that modify the shape of the curve. The rescaled optimal temperature α provides the location of the optimum, thereby controlling the skewness of the temperature response curve. The parameter s modifies the rate of increase to the optimum, with high values corresponding to "skinnier" and large values to "fatter" curves (Figure 3.1).

Thus in the full model, there are three parameters that determine the location and scaling of the shape given by the corresponding nondimensional model. The minimum temperature $T_{\min}$ provides the location of the curve in the T-axis, the maximum response $r_{\max}$ corresponds to the scaling in the r-axis, and the maximum temperature $T_{\max}$ (or, equivalently, the temperature range $T_{\max} - T_{\min}$ where the response is nonzero) determines the scaling in the T-axis (Figure 3.1).

A fixed-point iteration algorithm for finding the half-maximum growth temperatures

The minimum and the maximum growth temperatures $T_{\min}$ and $T_{\max}$ are explicitly parameters in the modified Briere model. However, the half-maximum growth temperatures are

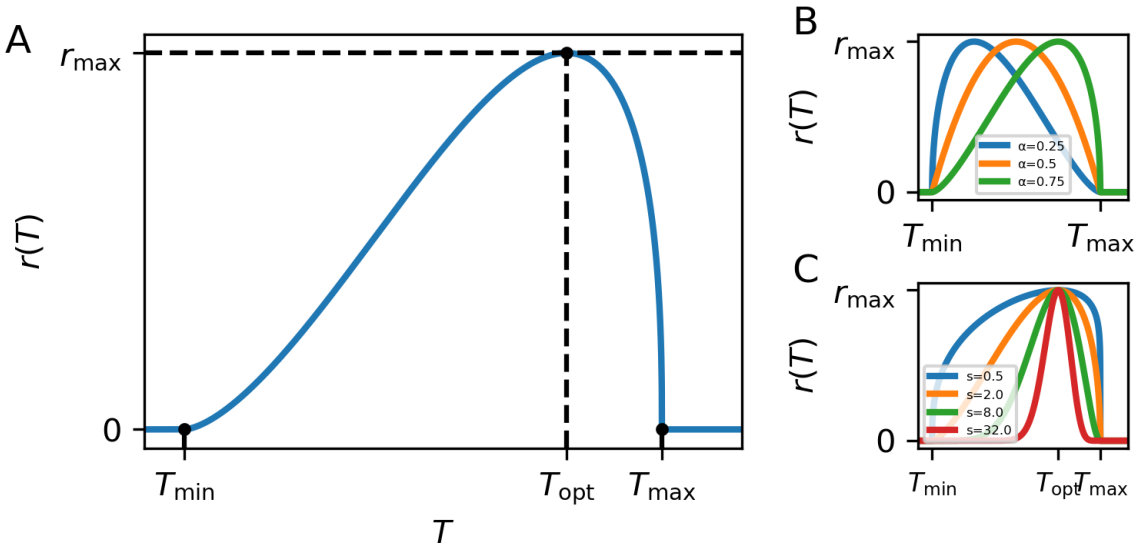

Figure 3.1: *Modified Briere model proposed here.* A: Schematic of the modified Briere model, which is parametrized in terms of biologically interpretable quantities: the minimum temperature $T_{\min}$, the maximum temperature $T_{\max}$, the maximum value of the response $r_{\max}$ and a choice of either the optimal temperature T_{opt} or the rescaled optimal temperature α. B: Effect of varying the parameter α, representing the position of T_{opt} relative to $T_{\min}$ and $T_{\max}$. C: Effect of varying the parameter s.

also often of interest to ecologists: this is because often there is less data collected at or near temperature extremes than near the central portions of the curve, so the half-maximum temperatures can often be estimated more reliably than the extremes.

It is not possible to solve analytically for the half-maximum temperatures for the modified Briere model (except for some specific values of α). However, as an alternative, we present here a simple fixed point algorithm for the numerical computation of half-maximum temperatures, and, more generally, for numerically finding the two temperatures that correspond to the solutions of the equation $w(\tau) = w_{\text{ref}}$, where $w_{\text{ref}} \in (0, 1)$.

Let τ_1, τ_2 be the two solutions to the equation $w(\tau) = w_{\text{ref}}$ where $w_{\text{ref}} \in (0, 1)$. Starting from the nondimensionalized model (Equation 3.8), we can "solve" for τ from either the $\frac{\tau}{\alpha}$

or the $\frac{1-\tau}{1-\alpha}$ factor to get the implicit equations

$$\tau = \alpha w_{\text{ref}}^{\frac{1}{\alpha s}} \left(\frac{1-\alpha}{1-\tau}\right)^{\frac{1-\alpha}{\alpha}} = f_1(\tau) \tag{3.9}$$

and

$$\tau = 1 - (1-\alpha) w_{\text{ref}}^{\frac{1}{(1-\alpha)s}} \left(\frac{\alpha}{\tau}\right)^{\frac{\alpha}{1-\alpha}} = f_2(\tau) \tag{3.10}$$

Since these expressions are algebraic rearrangements of Equation 3.8, τ_1 and τ_2 are also the solutions to Equations 3.9 and 3.10. We now use these expressions to construct an algorithm to find τ_1 and τ_2. Our approach is to start with an initial guess for the solutions and iterate through Equations 3.9 and 3.10 repeatedly.

If we use Equation 3.9 to define a discrete dynamical system, τ_1 and τ_2 correspond to fixed points, where the fixed point corresponding to τ_1 will be stable and the one corresponding to τ_2 will be unstable (see Figure 3.2). Likewise, for the dynamical system defined by Equation 3.10, τ_1 and τ_2 correspond to fixed points, where τ_1 will be unstable and τ_2 will be stable (see Figure 3.2). For a proof of the stability of these fixed points please see the appendix.

As such, we can construct an algorithm for numerically approximating the solution to the equation $w(\tau) = w_{\text{ref}}$ to some tolerance $\epsilon > 0$, starting from an initial guess $(\tau_1^{(0)}, \tau_2^{(0)})$ as follows:

$\tau_1 \leftarrow \tau_1^{(0)}$
while $|f_1(\tau_1) - \tau_1| > \epsilon$ **do**
    $\tau_1 \leftarrow \mathrm{f}_1(\tau_1)$
$\tau_2 \leftarrow \tau_2^{(0)}$
while $|f_2(\tau_2) - \tau_2| > \epsilon$ **do**
    $\tau_2 \leftarrow f_2(\tau_2)$

The obtained nondimensional temperatures (τ_1, τ_2) can then be checked to satisfy the equation $w(\tau) = w_{\text{ref}}$, and put back in the original scale through the transformations $T_1 = T_{\min} + (T_{\max} - T_{\min})\tau_1$ and $T_2 = T_{\min} + (T_{\max} - T_{\min})\tau_2$. For the computation of the half-

maximum growth temperatures, where $w_{\text{ref}} = \frac{1}{2}$, a simple choice for the initial values that seems to work well in practice is $\tau_1^{(0)} = \frac{\alpha}{2}$ and $\tau_2^{(0)} = \frac{3\alpha}{2}$.

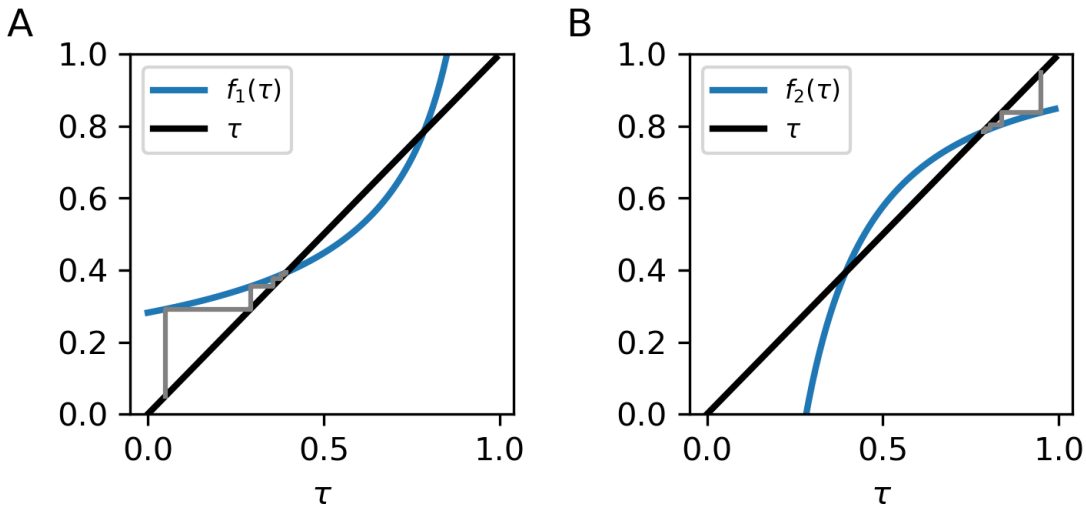

Figure 3.2: *Fixed point iteration algorithm to find half-maximum temperatures.* By construction, the intersection of the functions $f_1(\tau), f_2(\tau)$ with the identity line will occur at τ_1, τ_2, the nondimensional temperatures for which $w(\tau) = w_{\text{ref}} \in (0, 1)$. We can find these intersection points by iterating from an initial guess and applying f_1 and f_2 iteratively, treating these equations as discrete dynamical systems for which τ_1, τ_2 are fixed points. A: We show a plot of $f_1(\tau)$, which can be used to estimate τ_1 numerically, since τ_1 is a stable fixed point of f_1 and τ_2 an unstable fixed point. B: We show a plot of $f_2(\tau)$, which can be used to estimate τ_2 numerically, since τ_2 is a stable fixed point of f_2 and τ_1 an unstable fixed point.

3.3 Discussion

In this chapter, we modify the Briere model for temperature response curves to develop a flexible mathematical model to describe temperature response curves that is parametrized in terms of biologically meaningful quantities. We present various forms of this model that are useful for different purposes. A nondimensionalized version of the model with only two

parameters is best suited for theoretical work. We use this form of the model to develop an algorithm to obtain the half-maximum growth temperatures.

We also present two alternate parametrizations of the model that are useful for parameter inference. They differ on whether the optimal temperature is a parameter of the model in dimensional (T_{opt}) or dimensionless (α) form. Having the optimal temperature in dimensional form in the model allows for obtaining confidence intervals for T_{opt} when estimating the parameters through nonlinear least squares using standard statistical software, as is common in practice. In contrast, having the optimal temperature in dimensionless form α is convenient for Bayesian parameter inference, since $\alpha \in [0, 1]$ which allows setting a prior distribution with support over this interval.

We use the modified Briere model in practice to infer the optimal temperature and temperature niche of *E. coli* in the presence of antibiotics in Chapter 4 of this dissertation. This application requires a flexible model due to the very different curve shapes that are found in practice in this dataset. In future work, we will apply our model to other datasets and criteria to compare it to other models in the literature for common applications such as describing insect developmental rates. In doing so, we will evaluate the parameter ranges that occur most often in practice in common applications. This may make it possible to suggest a standard value for some parameters in the model, which may be helpful for applied scientists when the data available is scarce and a lower-dimensional model is needed and for setting prior distributions when taking a Bayesian approach to parameter inference. Future work could also focus on obtaining an approximate analytic expression for the half-maximum temperatures through asymptotic theory as an alternative to the fixed point algorithm presented here.

3.4 Appendix

Let $\alpha, w_{\text{ref}} \in (0, 1)$.

Lemma 1. *The function $w(\tau)$ increases monotonically for $\tau \in (0, \alpha)$ and decreases monotonically for $\tau \in (\alpha, 1)$.*

Proof. We have $\frac{dw}{d\tau} = w(\tau)\frac{d\log w}{d\tau} = sw(\tau)\left[\frac{\alpha}{\tau} - \frac{1-\alpha}{1-\tau}\right]$. If $\tau < \alpha$, then $\frac{dw}{d\tau} > 0$, so $w(\tau)$ increases monotonically in the interval $(0, \alpha)$. If $\tau > \alpha$, then $\frac{dw}{d\tau} < 0$, so $w(\tau)$ decreases monotonically in the interval $(\alpha, 1)$. □

Statement 1. *Let τ_1 and τ_2, with $\tau_1 < \tau_2$, be the solutions to the equation $w(\tau) = w_{ref}$, where $w(\tau)$ is the nondimensionalized modified Briere model (Equation 3.4) with domain $\tau \in (0, 1)$. For the discrete-time dynamical system $x_{n+1} = f_1(x_n)$, $x = \tau_1$ is a stable fixed point and $x = \tau_2$ is an unstable fixed point. For the system $x_{n+1} = f_2(x_n)$, τ_1 is an unstable fixed point and τ_2 is a stable fixed point.*

Proof. By Lemma 1, the function $w(\tau)$ increases monotonically in the interval $(0, \alpha)$ and decreases monotonically in the interval $(\alpha, 1)$. Since $w(\tau)$ has its only maximum at $\tau = \alpha$, it must be the case that $\tau_1 < \alpha < \tau_2$.

A well known result for one-dimensional discrete dynamical systems is that for a system $x_{n+1} = f(x_n)$, a fixed point x^* is stable if $|f'(x^*)| < 1$ and unstable if $|f'(x^*)| > 1$. Here we use this result to prove the stability of the fixed points of f_1 and f_2, respectively.

For notational simplicity, define $C_1 = \alpha w_{\text{ref}}^{\frac{1}{\alpha s}}(1-\alpha)^{\frac{1-\alpha}{\alpha}}$ and $m_1 = \frac{\alpha-1}{\alpha}$. Substituting, we can write $f_1(\tau) = C_1(1-\tau)^{m_1}$. Likewise, define $C_2 = (1-\alpha)w_{\text{ref}}^{\frac{1}{(1-\alpha)s}}\alpha^{\frac{\alpha}{1-\alpha}}$ and $m_2 = \frac{-\alpha}{1-\alpha}$ to write $f_2(\tau) = 1 - C_2\tau^{m_2}$.

By construction, τ_1 and τ_2 are fixed points of the equations $x_{n+1} = f_1(x_n)$ and $x_{n+1} = f_2(x_n)$ because these are algebraic rearrangements of Equation 3.4 with $w(\tau) = w_{\text{ref}}$. Thus, if x^* is either τ_1 or τ_2, we have $f_1(x^*) = x^*$ and $f_2(x^*) = x^*$. Specifically, we will have

$$
\begin{aligned}
f_1(x) &= C_1(1-x)^{m_1} \\
f_1'(x) &= -C_1 m_1 (1-x)^{m_1-1} \\
&= \frac{m_1}{1-x} f_1(x) \\
f_1'(x^*) &= -\frac{m_1}{1-x^*} x^*
\end{aligned}
$$

and

$$
\begin{aligned}
f_2(x) &= 1 - C_2 x^{m_2} \\
f_2'(x) &= -C_2 m_2 x^{m_2-1} \\
&= \frac{m_2}{x}(f_2(x) - 1) \\
f_2'(x^*) &= \frac{m_2}{x^*}(x^* - 1)
\end{aligned}
$$

Therefore, a fixed point x^* of f_1 will be stable if $|-\frac{m_1}{1-x^*}x^*| = \frac{1-\alpha}{\alpha}\frac{x^*}{1-x^*} < 1$, which implies $x^* < \alpha$. The same calculation with a greater than sign shows that x^* will be unstable when $x^* > \alpha$.

Since $\tau_1 < \alpha < \tau_2$, this implies τ_1 is a stable fixed point of f_1 and τ_2 an unstable fixed point for any $w_{\text{ref}} \in (0,1)$. Similarly, a fixed point x^* of f_2 will be stable if $|\frac{m_2}{x^*}(x^* - 1)| = \frac{\alpha}{1-\alpha}\frac{1-x}{x} < 1$, which implies $x^* > \alpha$. Repeating the calculation with a greater than sign shows that x^* will be unstable when $x^* < \alpha$. Thus τ_1 is an unstable fixed point, and τ_2 a stable fixed point of f_2 for any $w_{\text{ref}} \in (0,1)$.

□

CHAPTER 4

Antibiotics shift the temperature response of *Escherichia coli* growth

Note: The contents of this chapter is based on an article published in mSystems [CTK21a].

Temperature variation—through time and across climatic gradients—affects individuals, populations, and communities. Yet how the thermal response of biological systems is altered by environmental stressors is poorly understood. Here, we quantify two key features—optimal temperature and temperature breadth—to investigate how temperature responses vary in the presence of antibiotics. We use high-throughput screening to measure growth of *Escherichia coli* under single and pairwise combinations of 12 antibiotics across seven temperatures that range from 22°C to 46°C. We find that antibiotic stress often results in considerable changes in the optimal temperature for growth and a narrower temperature breadth. The direction of the optimal temperature shifts can be explained by the similarities between antibiotic-induced and temperature-induced damage to the physiology of the bacterium. We also find that the effects of pairs of stressors in the temperature response can often be explained by just one antibiotic out of the pair. Our study has implications for a general understanding of how ecological systems adapt and evolve to environmental changes.

4.1 Introduction

Many environments experience daily and seasonal temperature fluctuations that affect rates of physiological processes. These changes in turn affect biological and ecological traits and

ultimately impact the behavior of communities [CR54, HK89, LG87, FSS16, Som10, OMS08, Ben80, SGB04, Ali70, ACU17]. In this manner temperature fluctuations can drive the evolution of organisms through variation in thermal sensitivity—the ability to function and survive at different temperatures [HK89, PYB16, Par06, BRI02, BH16, Ang09, ABG06].

Measuring the growth of a living organism at different temperatures yields a temperature response curve (Figure 4.1a). Typically, temperature response curves have a single peak, corresponding to an optimal temperature where growth is maximized [HK89]. As the temperature changes away from the optimum in either direction, the growth rate decreases, with an especially steep decline at higher temperatures. The range of temperatures in which an organism can grow to a certain extent (e.g., at least half of the maximum growth) is termed the temperature breadth. Living organisms are said to experience either cold or heat stress at extreme temperatures where growth is substantially less than optimum.

Thermal response curves are fundamental to grasping the variability of physiological and ecological traits in response to temperature changes in different taxonomic groups and habitats. Because shifts in the thermal response curves are representative of average fitness performance and temporal niches [GBL13], optimal temperature and thermal breadth are indicative of evolution and acclimation patterns based on how species' performance contributes to survivorship or fecundity [Ang09]. For instance, seasonal variation in temperature could lead to an evolution of different attack and escape speeds that would allow individuals to perform best when they are predator or prey [DPS11]. Another example is given by the *Micromonas* genus of marine phytoplankton, where niche partitioning has been observed, with various thermal responses according to their geographic location [DBM19].

At a cellular level the performance of an organism across different temperatures can lead to various genetic and physiological adaptation mechanisms. For example, in bacteria thermal sensitivity is related to many physiological and genetic modulations in metabolism, including outer membrane rigidity [RS80, MCA04], chemotaxis [MIS76, PJZ17], enzymatic thermostability [TTC04, LMH86], and other general adaptive responses [CFM18, RHB10].

Moreover, the heat shock response—a cellular mechanism to deal with the deleterious effects of high temperatures, such as protein misfolding and aggregation—is highly conserved in both prokaryotes and [RHB10, MB05]. Understanding responses to temperature changes is important to infer general patterns of how organisms, species, communities, and ecosystems are adapting to fluctuations in climate patterns and different environmental conditions.

Any environmental feature that kills a living organism or reduces its growth can be considered a stressor. Temperature can interact with other environmental stressors such as light, precipitation, pH, and salinity. Exposure to different stressor types and intensities can lead to phenotypic variation in an organism's ability to respond to temperature changes [RSW11, TAK17]. Nevertheless, how the effects of environmental stressors interact with temperature responses is not well understood. Therefore, insights on whether temperature responses—as described by optimal temperatures and temperature breadths—can change rapidly and plastically in the presence of other environmental stressors have been lacking. In fact, it has been commonly assumed that thermal responses are not altered in the presence of other stressors [MH08, DTH08, AS12].

A systematic approach that informs how optimal temperatures and temperature breadths are shifted by stressors (Figure 4.1) is needed to uncover these ambiguities and provide additional insights on fitness tradeoffs and thermal adaptation strategies. Here, we use a combined empirical-theoretical approach to study if the characteristics of thermal response curves change in response to additional environmental stressors. In particular, we use an experimental system of *Escherichia coli* and antibiotics as stressors in order to investigate how a physiological trait—growth of the bacterium—responds to variation in temperature in the presence of different stressor conditions. We obtain temperature response data for *E. coli* in 12 single-drug and 66 two-drug combination environments, where antibiotics are chosen to cover a wide range of mechanisms of action (Table 1). We then quantify both the optimal temperature and the temperature breadth of *E. coli* in the presence of these different environments.

Antibiotic	*Abbreviation*	*Color*	*Mechanism of Action*	*Dose (μg/mL)*	*Temperature similarity*
Ampicillin	AMP		cell wall synthesis inhibitor	1.2	None
Cefoxitin	FOX		cell wall synthesis inhibitor	1.2	None
Levofloxacin	LVX		fluoroquinolone, DNA gyrase inhibitor	0.01	cold (22-37°C)
Ciprofloxacin	CPR		fluoroquinolone, DNA gyrase inhibitor	0.005	cold (22-37°C)
Nitrofurantoin	NTR		DNA damaging, multiple mechanisms	2	hot (44°C)
Trimethoprim	TMP		folic acid synthesis inhibitor	0.1	hot (44°C)
Tobramycin	TOB		aminoglycoside	1.5	very hot (46°C)
Gentamycin	GEN		aminoglycoside	1	very hot (46°C)
Streptomycin	STR		aminoglycoside	2	very hot (46°C)
Clindamycin	CLI		protein synthesis inhibitor, 50S	40	very cold (22-25°C)
Erythromycin	ERY		protein synthesis inhibitor, 50S	50	very cold (22-25°C)
Tetracycline	TET		protein synthesis inhibitor, 30S	0.25	cold (22-37°C)

Table 4.1: Antibiotics and doses used for the temperature curve experiments.

We first show that individual stressors can have a substantial impact on the optimal temperature and temperature breadth. Next, we evaluate if the directions of the shifted thermal responses are related to the mechanism of action of the antibiotics. Previously, we determined that some specific classes of antibiotics have similar physiological effects as either heat or cold stress in E. coli [CKL19]. This classification was based on comparing the experimentally determined interaction profile (synergies and antagonisms with other stressors) of antibiotics and various growth temperatures (Table 4.1). We find that in most cases the direction of the shifts in the thermal responses under antibiotic stress can be explained through these groups. Lastly, we investigate how pairs of stressors move optimal temperatures in different directions compared to the optimal temperatures under single-stressor conditions. In particular, we evaluate the extent to which the optimal temperatures

result from integrated effects of both stressors, or whether a single stressor is the key driver of the temperature response. We infer from our results that a single drug often plays a dominant role in determining the optimal temperature response of a combined treatment.

Our experimental and theoretical framework on temperature response curves of *E. coli* presented here allows us to better understand how thermal sensitivities change in response to stressors. Therefore, our analysis will shed light on fundamental features shaping the ecological and evolutionary responses of organisms facing complex environmental conditions. By using antibiotics as stressors and a bacterium as a model organism, our study system is particularly valuable for its experimental tractability and reproducibility.

4.2 Materials and Methods

Experimental framework

The experiments for determining *E. coli* growth in the presence of antibiotics and temperatures were done under the same procedures as detailed in Chapter 2.

To explore the effects of antibiotic concentration on the temperature curves, additional growth experiments were performed for a representative cold-similar (ERY) and heat-similar (TMP) antibiotic (Figures 4.4 and 4.5). For these experiments, ten antibiotic concentrations were chosen as a linear gradient ranging from the absence of drug to a near-inhibitory drug concentration (ERY, 1,000 μg/μL; TMP, 0.14 μg/μL) in order to clearly see changes in the shape of the temperature response. Four replicates of each antibiotic concentration were incubated at each of 14 temperatures, ranging from 18°C to 50°C.

Mathematical framework

Modified Briere model for characterizing temperature response curves

To infer the optimal temperature for growth and other parameters from our data on *E. coli* growth in the presence and absence of antibiotics, we fit the modified Briere model (developed in Chapter 3)

$$g(T) = g_{\max}\left[\left(\frac{T - T_{\min}}{\alpha}\right)^{\alpha}\left(\frac{T_{\max} - T}{1-\alpha}\right)^{1-\alpha}\left(\frac{1}{T_{\max} - T_{\min}}\right)\right]^{s}$$

where $T_{\min}$ and $T_{\max}$ are the minimum and maximum temperatures for growth. The parameter α is a rescaled optimal temperature, from which the unscaled optimal growth temperature can be obtained through the equation $T_{\text{opt}} = \alpha T_{\max} + (1-\alpha)T_{\min}$. The parameter $g_{\max}$ is the maximum growth, which is attained when $T = T_{\text{opt}}$.

Bayesian parameter estimation

The modified Briere model was fitted to the temperature growth curve for the bacterium under all conditions through a Bayesian methodology with the PyMC3 library of the Python programming language [SWF16].

Denote the parameters of the extended Briere model as $\mathcal{P} = \{g_{\max}, T_{\min}, T_{\max}, \alpha, s\}$. In order to do parameter inference, we took a Bayesian approach. We first extend the deterministic modified Briere model to an explicit statistical model.

Denote the ith observed data point for growth after 24 hours as y_i, and let T_i be the temperature at which it was observed. We model the data as a nonlinear regression, with

$$y_i|\mathcal{P}, \sigma_{Ti}, T_i \sim \text{Gamma}(\mu = g(T_i; \mathcal{P}), \sigma = \sigma_{T_i})$$

(where a Gamma distribution was chosen since growth is strictly positive). Note that the Gamma distribution is parametrized in terms of the mean and standard deviation. The mean of the distribution $g(T_i : \mathcal{P})$ corresponds to the deterministic modified Briere model

with parameters P. A different set of parameters was fit for each condition (antibiotic or antibiotic combination).

The observed standard deviation was clearly different across temperatures. However, there was no clear trend as a function of T_i or y_i that was consistent across the different growth conditions. We took a hierarchical approach to model the standard deviation

$$\gamma_{T_i}|\beta \sim \text{halfCauchy}(\beta)$$
$$\beta \sim \text{halfCauchy}(0.3)$$

The halfCauchy family is a common choice for variance parameters in hierarchical models, as recommended by [Gel06]. According to these recommendations, the scale parameter for the halfCauchy was chosen to be a plausible, but high, value for a standard deviation. The purpose for this weakly informative prior is to not have much effect in the parameter inference in the region of plausible values of the standard deviations (values around 0.3 or smaller), but for it to rule out implausible values that are much higher (which can cause problems when using uniform priors). The optical density data ranges roughly from 0 to 1, so this is a conservative upper bound.

The following weakly informative priors were used for the temperatures $T_{\min}$ and $T_{\max}$:

$$T_{\min} \sim \text{Normal}(\mu = 12.5°\text{C}, \sigma = 12.5°\text{C})$$
$$T_{\max} \sim \text{Normal}(\mu = 47°\text{C}, \sigma = 7.5°\text{C})$$

While these priors are informative, these choices are quite conservative in a biological sense. They correspond to a prior belief that the minimum temperature for growth of *E. coli* (under the experimental conditions) is 95% likely to be in the interval $[-12.5°\text{C}, 37.5°\text{C}]$ and that the maximum temperature for growth of is 95% likely to be in the interval $[32°\text{C}, 62°\text{C}]$. From previous experiments, it is known that the optimal temperature for *E. coli* growth is

around 37°C and that no growth is observed past approximately 46°C to 50°C [SSM81]. The means and standard deviations for the normal priors were chosen to be consistent with these previous experiments.

By definition, the rescaled optimal temperature α is constrained to the interval $0 \leq \alpha \leq 1$. For simplicity, the same prior distribution for the parameters were used for all conditions. In order to not put a higher prior belief in left-skewed or right-skewed curves, the prior distribution for this parameter was chosen as

$$\alpha \sim \text{Uniform}(0, 1)$$

From previous experiments using the same equipment to measure optical density of *E. coli* cultures, it is known that the optical density of cultures is almost always less than 1. This informed the upper bound of the prior for the maximum growth $g_{\max}$.

$$g_{\max} \sim \text{Uniform}(0, 1)$$

Lastly, the prior distribution for s was chosen to be weakly informative, placing weak constraints in $s = a + b$ to be small by penalizing very large values of s.

$$s \sim \text{halfCauchy}(20)$$

This prior can be thought as a form of regularization, with the goal of preventing overfitting. It corresponds to a prior belief that smoother curves should be preferred if possible (where the growth changes smoothly, rather than abruptly, with temperature). This gives smaller prior probability to curves where there are very abrupt changes in growth with small changes in temperature. Here, we took $s = 20$ to be a plausible, but high value of the parameter.

Data availability

The data and code used in this paper are available in the Dryad Digital Repository [CTK21b].

4.3 Results

In this chapter we explore how different stressors (antibiotics) alter an organism's response to temperature, both in isolation and in combination. To do this, we determine the temperature optimum and temperature niche/breadth of *E. coli* by fitting the modified Briere model (developed in Chapter 3) to experimental data of bacterial growth collected under different (unstressed and stressed) growth environments across seven temperatures (22°C, 25°C, 30°C, 37°C, 41°C, 44°C, and 46°C). The entire data set and model fits are shown in Figure 4.2.

First, we explore how the optimal growth temperature of *E. coli* changes under single-stressor conditions (Figure 4.1a and b). We find that the majority of the single-drug environments exhibit left shifts—meaning the optimal temperature (T_{opt}) is lower (Figure 1c)—compared to the no-drug condition, $T_{\text{opt}} = 37.7$°C, 95% credible interval (CI) (36.7°C, 38.6°C). Right shifts are both less common and of lower magnitude than the observed left shifts. In addition, we find that the thermal niche breadth typically becomes narrower under antibiotic stress, meaning that *E. coli* can survive and properly function at a reduced temperature range.

Next, we investigate whether the physiological effects of antibiotics bear any relation to the direction of the observed shifts in the temperature responses (Figure 4.3). To do this, we group the antibiotics according to the similarity of their physiological effects to those of low or high temperatures, as determined previously [CKL19]. We observe the direction of the shifts for both single drugs (Figure 4.3a, left panels) and drug combinations that contain one or more of the antibiotics in the group (Figure 4.3a, right panels). We find that —for both single drugs and combinations— cold-similar antibiotics (i.e., with effects on bacteria similar to those caused by low temperatures) tend to either leave the optimal temperature unchanged or shift it slightly to the right (i.e., to higher optimal temperatures). In contrast, heat-similar antibiotics (i.e., with effects on bacteria similar to those caused by high temperatures) tend to result in unchanged optimal temperatures or shifts to the left (i.e.,

to lower optimal temperatures). In fact, bacteria exposed to aminoglycosides (tobramycin [TOB], gentamicin [GEN], and streptomycin [STR]), which induce misfolding of membrane proteins and have similar physiological effects as very high temperatures (Figure 4.3), show the greatest shifts toward the left. This is not the case for other protein synthesis inhibitors such as erythromycin (ERY) or clindamycin (CLI) that are similar to cold. Interestingly, beta-lactams shift the temperature curves in a similar way as heat-similar drugs when used in combinations, despite them having a different mechanism of action (inhibition of cell wall synthesis) that was not found to be heat similar.

Furthermore, to evaluate the extent to which these changes are concentration dependent, we measure the growth of *E. coli* at 12 growth temperatures and increasing antibiotic concentrations (ranging from no antibiotic to near inhibitory) for two antibiotics: ERY and trimethoprim (TMP) (Figure 4.4 and 4.5). We find that growth decreases with increasing antibiotic concentration, but this decrease is not uniform at all temperatures. For both antibiotics, the growth decrease at temperature extremes is sharper than at the central part of the curve. However, for TMP (a heat-similar drug), growth at high temperatures decreases more sharply than at low temperatures. In contrast, for ERY (cold similar), growth decreases more sharply at low temperatures than at high temperatures. The observed shifts in optimal temperature seem to be due to this asymmetry in the growth decrease which causes the position of the central part of the curve to change. From these experiments, we conclude that both the magnitude of the optimal temperature shifts and the extent of the decrease in temperature breadth depend on the antibiotic concentration. However, the direction of the optimal temperature shifts seems to remain consistent when varying antibiotic concentrations.

We then compare the optimal temperature and temperature niche—the range between the temperatures that result in half-maximum growth—for bacteria under all antibiotic combinations to those under the single-drug conditions (Figure 4.3b). For some antibiotics (e.g., ERY and ciprofloxacin [CPR]), the optimal temperature and the thermal niche range

are similar to those of the single drug when combined with most other antibiotics. In contrast, there are other antibiotics for which these features show much more variation when combined with others (e.g., GEN, STR, TOB, and cefoxitin [FOX]). This suggests that some antibiotics may act as the main drivers of the temperature response curve of antibiotic combinations.

Following this idea, we further explored how the optimal growth temperature is determined under combinations of stressors relative to the optimal temperature under single-stressor conditions. We contrast the observed optimal temperatures with the predictions of five candidate models of how the combination optimal temperature could be determined from that of the single stressors (see Materials and Methods) (Figure 3a). The min and max models assume that the optimal temperature of the combination is determined by the optimal temperature of a single drug (the minimum or the maximum of the pair, respectively). These models best describe most (65%) multidrug combinations (Figure 3b). The attenuated and elevated models assume that the optimal temperature of the combination is either lower or higher, respectively, than for both single drugs. These models best describe 18% of the combinations. Lastly, the mean model assumes that the temperature of the combination is determined by the average of the single-drug optimal temperatures. This model best described only 17% of the drug combinations. These results suggest that the optimal temperature of antibiotic combinations is often determined by a single drug.

Finally, we explore cases where single-driver models (min, max, attenuated, and elevated) represent the best optimal temperature model over the mean model, where both stressors compromise to result in the optimal temperature of an organism in the presence of combined stressors (Figure 3c). Interestingly, we rarely observe aminoglycosides (GEN, STR, and TOB), antibiotics similar to high heat, being drivers. In contrast, some cold-similar drugs (ERY, LVX, CPR), but not all (CLI, TET), frequently drive the optimal temperature of the combination. To account for the possibility that some antibiotics appear to be a driver more often than others purely by chance, we used a permutation test to evaluate our data against the null model that all drugs are equally likely to be a driver (see D-statistic in Text

S1 for details). This test provides strong evidence ($P = 0.002$) that some antibiotics have a greater tendency to be drivers than others by testing the entire data set simultaneously. We also tested if specific antibiotics are drivers more often than expected by chance (see M-statistic in Text S1). However, we did not obtain statistically significant results for individual drugs, after correcting for multiple comparisons. We believe this may be due to a lack of statistical power to detect differences due to the smaller number of observations for individual antibiotics than for the full data set.

4.4 Discussion

Through a systematic analysis of growth response curves of bacteria across different temperatures and under different stressor environments, we investigate the effects of stressors on the phenotypic variation in temperature response traits—optimal temperature and temperature breadth. We see that stressors often decrease the temperature breadth and shift the optimal temperature in a direction that depends on their physiological mechanism of harm. In addition, our results suggest that left shifts—where the optimal temperature in a stressed environment is lower than the optimal temperature under unstressed environmental conditions—are more common and dramatic as opposed to right shifts toward higher optimal temperatures. This may be partially due to the asymmetry of temperature response curves, where the interval between the minimum and optimal growth temperatures is larger than that between the optimal and maximum growth temperatures.

High temperature harms living organisms through multiple mechanisms, including misfolding and aggregating proteins, damaging nucleic acids, and increasing membrane permeability [RHB10]. The heat shock response attempts to prevent and/or repair this damage by producing chaperones that aid the correct folding of proteins [VRH10]. It has previously been shown that certain kinds of antibiotics can activate components of the heat shock response [CKL19, VN90, CGW10]. Moreover, heat shock chaperones have been shown to help

combat aminoglycoside-induced protein misfolding [GGB13]. However, adding antibiotics to heat stress is unlikely to help the cell survive high temperatures, since the heat shock response is already induced by the high temperature alone. Thus, right shifts in the optimal temperature may be rare because it is unlikely that adding a second stressor can reduce or repair the high-temperature-induced damage. In most cases where we do observe a right shift, it seems to be due to asymmetrical effects on the temperature response curve, where the left portion (i.e., below the unstressed optimal temperature T_{opt}) is more depressed by the antibiotic than the right portion (Figure 4.3a; see also Figure 4.4 and 4.5).

In contrast, cold temperatures predominantly slow down cell growth by suppressing DNA replication or protein translation [HCB12, SPK13]. Since the effects of low temperature seem to be primarily mediated by slowing down metabolism and growth rather than the accumulation of physical damage, it seems more likely that stressors can shift the optimal temperature to the left, especially when the stressor is more harmful at higher temperatures. In some cases, cold temperatures might allow cells to sustain antibiotic killing because certain antibiotics are effective against only actively growing cells [Lew07]. Low temperatures have also been shown to alter the structural stability [MUT14] or the global uptake of some antibiotics such as gentamicin, thus impairing killing efficiency [LHK16].

Antibiotics damage bacteria through various mechanisms of action, such as interfering with cell wall synthesis [BB16], binding the ribosome to either inhibit protein translation or increase the translational error rate [LZS18], and modifying DNA supercoiling [LeB88]. Based on network clustering methods [YTK06, SDC05], we previously found that certain antibiotic classes have similar physiological effects as either heat or cold in *E. coli* [CKL19]. These temperature-drug groups were shown to correlate with changes in drug sensitivity of high-temperature-adapted strains obtained by Rodríguez-Verdugo et al. [RGT13] and are consistent with previous work comparing the protein expression profile of *E. coli* under various antibiotics with that induced under heat shock and cold shock [VN90]. Interestingly, here we find that in most cases the direction of the shifts in the optimal temperature can be

predicted from these groups. Cold-similar drugs tend either to leave the optimal temperature unchanged or to shift it slightly to the right. In contrast, heat-similar drugs tend to result in larger shifts to the left or leave the optimal temperature unchanged (Figure 4.3). Similar trends are exhibited by antibiotic combinations containing drugs in these groups.

We propose a shared-damage hypothesis to explain this phenomenon: antibiotics that damage the same cellular functions as those damaged by temperature stress (heat or cold) will cause an increased burden to the cell machinery that repairs this damage. For example, simultaneous exposure to aminoglycosides and high temperatures will result in more misfolded proteins than either stressor on its own. Upon addition of an antibiotic, the stress-response machinery of the cell could be overwhelmed at less extreme temperatures, causing a greater reduction in growth at temperatures that cause similar physiological damage to the drug. The effect of these kinds of antibiotics in the temperature response curve will thus be asymmetrical. Growth will be more strongly reduced in the direction (heat or cold relative to T_{opt}) where the drug and temperature damage overlap, and the optimal temperature will often shift toward the opposite direction because it suffers less from growth reduction. In terms of stressor interactions based on the Bliss independence framework, the shared-damage hypothesis implies that stressors (e.g., antibiotics and temperatures) with overlapping damage mechanisms will tend to interact synergistically, decreasing growth more than what would be expected given the effects of the individual stressors (Figure 4.7).

The most pronounced shifts in optimal temperature tend to occur in cases with lower peak growth (Figure 4.3a). This suggests that perhaps these shifts become more pronounced when increasing antibiotic concentration, as we see for ERY and TMP (Figure 4.4 and 4.5). However, when evaluated across all antibiotic backgrounds in our study, maximum growth is uncorrelated with the magnitude of the optimal temperature shifts (Figure S6). Our results suggest that not all antibiotics elicit optimal temperature shifts, but for those that do, the magnitude of shifts is concentration dependent. We hypothesize that increasing the concentration of heat-similar drugs will result in greater shifts to the left and that doing so

for cold-similar drugs will result in greater shifts to the right.

Notably, although the aminoglycosides (TOB, GEN, and STR) share the same cellular target—the ribosome—as the other protein synthesis inhibitors (CLI, ERY, and TET) used in our study, they result in distinct effects on the thermal response. Previously, differences in the effects of aminoglycosides and other protein synthesis inhibitors at different growth rates have been attributed to the reversibility of ribosomal binding [GSE15]. In that study, the authors found that STR is more effective when the growth rate is lower, which does not agree with our results at low temperatures. This discrepancy may be because the reduction in growth was previously manipulated by nutrient limitation as opposed to the temperature variation in our study.

Instead of binding reversibility, we could explain the different effects of these drugs by their mechanisms of action being qualitatively different, with the aminoglycosides being heat similar and the other protein synthesis inhibitors being cold similar. This is because aminoglycosides, unlike other protein synthesis inhibitors, induce mistranslation by the ribosome that decreases translational accuracy and causes protein misfolding [MGT99]. Cold temperatures may counteract this effect by slowing down ribosomal activity and increasing accuracy [VN90], thus causing aminoglycosides to be less effective when bacterial growth is suppressed at lower temperatures, as we observe. Reduced drug uptake at low temperatures could also play a role [LHK16].

Interestingly, beta-lactams have a similar effect in the temperature response as heat-similar drugs. We speculate that this may be due to increased effectiveness at high temperatures due to a synergy between the cell wall damage caused by the antibiotic and the increased membrane permeability caused by high temperatures. Further disentangling these processes in future studies will help increase our understanding of the connection between antibiotic susceptibility and bacterial physiology.

The breadth of the temperature niche is typically reduced in the presence of antibiotics, both in isolation and in combination. The molecular mechanisms involved in this reduction of

the temperature breadth by antibiotics have not yet been studied experimentally. However, in the absence of antibiotics the lower and upper limits of growth are believed to be set by chemical and physical limits on the biological processes necessary for bacterial physiology, growth, and cell division [HK89]. Since drugs introduce physiological damage in addition to that caused by temperature extremes, it seems likely that in most cases antibiotics would further constrain the temperature response by killing off barely surviving populations at the extreme temperatures. Previous studies have also observed the temperature niche being reduced upon exposure to stressors [OVS15, FDF10]. From our results it is apparent that stressors can reduce the temperature niche of living organisms at either temperature extreme. Thus, species that experience a wide range of stressful conditions at different times could perhaps experience selection for a broader temperature breadth that can be adapted to various environmental stressors [GBL13].

The temperature niche is measured as the range between the low and high temperatures for half-maximum growth: its definition is therefore relative to the maximum growth. Consequently, conditions that decrease the right and central portions of the curve (i.e., near T_{opt}) more than the left portion can result in a temperature niche that is shifted to the left (and vice versa) in the absence of increased growth at temperature extremes. These effects can lead to apparently surprising cases where adding a drug extends the limits for the thermal niche of the unstressed condition without increased growth at temperature extremes. This suggests that microbial communities may experience shifted thermal niches—giving rise to a different competitive landscape (e.g., due to reduced invasibility of high-temperature habitats under aminoglycosides)—in the presence of certain antibiotics. These effects could be particularly important in the presence of variation in adaptations to antibiotics within microbial communities, which might cause the severity of their effects on the temperature curves to be species dependent. We expect antibiotics to change the competitive landscape the most in mixed populations with both antibiotic-resistant and nonresistant microbes, since the latter would be expected to show larger antibiotic-induced changes in the thermal

response than the former under the shared-damage hypothesis.

We find that in most cases the shift in optimal temperature of *E. coli* due to antibiotic pairs is primarily determined by a single antibiotic. However, we also found cases where interactions between antibiotics seem to be important for determining the optimal temperature. For example, aminoglycosides (TOB, GEN, and STR) show the largest degree of downshifting of the optimal temperature. However, when a second drug is added, this downshifting tends to be alleviated. Thus, in combinations of stressors, aminoglycosides are not the dominant driver for changing optimal temperature despite their large effects when used alone. When a shift in the thermal optimum is alleviated by addition of a second antibiotic, this does not imply that the reduced growth is also alleviated. Typically, these shifts are due to the second antibiotic decreasing some regions of the temperature response curve more sharply than others (Figure 4.2). A notable exception involves interactions between certain aminoglycosides (GEN and STR) and other protein synthesis inhibitors (ERY, TET, and other aminoglycosides), possibly because inhibition of protein synthesis reduces the aminoglycoside-induced production of misfolded protein aggregates.

The growth response to multiple environmental factors such as temperature, CO_2, and pH has been measured in green algae [BC15]. Under conditions with a large number of factors present simultaneously, the response is dominated by a single, severely detrimental driver. In contrast, in environments with a smaller number of factors, specific interactions between drivers were found to determine overall growth rather than the response to an overriding factor. These results were explained by the authors by the presence of a severely detrimental driver limiting the growth reduction that can be obtained by additional stressors, making the severe driver the primary determinant of the response. In contrast, we find that the effects of an antibiotic can sometimes be partially undone by another (e.g., aminoglycosides and other protein synthesis inhibitors). This suggests that, while identifying a dominant environmental driver can be a simplified approach to understanding organismal response to a complex system, this needs to be done with care since interactions between drivers can be

a contributing factor as well.

The thermal optimum is often below the mean environmental temperature. This is because thermal response curves typically decrease sharply at high temperatures, so the penalty of going above the optimal temperature is much steeper than going below. The exact distance between the thermal optimum and the mean is determined by the temperature variability in the environment [MH08, DTH08, AS12]. It is thus often tacitly assumed that the optimum temperature of individuals closely aligns with the environment in which the individual has been reared and/or the species has evolved. For this reason, the optimal temperature is not expected to quickly shift in response to other stressful conditions. This is a common assumption in mathematical models that describe the combined effects of temperature and other stressors such as pH [RLB95], nutrient limitation [KZE96], and humidity [PM04]. In contrast, we observe that stressors can substantially and quickly change the optimal temperature for growth of a bacterium. A study that evaluated the combined effects of temperature and salt in slime molds [COB97] also found shifts in the thermal optimum, suggesting that this phenomenon is not limited solely to antibiotics.

Any physical or chemical environmental feature that kills a living organism or slows its population growth can be considered a stressor. Antibiotics are stressors to bacteria in clinical settings, but they may not always take this role in nature. It has been proposed that some antibiotics may participate in communication or be by-products of metabolism in their natural environments [Mlo09, Mar08, DTP08]. Since we explain thermal optimum shifts through differences in growth reduction, our shared-damage hypothesis predicts antibiotic-induced thermal optimum shifts will occur when antibiotics are acting as stressors. However, this will not necessarily happen when antibiotics have a different role at much lower concentrations than those relevant in the clinic. In these cases, we would expect thermal optima to change only if there is a nonnegligible fitness decrease caused by the antibiotic. Further work could test this by measuring the effects of an antibiotic on the thermal responses of microbes that naturally occur in the same environments as the antibiotic.

An exciting potential application of the shared-damage hypothesis is in predicting the effect of other stressors on the thermal optima of living organisms. To do this, further studies are necessary to evaluate the extent to which the physiological damage caused by other environmental stressors—such as pressure and pH—is similar to either temperature stress or antibiotics. This can be done by comparing either the gene-expression profile or the interaction profile (i.e., synergies and antagonisms with other stressors) of the environmental stressor of interest with those of extreme temperatures and/or antibiotics, as has been done to explore the overlap between antibiotics and temperature [CKL19, VN90]. Our hypothesis would then predict that stressors that induce similar damage as high temperature will result in left shifts in T_{opt} (and vice versa). Moreover, the direction of the shift induced by a stressor should be the same as that of other stressors (e.g., antibiotics) that cause similar physiological damage. For example, beta-lactam antibiotics compromise the integrity of the bacterial cell wall, so we speculate that the induced damage to the cell could have certain similarities to osmotic shock. If this were true, it seems possible that osmotic shock might change the temperature responses in a similar way as beta-lactams.

Although there has been substantial interest in understanding thermal response curves because of their potential to predict responses to climate change [DPS11, DBM19, HK11, RCC18], the implications might be even broader. For example, an intriguing recent study showed that increased local temperatures were associated with increasing antibiotic resistance [MMF18]. This may be because temperature or seasonality affects environmental growth of resistant strains [GBN11, MMP11] and horizontal gene transfer—one method of facilitating resistance transmission [LW94, WWL11]. Another study showed that adaptations to long-term temperature changes unexpectedly coincided with mutations conferring resistance to rifampin, an antibiotic that impairs RNA polymerase [RGT13]. Climate change has also been linked to changes in host-parasite dynamics that alter the frequency and severity of many infectious diseases [MKH13, HMW02]. Our work here and elsewhere shows that certain classes of antibiotics are more effective at different temperatures and that there is

substantial overlap in the response mechanisms to temperature and some kinds of antibiotics [CKL19, VN90, GGB13, RLC20]. This suggests the hypothesis that climate change might favor the evolution of resistance to specific (i.e., heat-similar) antibiotics indirectly due to its overlap with resistance to high-temperature stress.

From our results it also appears that drugs can be used to modify temperature response curves in predictable ways. A temperature-drug system could perhaps be used to examine scenarios for biological responses to climate change via a variety of thermal responses in a laboratory setting. Going forward, such a system could serve as a simplified model for examining changes in response to temperature across seasons, geographic gradients, and climate change. Finally, it is worth nothing that exact estimates of the optimal temperature and temperature niche depend somewhat on the choice of mathematical model [**?**]. This is why the abilities of a model to provide a good fit to the data and have biologically interpretable parameters are important considerations in choosing an appropriate model [ACU17]. In order to fit the variety of shapes and skews we observe here for temperature responses, we developed a novel flexible temperature response model that is reparametrized in terms of biologically meaningful parameters (Chapter 3).

Temperature is one of the fundamental drivers of biological processes. By using antibiotics as stressors, our study system is particularly valuable for its tractability, reproducibility, and potential to study temperature-stressor interactions beyond the pairwise level. Our results provide insights into the interactions between temperature and other stressors. Particularly, we show that stressors can modify the temperature response curves of a living organism and that these changes can be predicted from the way the stressor harms its physiology. More broadly, our results imply that the chemical environment of a living organism—or potentially the presence of other stressors—can influence how it interacts with both abiotic (temperature) and biotic (modified competition due to changes in its thermal niche) factors. Investigating stressor effects on the physiological and ecological trait responses to temperature changes under this framework could lead to future research directions in exploring other

environmental stressors that may aid in predicting the stability and diversity of ecological systems.

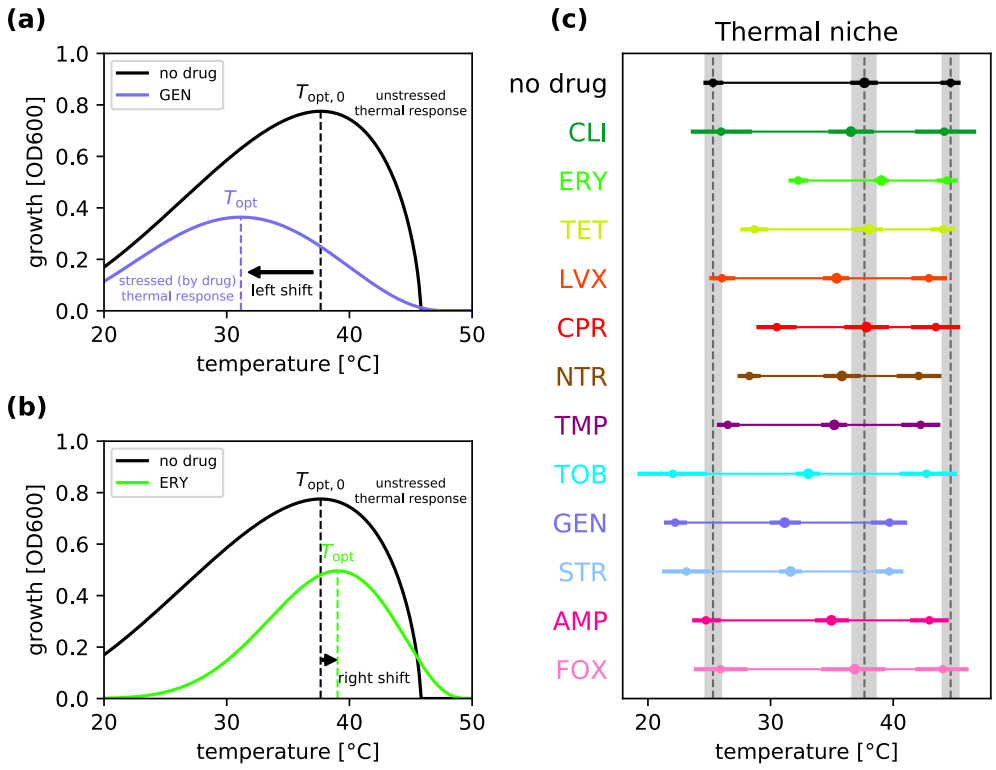

Figure 4.1: *Temperature response curves change under antibiotic stress.* (a) An example of a left shift of optimal temperature with antibiotic GEN. (b) An example of a right shift of optimal temperature with antibiotic ERY. (c) Optimal growth temperature (middle circle) and temperature niche (thin line joining the half-maximal growth temperatures, left and right circle) observed under each antibiotic used in this study. Point estimates for the optimal and half-maximal growth temperatures are shown as circles. To show the uncertainty in the estimates, 95% credible intervals (CIs; see Materials and Methods) are drawn as thick lines. The CIs for the no-drug condition are shaded in the plot to facilitate comparison.

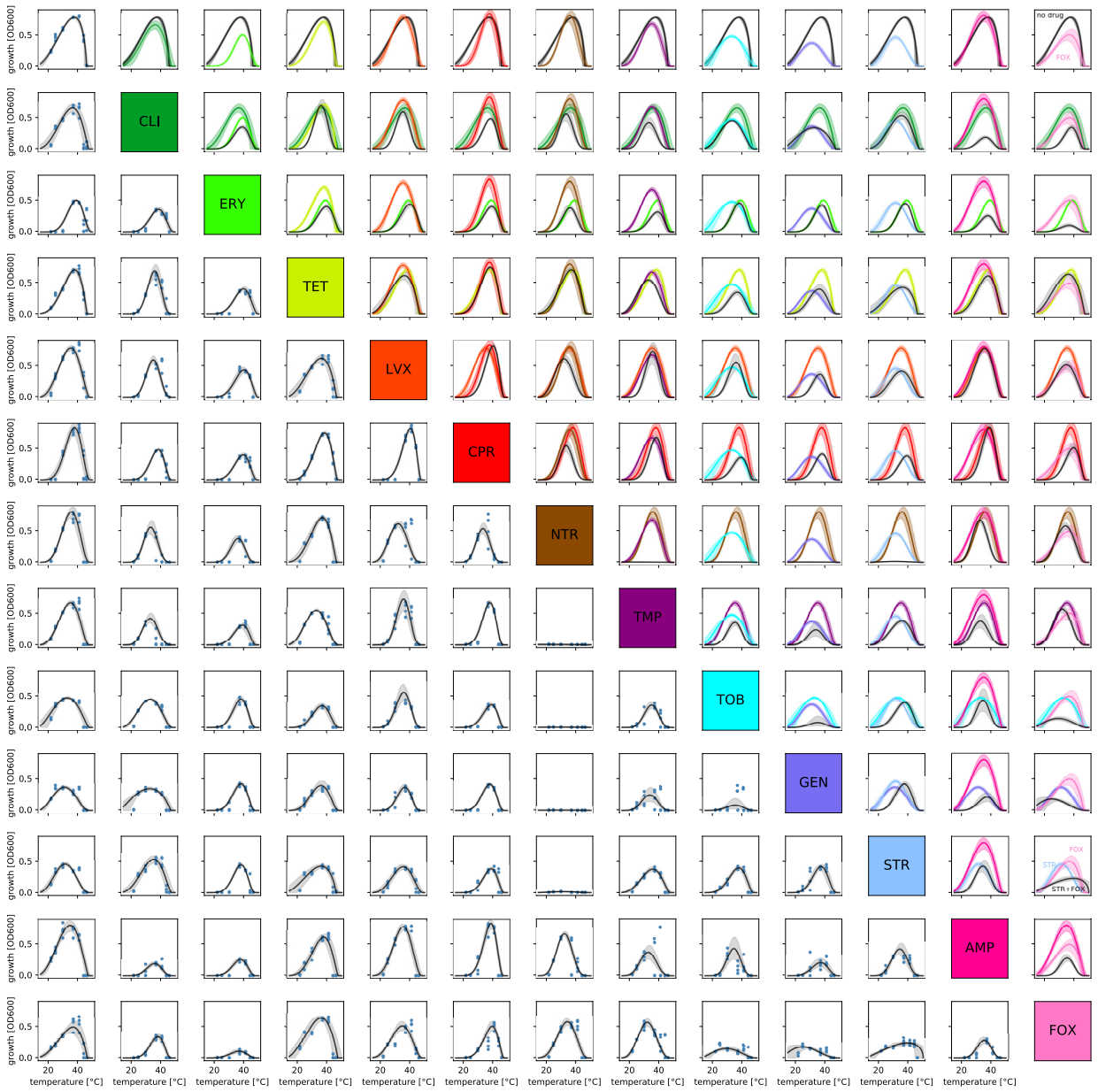

Figure 4.2: *Full data set and model fits.* (Lower half) The growth data for all antibiotic combinations (blue dots) and the fitted modified Briere model (black lines) are shown, as well as 95% credible intervals for the modified Briere model. The upper left corner corresponds to the no-drug case. (Upper half) The fitted curves corresponding to each drug combination are shown in black, and the fits corresponding to each single drug are shown in their corresponding color. In the uppermost row, the growth curve in the absence of antibiotics is shown in black and the single-drug curves are shown in the corresponding color. The entries corresponding to FOX and STR+FOX in the upper quadrant are labeled to aid interpretation.

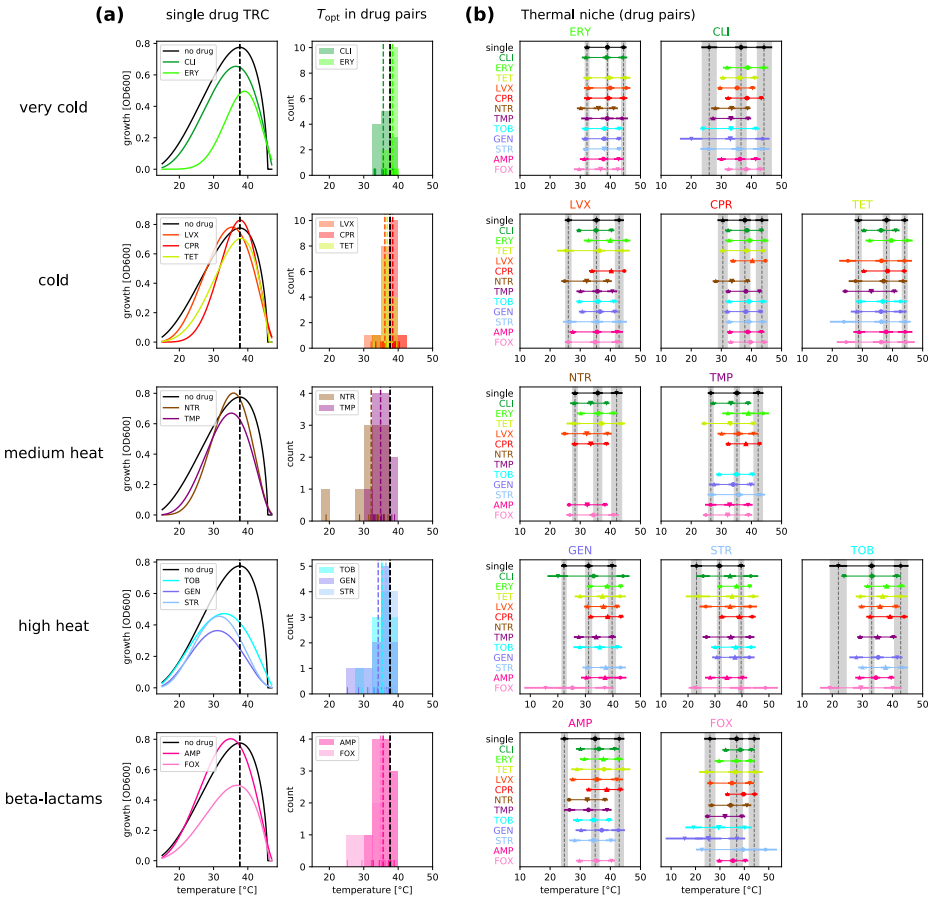

Figure 4.3: *Physiological effects of antibiotics predict the direction of shifts in the optimal temperature.* (a) (Left) The fitted temperature response curve (TRC) in the presence of single antibiotics is compared to the unstressed growth condition. Drugs are grouped according to the similarity of their effects to temperature. (Right) Histogram of shifts in the optimal temperature under all pairwise drug combinations involving the drugs in the group. The individual estimates are shown as short lines in the bottom. The mean of the optimal temperature estimates involving each drug (including combinations) is shown as a dashed colored line. The unstressed optimal temperature is shown as a black dashed line in both sets of plots. (b) Optimal growth temperature and temperature niche observed under each antibiotic combination used in this study. The first drug in the combination is shown at the top of the plot. The second drug is shown on the y-axis using its assigned line color. The single-drug conditions are shown with shaded 95% credible intervals to facilitate comparisons and the point estimates are marked as in Figure 4.1c. Conditions under which the maximum growth was too small to estimate parameters reliably were removed.

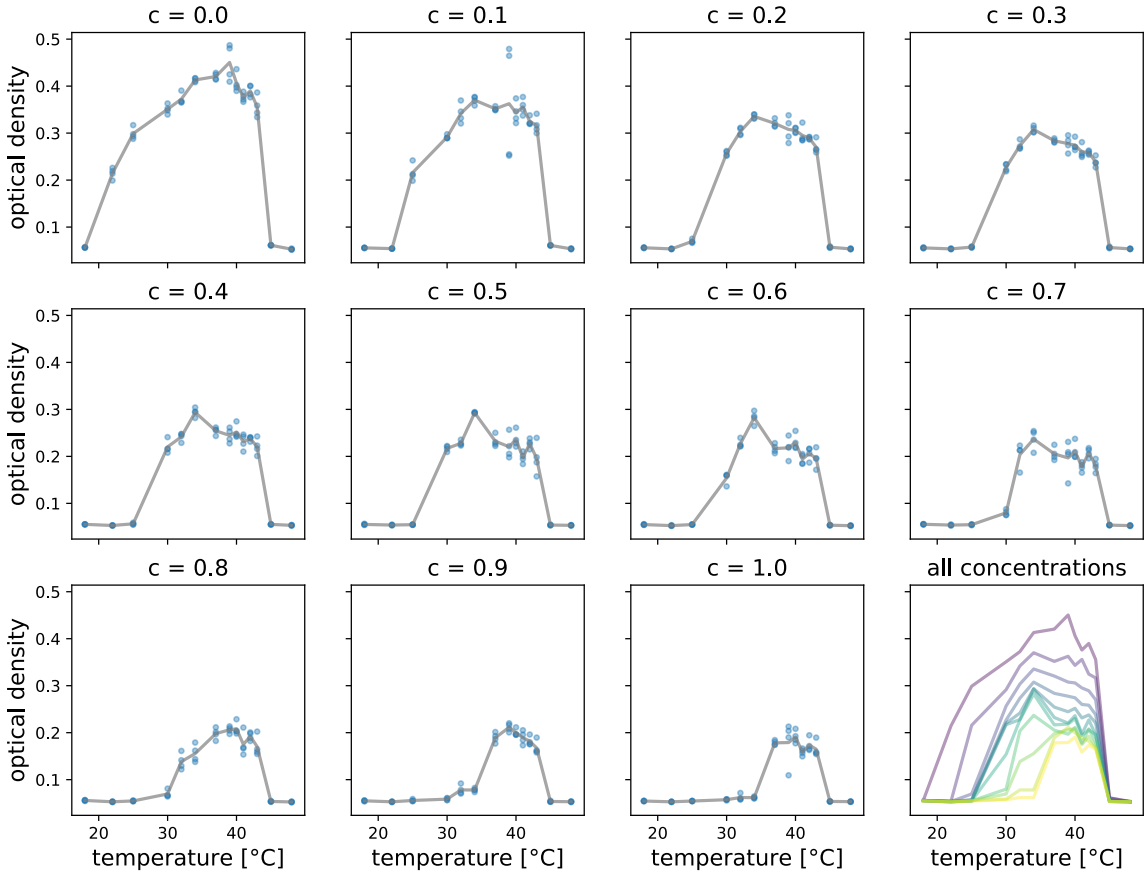

Figure 4.4: *Effects of increasing antibiotic concentration for erythromycin in the temperature response curve.* The temperature curves for *E. coli* under increasing ERY concentration c are shown. The concentrations c are shown as a proportion of the maximum concentration used (where $c = 1$ corresponds to 1000 μg/μl). The individual data points are shown as blue dots. The mean at each measured temperature is shown as a gray line in each panel. The curves for the mean growth for all concentrations are shown simultaneously in the bottom right panel. The curves are color coded from low (purple) to high (yellow) concentration.

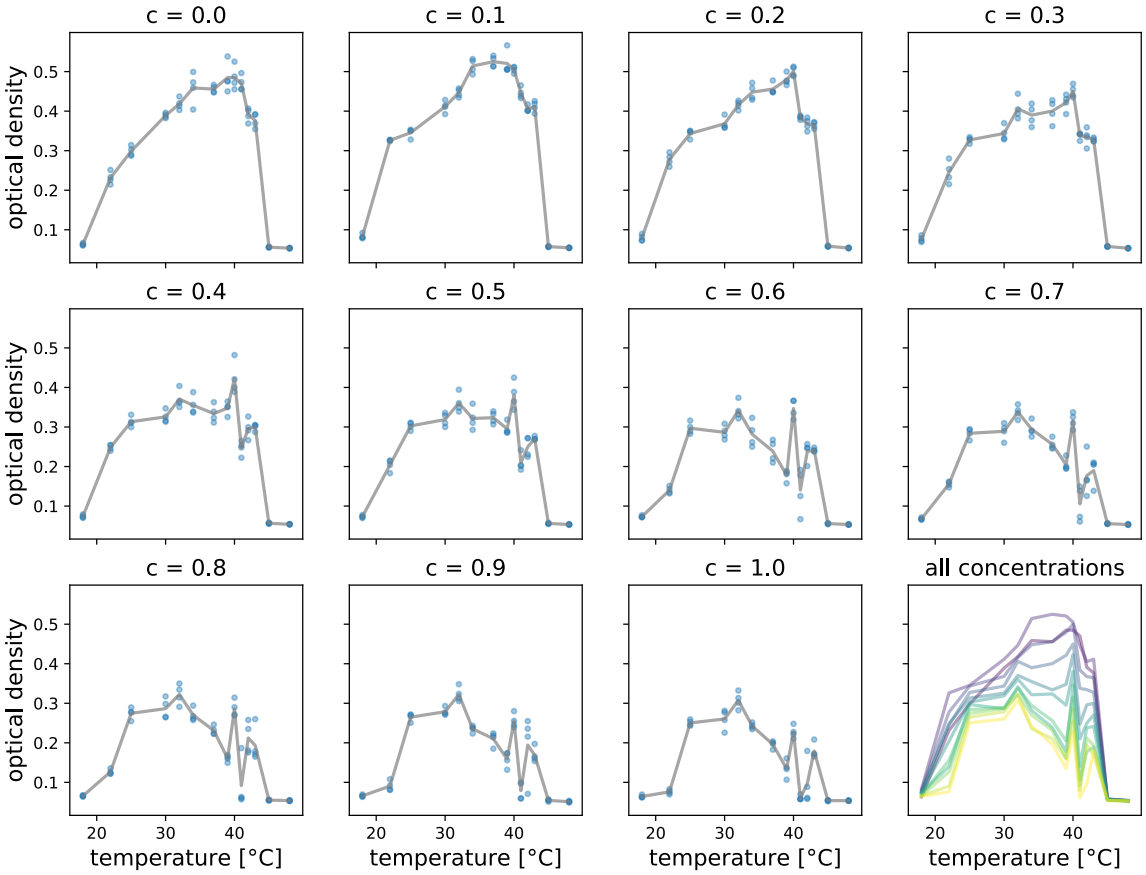

Figure 4.5: *Effects of increasing antibiotic concentration for trimethoprim in the temperature response curve.* The temperature curves for *E. coli* under increasing ERY concentration c are shown. The concentrations c are shown as a proportion of the maximum concentration used (where $c = 1$ corresponds to 0.14 μg/μl). The individual data points are shown as blue dots. The mean at each measured temperature is shown as a gray line in each panel. The curves for the mean growth for all concentrations are shown simultaneously in the bottom right panel. The curves are color coded from low (purple) to high (yellow) concentration.

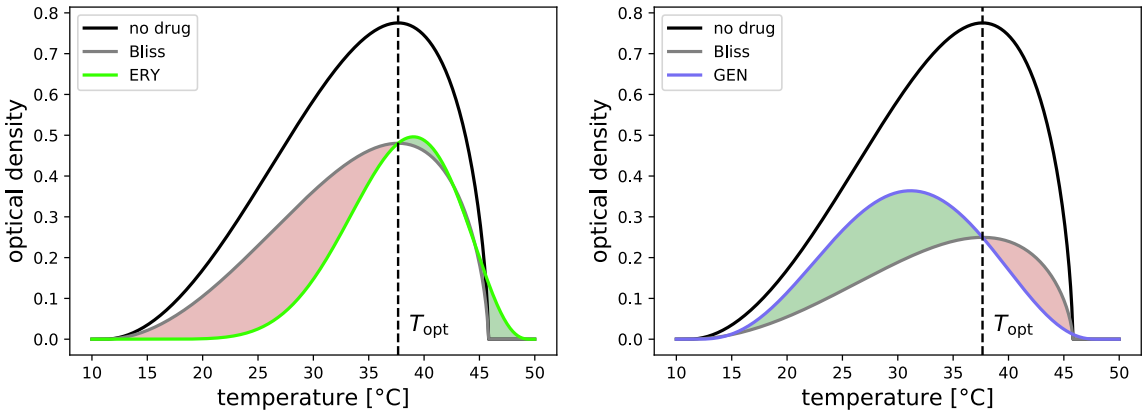

Figure 4.6: *Relationship between antibiotic-temperature interactions based on Bliss independence and temperature response curves.* The black curve corresponds to the fitted temperature response in the absence of antibiotic $g_0(T)$ in E. coli. The colored line corresponds to the response under an antibiotic $g_a(T)$ (ERY, a cold-similar antibiotic, left, and GEN, a heat-similar antibiotic, right). The temperature response curve predicted by the Bliss independence null model $\tilde{g}_a(T)$ is shown in gray (see Text S1 for details). A temperature interacts synergistically with the antibiotic if growth is reduced more than predicted by the null model (red-shaded area) and antagonistically if growth is higher than predicted (green-shaded area). Note the opposite patterns in interactions below and above the optimal temperature in the absence of drugs.

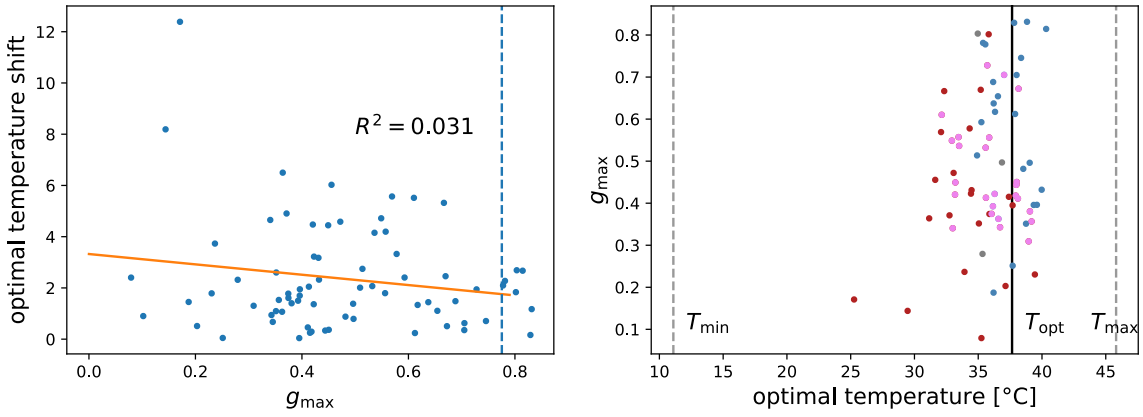

Figure 4.7: *The magnitude of optimal temperature shifts is uncorrelated with maximum growth.* (Left) The maximum growth rate $g_{\max}$ for all conditions is plotted against the absolute magnitude of the shift in the optimal temperature. The maximum growth in the absence of antibiotics is shown as a dotted line. The line of best fit is shown in orange. There is no apparent correlation between the maximum growth rate and the magnitude of the temperature shifts. All point estimates shown in the plot correspond to mean posterior values. (Right) The estimated maximum growth rate $g_{\max}$ is shown as a function of the estimated optimal temperature for each antibiotic background (including both single drugs and pairs). For comparison purposes, the minimum ($T_{\min}$), optimum (T_{opt}), and maximum ($T_{\max}$) temperatures in the absence of drugs are shown as vertical lines. The antibiotic backgrounds are color coded (purple, a heat-similar and a cold-similar drug are present simultaneously; red, heat-similar but not cold-similar drugs are present; blue, cold-similar but not heat-similar drugs are present; gray, neither heat-similar nor cold-similar drugs are present).

CHAPTER 5

A mathematical model for the evolution of stress responses in living organisms

In this chapter, we present a theoretical framework to explore the evolution of stress responses based on evolutionary game theory. This includes results regarding the favorability of evolutionary strategies with stress responses to biostatic stressors (that primarily act in the growth rate) and biocidal stressors (that primarily act in the death rate). We are also interested on exploring the tradeoffs in the evolution of specialist stress responses, that provide strong protection against a single stressor and generalist stress responses, that provide weaker protection against many different stressors. This follows up on the results of the Chapter 2 of this dissertation, which suggest that stress responses can be co-opted to deal with many different stressors.

5.1 Introduction

Living organisms are constantly exposed to stressors in their environment. In order to improve their survival and reproductive success upon encountering stressors, they have developed *stress responses*, changes in their physiology that reduce the negative impacts of a stressor [Boo06, CZJ20, CHK20, GYK18, Wen97]. Maintaining a stress response comes at a cost, both in terms of additional energy expenditure that could otherwise be spent in reproduction and also in needing to maintain the associated genetic material and regulatory mechanisms.

Some environmental stressors are biocidal, primarily killing living organisms, while others are biostatic, slowing down their rate of growth or reproduction [ASC19, BSP13, PS04]. One question we explore here is whether there are different constraints in the evolution of stress responses to biocidal or biostatic stressors. A better understanding of these evolutionary tradeoffs will be helpful in making rational treatment choices to slow down the evolution of resistance to stressors of clinical relevance. For example, some antibiotic classes are bacteriostatic and others bacteriocidal.

Ultimately, a stressor harms a living organism through damaging some aspect of its physiology. Because of this, different kinds of stressors can overlap in terms of the physiological processes harmed [CKL19, VN90] (see also Chapters 2 and 4). This may be the reason that some stress responses can protect a living organism against multiple kinds of stress [PKM16, BMG11, Poo12a]. For example, stress responses to stressors like nutrient limitation, reactive oxygen and nitrogen species, membrane damage, elevated temperature and ribosome disruption have been shown to also provide some protection to antibiotics and other antimicrobial compounds [Poo12a].

Stress responses can thus vary in their specificity. Some can be considered specialist stress responses that grant strong protection against the effects a specific stressor while providing little or no protection to other stressors. Enzymes that degrade specific harmful chemical compounds are an example of this kind of specialist stress response. In contrast, generalist stress responses can provide protection against many different stressors (albeit possibly less protection than a specialist stress response). One striking example is the general stress response in bacteria, which helps bacteria mitigate the damaging effects of stressors as diverse as UV radiation, acid, osmotic shock, oxidative stress, and nutrient deprivation [BMG11].

In this work, we are interested in the tradeoffs involved in the evolution of specialist and generalist stress responses. On one hand, a specialist stress response is likely to be more effective at dealing with a specific stressor. Thus, specialist stress responses may be

a better strategy to deal with commonly encountered stressors that have large detrimental effects on fitness. However, living organisms typically have stress responses to many different environmental stressors, and the presence of each additional stress response will require investment in terms of energy expenditure, genetic material and regulatory mechanisms. These increased requirements will eventually make it unfeasible to have a separate specific stress response for each stressor that can be encountered. Because of this, generalist stress responses that can deal with multiple stressors simultaneously may be a better strategy for dealing with stressors that are encountered more rarely and have smaller effects on fitness. The mathematical model proposed here aims to provide a framework to understand these tradeoffs quantitatively by exploring the conditions in which it is favorable to evolve a specialist or a generalist stress response, in terms of the energy expenditure, probability to encounter the stressor, the severity of the effects of the stressor and the degree of resistance.

The presence or absence of stressors is often unpredictable in natural environments. Indeed, environmental stochasticity, defined as unpredictable fluctuations in environmental conditions, is a common feature in ecological systems that influences the evolution of living organisms [FT17, HH00]. In order to deal with uncertain future conditions, living organisms employ bet-hedging strategies that improve their fitness under possible future environments at the cost of reducing their fitness in the current environment [MHK22]. For example, persister bacterial cells are a small subpopulation of cells that are dormant/non-growing but are resistant to many different biocidal stresses [KKB05]. These subpopulations prevent the bacterial population from being eliminated when encountering biocidal stressors. The effects of stochastic environmental stress in the evolution of living organisms has been studied experimentally in various contexts, such as its interactions with deleterious mutations [KL03], and how it affects the evolution of resistance to a single or multiple stressors [LPB21].

To complement and extend these experimental studies, there is a need for a quantitative framework to further understand how living organisms respond to stressors in their environment and which tradeoffs are involved in the evolution of stress responses. As an approach

to explore these questions, we propose a simple mathematical model for the evolution of stress responses where stressors are present stochastically in the environment. This model is based on evolutionary game theory [Smi82, SN99, NS04, NTA10], and considers competing strategies for survival that consist of organisms of the same species that have different sets of stress responses. The proposed model incorporates the energetic costs of the stress response and their effects on fitness, both in the presence and absence of stressors. The goal is to use it as a framework to explore questions regarding the favorability of evolving stress responses depending on energetic constraints, and the conditions under which specialist or generalist stress responses are a better strategy.

5.2 Methods

Mathematical model for the evolution of stress responses

The mathematical model for stress response evolution proposed here consists of three parts: a) a simple stochastic model for stress, b) deterministic population dynamics and c) a model for how stressors and stress responses interact in affecting fitness. Each portion of the model is described in turn in the following sections.

A simple stochastic model for environmental stress

Environmental stressors are modeled through a continuous time Markov chain. The random variable $S_t \in \{0, 1, 2, \ldots, m\}$ represents the state of the environment at time t. The state corresponding to $S_t = 0$ is taken as the reference (unstressed) state, with other values of S_t corresponding to one of m possible stressors being present in the environment. For simplicity, environmental stressors are assumed to only be present individually. Stressors are assumed to be relatively rare relative to the unstressed state, so that stressor interactions can be ignored and so that the system needs to return to the unstressed state before a new stressor

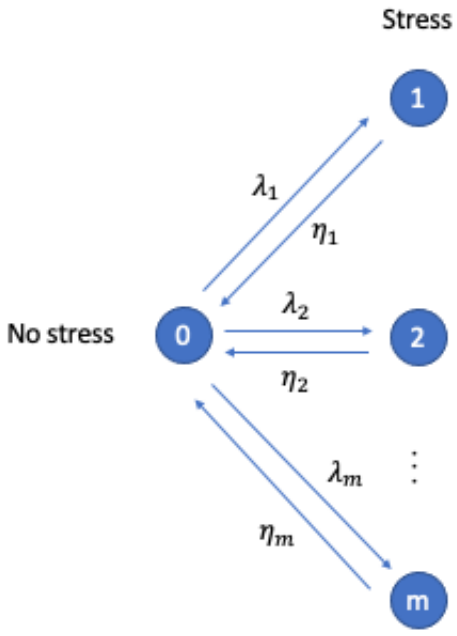

Figure 5.1: A simple stochastic model for environmental stress. The random variable S_t represents the stressor environment at time t, with $S_t = 0$ corresponding to the absence of a stressor and $S_t = 1, 2, \ldots, m$ to one of m different stressors being present in the environment.

is active.

A schematic for the Markov chain for environmental stress is shown in Figure 5.1. When in the unstressed state, the system can change stochastically to stress of type s with rate λ_s. When in the stressed state, the system returns to the unstressed state with rate η_s. The simplifying assumption that stressors are rare relative to the unstressed state allows for each stressor state $s \neq 0$ to be described by only two parameters λ_s (the rate of switching to stressor state s) and η_s (the rate of switching from stressor state s back to the unstressed state). More general frameworks that allow for switching between different stressor states and for multiple stressors to be present simultaneously can be considered in future work.

Since the Markov chain described in in Figure 5.1 has a finite state space and the chain is irreducible (that is, all states communicate with each other), it has a unique equilibrium

distribution. This equilibrium distribution can be found as the solution of the system of equations consisting of the balance conditions:

$$\lambda_s \pi_0 = \pi_s \eta_s \qquad \forall s > 0 \tag{5.1}$$

and the constraint $\sum_{s=0}^{m} \pi_s = 1$ which must be true because probability distributions must sum to unity. Solving this system of equations yields the following result for the equilibrium distribution of the chain.

$$\pi_s = \begin{cases} \frac{1}{1+\sum_{j=1}^{m} \lambda_j/\eta_j} & s = 0 \\ \frac{\lambda_s/\eta_s}{1+\sum_{j=1}^{m} \lambda_j/\eta_j} & \text{otherwise} \end{cases} \tag{5.2}$$

Population dynamics

We model the dynamics of competing members of the same species that have different *strategies* to combat environmental stress. Each strategy k consists of a collection of stress responses that modify the growth and death rates of the living organisms when different stressors are present. We assume there are U stress responses in total, which yield 2^U possible strategies (where each stress response can be present or absent). The number of organisms under strategy k is modeled by logistic growth where the growth and death rates depend on the stressor environment:

$$\frac{dn_k}{dt} = \left[r_k(S_t) \left(1 - \frac{n}{K} \right) - \delta_k(S_t) \right] n_k \tag{5.3}$$

where the total population size across all strategies is $n = \sum_k n_k$ and the individuals are assumed to be members of the same species that are in competition with each other, with a shared total carrying capacity K. Note that although Equation 5.3 defines a system of ordinary differential equations, it depends on the (stochastic) stressor environment S_t, so population growth will be stochastic.

Each strategy is associated with a vector $z_k \in \{0, 1\}^U$, where $z_{ku} = 1$ indicates that stress response u is present in strategy k and $z_{ku} = 0$ that it is absent. Strategy $k = 0$ is assumed

to correspond to the case where no stress response is active (i.e. $z_{0u} = 0$ for all u). Since every stress response can be present or absent, there can be 2^U different strategies.

The stochastic model for stress presented here is somewhat simplistic. Some of its limitations are that it ignores that multiple stressors can be present simultaneously and that most stressors are not simply discrete on-off phenomena, but have an associated strength as well (for example, temperature, pressure, antibiotic concentration). Also, some stresses may not be purely stochastic, but might also have deterministic components (such as stressors that depend on day-night cycles or different seasons). Nonetheless, the simplicity of this model allows for the mathematics to be relatively straightforward and it should be a good starting point to investigate evolutionary tradeoffs between different stress responses.

Effects of the stress responses on growth and death rates

Each stress response is assumed to have an energetic cost, so that the total amount of energy available for reproduction decreases with each additional response present in a living organism. The total energy available for reproduction under strategy k is given by

$$E_k = E_T - \sum_{u=1}^{U} z_{ku} E_u^{(S)}$$

where E_T is the total energy available for reproduction when there is no stress responses, $E_u^{(S)}$ is the energetic cost of stress response u and z_{ku} is an indicator variable that is one when strategy k contains stress response u and is zero otherwise (as defined above).

Growth and death rates in unstressed conditions

The growth rate of a strategy under unstressed conditions (i.e. $S_t = 0$) is assumed to be proportional to the available energy for reproduction. That is,

$$\frac{r_k(0)}{r_0(0)} = \frac{E_k}{E_T}$$

Thus, substituting E_k from the previous expression

$$r_k(0) = r_{\max}\left(1 - \sum_{u=1}^{U} z_{ku}\phi_u\right) \tag{5.4}$$

where $r_{\max} = r_0(0)$ is the growth rate of a strategy without any stress responses in the absence of stress, while the energy fraction $\phi_u = \frac{E_u^{(S)}}{E_T}$ is the proportion of the total energy that is allocated to the stress responses instead of reproduction. The death rate under unstressed conditions is assumed to be the same for all strategies: in other words $\delta_k(0) = \delta_{\min}$. This represents the assumption that maintaining a stress response will have a cost in terms of a reduced amount of energy that can be destined for growth and reproduction (which should be true for most/all stress responses), but that having a stress response in and on itself will not lead to increased death in the absence of stress. This simplifying assumption may not be true for all stress responses (for example, if a stress response affects the ability of the organism to e.g. escape predation), so it could be relaxed in future work.

Growth and death rate under environmental stress

In this section, we describe how environmental stress modifies the growth and death rates. We assume that stressors can have separate effects in the growth and death rates, and that whenever a strategy k has stress responses to deal with a stressor, this results on partial or total resistance to these effects at the cost of a decreased growth rate in the absence of stress. The parameters of the model involving the stressors and stress responses are summarized in Table 5.1.

The effects of a stressor $s \neq 0$ on the growth rate are modeled by introducing a parameter $\alpha_s \in [0, 1]$ that represents the strength of the effect of the stressor, with $\alpha_s = 0$ corresponding to no effect in the growth rate and $\alpha_s = 1$ to complete inhibition of growth. Another parameter $\beta_{ks} \in [0, 1]$ is introduced to represent the amount of resistance strategy k has to stressor s, with $\beta_{ks} = 0$ corresponding to no resistance and $\beta_{ks} = 1$ to complete resistance to the effects of the stressor in the growth rate. The growth rate $r_k(s)$ of strategy k when

Parameter	Description
$r_{\max}$	Maximum growth rate.
$\delta_{\min}$	Minimum death rate.
α_s	Effect of stressor s on the growth rate.
ρ_s	Effect of stressor s on the death rate.
β_{ks}	Resistance of strategy k to the effect of stressor s on the growth rate.
θ_{ks}	Resistance of strategy k to the effect of stressor s on the death rate.
ϕ_u	Energy cost of having stress response u (as a fraction of total energy).
z_{ku}	Indicator of whether strategy k has stress response u.

Table 5.1: Parameters involving the effects of stressors and stress responses in the growth and death rates.

stressor s is present is modeled with following equation:

$$\begin{aligned} r_k(s) &= \left[1 - (1 - \beta_{ks})\,\alpha_s\right] r_k(0) \\ &= r_{\max}\left(1 - \sum_{u=1}^{U} z_{ku}\phi_u\right)(1 - \alpha_s + \alpha_s\beta_{ks}) \end{aligned}$$

where . The growth rate of strategy k is thus reduced by two factors relative to the maximum growth rate: a) a factor that depends on the total energy investment in stress responses $\sum_{u=1}^{U} z_{ku}\phi_u$, and b) a factor that depends on the effect of the stressor in the growth rate, which depends on α_s, the strength/severity of the effect and β_{ks}, the amount of resistance that strategy k has to the effect of stressor s in the growth rate.

Living organisms can have multiple stress responses, and each stress response can grant partial or total resistance to a subset of the stressors that can be encountered in the environment. Whenever a strategy has multiple stress responses, it is assumed to always use the best stress response available to deal with a stressor. Because of this, the amount of resistance that strategy k has against stressor s is assumed to be the maximum resistance granted by the individual stress responses it possesses. More precisely, we model $\beta_{ks} = \max\{\tilde{\beta}_{us} : z_{ku} = 1\}$

where $\tilde{\beta}_{us} \in [0,1]$ is the amount of resistance stress response u gives to stressor s. However, having multiple stress responses that provide resistance to the same stressor is assumed to provide no greater benefit than that conferred by the single best stress response against that stressor.

Similarly, the effects on the death rate are modeled by the equation

$$\begin{aligned}\delta_k(s) &= (1 + (1 - \theta_{ks})\,\rho_s)\,\delta_k(0) \\ &= (1 + (1 - \theta_{ks})\,\rho_s)\,\delta_{\min}\end{aligned}$$

where $\rho_s \geq 0$ represents the strength of the effect of stressor s in the death rate and $\theta_{ks} \in [0,1]$ the amount of resistance strategy k has to the effects of stressor s on the death rate. As before, a strategy is assumed to always use the best stress response available so $\theta_{ks} = \max\{\tilde{\theta}_{us} : z_{ku} = 1\}$ where $\tilde{\theta}_{us} \in [0,1]$. Note that unlike the equation for the growth rate, the death rate is assumed to not change due to the energy investment in stress responses.

Average growth and death rates

We can use the above expressions to calculate the expected growth and death rates when averaging over the different environments, assuming we are at the equilibrium distribution of the Markov chain. We have

$$\begin{aligned}\bar{r}_k &= \mathrm{E}_\pi\left[r_k(s)\right] \\ &= \sum_{s=0}^{m} \pi_s r_k(s) \\ &= \pi_0 r_k(0) + \sum_{s=1}^{m} \pi_s r_k(s) \\ &= r_{\max}\left(1 - \sum_{u=1}^{U} z_{ku}\phi_u\right)\left[\pi_0 + \sum_{s=1}^{m} \pi_s\left(1 - \alpha_s + \alpha_s\beta_{ks}\right)\right] \\ &= r_{\max}\left(1 - \sum_{u=1}^{U} z_{ku}\phi_u\right)\left[1 - \sum_{s=1}^{m} \pi_s\alpha_s\left(1 - \beta_{ks}\right)\right]\end{aligned}$$

where $\beta_{ks} = \max\{\tilde{\beta}_{us} : z_{ku} = 1\}$.

A similar procedure for the death rate yields the following result:

$$\begin{aligned}
\bar{\delta}_k &= \mathrm{E}_\pi \left[\delta_k(S)\right] \\
&= \sum_{s=0}^{m} \pi_s \delta_k(s) \\
&= \sum_{s=0}^{m} \pi_s \left[1 + (1 - \theta_{ks})\, \rho_s\right] \delta_{\min} \\
&= \delta_{\min} \left[1 + \sum_{s=0}^{m} \pi_s \left(1 - \theta_{ks}\right) \rho_s\right]
\end{aligned}$$

where $\theta_{ks} = \max\{\tilde{\theta}_{us} : z_{ku} = 1\}$.

Deterministic approximation

Next, we propose a deterministic approximation to the model in order to explore the relationship between the modeled parameters and the outcome of the modeled populations. We construct this approximation by replacing the stochastic growth and death rates with their averages according to the equilibrium distribution of the Markov chain representing the stressor environment. This results in the following deterministic model

$$\frac{dn_k}{dt} = \left[\bar{r}_k \left(1 - \frac{n}{K}\right) - \bar{\delta}_k\right] n_k \tag{5.5}$$

where $k = 0, 1, \ldots, 2^U - 1$. Here, we note that we are averaging over the growth and death rates rather than over the population numbers (which are the quantities of interest). However, it is tricky to average in terms of the population numbers since this is the solution to a differential equation that cannot be solved analytically. Because of this, we use this approximation to explore the tradeoffs involved in the stress responses. We expect this deterministic model to be a better approximation to the stochastic model when the stressor environment

changes very rapidly relative to changes in the population numbers, which should result in the stochastic environmental changes being averaged out, and worse when the environment changes at a similar rate or more slowly than the populations.

This deterministic approximation is not constructed based on a rigorous mathematical argument. However, later in this work we compare stochastic simulations with the deterministic approximation (see Stochastic simulations section below and Figure 5.4). Our simulations show that this deterministic approximation seems to approximate the stochastic model reasonably well in practice, at least for the parameter values in the simulations.

We now proceed to find the nontrivial fixed points of this system to explore the long term behavior of the model. Note that at equilibrium,

$$0 = \left[\bar{r}_k \left(1 - \frac{n^*}{K}\right) - \bar{\delta}_k\right] n_k^*, \qquad k = 0, 1, \ldots, 2^U - 1$$

For all nonzero n_k^*, we can rearrange this expression to yield the condition

$$n^* = K\left(1 - \frac{\bar{\delta}_k}{\bar{r}_k}\right) \tag{5.6}$$

where $n^* = \sum_j n_j^*$ is the total population at equilibrium.

If we assume that there exist multiple $n_k^* \neq 0$ with different $\frac{\bar{\delta}_k}{\bar{r}_k}$, this leads to a contradiction, since $n^* = K\left(1 - \frac{\bar{\delta}_k}{\bar{r}_k}\right)$ would need to take multiple values simultaneously. It follows that for all k such that $n_k^* \neq 0$, $\frac{\bar{\delta}_k}{\bar{r}_k}$ must be identical. In practice, since different strategies will vary on their resistance to stressors, models will usually consist of strategies for which there are no identical $\frac{\bar{\delta}_k}{\bar{r}_k}$. In this case, the expression above implies that there can only be at most one nonzero n_k^* at a fixed point. When this is the case, $n_k^* = n^* = K\left(1 - \frac{\bar{\delta}_k}{\bar{r}_k}\right)$. Thus, besides the trivial fixed point where all $n_k^* = 0$, there will be 2^U more fixed points, corresponding to a single strategy k taking over the population.

Now we show that, under the assumption that all $\frac{\bar{\delta}_k}{\bar{r}_k}$ are different, the fixed point with $n_k^* \neq 0$ is stable when $\frac{\bar{\delta}_k}{\bar{r}_k} = \min_j \frac{\bar{\delta}_j}{\bar{r}_j}$. Thus, the winning strategy will be the one that minimizes $\frac{\bar{\delta}_k}{\bar{r}_k}$: this will outcompete all other strategies and take over the population in the long run.

We start by calculating the Jacobian matrix from the system defined by Equation 5.5. Note that

$$\frac{\partial \dot{n}_k}{\partial n_j} = \begin{cases} \bar{r}_k - \bar{\delta}_k - \frac{\bar{r}_k}{K}\sum_{j\neq k} n_j - 2\frac{\bar{r}_k}{K} n_k & j = k \\ -\frac{\bar{r}_k}{K} n_k & j \neq k \end{cases}$$

(where the notation $\dot{n}_k = \frac{dn_k}{dt}$ is used for simplicity). To simplify our calculations we temporarily change our ordering convention only for the rest of this section. Rather than setting $k = 0$ as the strategy with no stress responses, without loss of generality we rearrange the strategies so that n_0 corresponds to the strategy that has a nonzero population in the fixed point we are evaluating. With this reordering we have $n_0^* = K\left(1 - \frac{\bar{\delta}_0}{r_0}\right)$ and all other $n_j^* = 0$. The Jacobian evaluated at this fixed point is then

$$J = \begin{bmatrix} \bar{\delta}_0 - \bar{r}_0 & \bar{\delta}_0 - \bar{r}_0 & \bar{\delta}_0 - \bar{r}_0 & \bar{\delta}_0 - \bar{r}_0 & \dots & \bar{\delta}_0 - \bar{r}_0 \\ 0 & \bar{r}_1\frac{\bar{\delta}_0}{\bar{r}_0} - \bar{\delta}_1 & 0 & 0 & \dots & 0 \\ 0 & 0 & \bar{r}_2\frac{\bar{\delta}_0}{\bar{r}_0} - \bar{\delta}_2 & 0 & \dots & 0 \\ \vdots & \vdots & \vdots & \vdots & \ddots & \vdots \\ 0 & 0 & 0 & 0 & \dots & \bar{r}_{(2^U-1)}\frac{\bar{\delta}_0}{\bar{r}_0} - \bar{\delta}_{(2^U-1)} \end{bmatrix}$$

and its eigenvalues are the solutions of the characteristic polynomial

$$\begin{aligned} 0 &= \det(\lambda I - J) \\ &= \left[\lambda - (\bar{\delta}_0 - r_0)\right] \prod_{k>0} \left[\lambda - (\bar{r}_k \frac{\bar{\delta}_0}{\bar{r}_0} - \bar{\delta}_k)\right] \end{aligned}$$

The eigenvalues for this fixed point are $\lambda_0 = \bar{\delta}_0 - \bar{r_0}$ and $\lambda_k = \bar{r}_k\frac{\bar{\delta}_0}{\bar{r}_0} - \bar{\delta}_k$ for $k = 1, 2, \dots, 2^U - 1$. The fixed point will be stable whenever all of the eigenvalues are negative. This means that the conditions for the fixed point where $n_0^* = K\left(1 - \frac{\bar{\delta}_0}{\bar{r}_0}\right)$ and all other $n_j^* = 0$ to be stable

are

$$\begin{aligned} \bar{r}_0 &> \bar{\delta}_0, && \text{and} \\ \frac{\bar{r}_0}{\bar{\delta}_0} &> \frac{\bar{r}_k}{\bar{\delta}_k} && \forall k \neq 0 \end{aligned}$$

Since the previous argument does not rely on n_0 being any particular strategy, this shows that for a strategy n_k to be winning (and take over the population) it must satisfy two conditions: $\bar{r}_k > \bar{\delta}_k$ (that is, the trivial condition that it should be able to grow) and $\frac{\bar{r}_k}{\bar{\delta}_k} > \frac{\bar{r}_j}{\bar{\delta}_j}$ for all $j \neq k$ (that is, that it will outcompete the other strategies).

5.3 Some preliminary analytic results

Favorability of evolving a stress response

In this section, we will consider the simplest case, where there is only one stressor and only two strategies, corresponding to a single stress response being present or absent. The Markov chain for environmental stress reduces to two states where $\pi_0 = \frac{\eta}{\lambda+\eta}$, $\pi_1 = \frac{\lambda}{\lambda+\eta}$ are the equilibrium probabilities for an unstressed and stressed environment, respectively. Given that there are only two states for the environment (stressor present or absent), I will henceforth refer to the equilibrium probability for the stressor to be present π_1 simply as p, since $\pi_0 = 1 - \pi_1 = 1 - p$. Then the expected growth and death rates for the no-stress response strategy are

$$\begin{aligned} \bar{r}_0 &= r_{\max}\left[1 - \left(\frac{\lambda}{\eta+\lambda}\right)\alpha\right] = r_{\max}\left(1 - p\alpha\right) \\ \bar{\delta}_0 &= \delta_{\min}\left[1 + \left(\frac{\lambda}{\eta+\lambda}\right)\rho\right] = \delta_{\min}\left(1 + p\rho\right) \end{aligned}$$

and the expected growth rate for the stress response strategy is

$$\bar{r}_1 = r_{\max}(1-\phi)\left[1-p\alpha(1-\beta)\right] \tag{5.7}$$

$$\bar{\delta}_1 = \delta_{\min}\left[1+p\rho(1-\theta)\right] \tag{5.8}$$

The stress response strategy will be better relative to not having a stress response when

$$\begin{aligned}
\frac{\bar{r}_1}{\bar{\delta}_1} &> \frac{\bar{r}_0}{\bar{\delta}_0} \\
\frac{r_{\max}(1-\phi)\left[1-p\alpha(1-\beta)\right]}{\delta_{\min}\left[1+p\rho(1-\theta)\right]} &> \frac{r_{\max}\left[1-p\alpha\right]}{\delta_{\min}\left[1+p\rho\right]} \\
1-\phi &> \frac{(1-p\alpha)\left[1+p\rho(1-\theta)\right]}{(1+p\rho)\left[1-p\alpha(1-\beta)\right]}
\end{aligned}$$

This expression necessary for the stress reponse strategy to be favorable relates the energy fraction used for the stress response with the probabilty of encountering the stressor, the strength of the stressor effects in the growth and death rate, and the resistance to each conferred by the stress response.

We use this result to compare the cases when a stressor is biostatic (i.e. only modifies the growth rate) and biocidal (only modifies the death rate). A purely biostatic stressor will have no effect on the death rate or resistance to this effect, so $\rho, \theta = 0$. The strategy with the stress response will be favorable when the following condition relating the energy fraction ϕ allocated to the stress response is satisfied.

$$1-\phi > \frac{1-p\alpha}{1-p\alpha(1-\beta)}$$

We can solve for the amount of resistance β to show that the stress response strategy is advantageous when

$$\beta > \left(\frac{\phi}{1-\phi}\right)\left(\frac{1-p\alpha}{p\alpha}\right)$$

(where $p = \frac{\lambda}{\eta+\lambda}$).

We use this result to explore the relationship between stressor strength, energy expenditure and the necessary stress resistance in order for the stress response to be advantageous

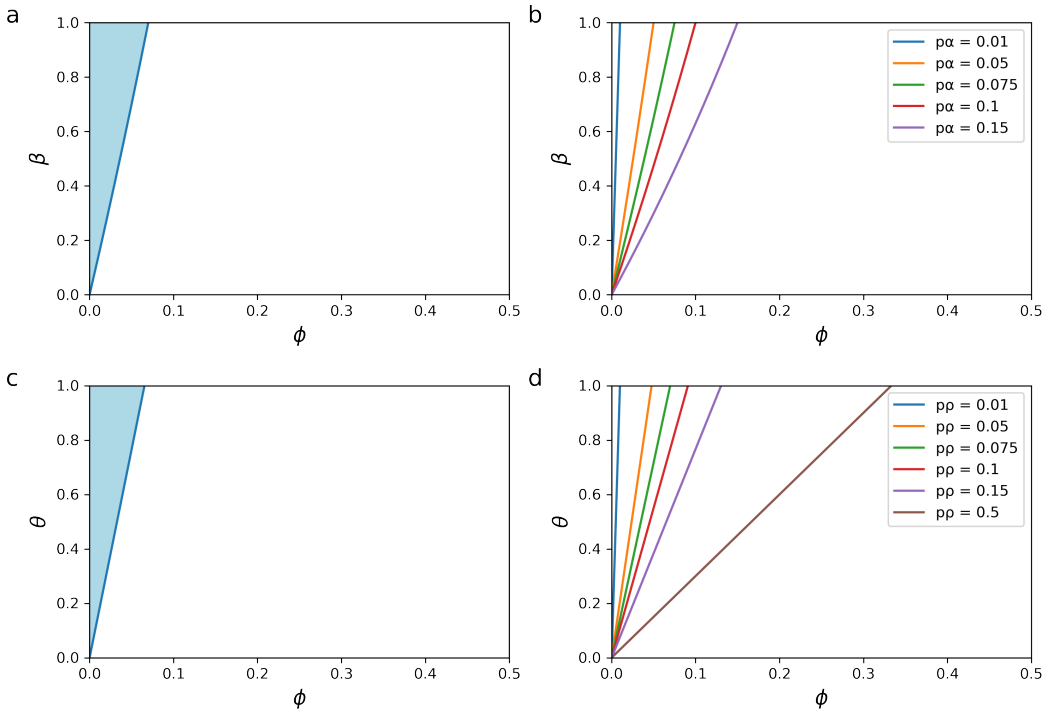

Figure 5.2: *Parameter values for which the stress response strategy is favorable.* a) The necessary stress resistance strength β for the stress response strategy to outperform the no-stress response case is shown as a function of the energy expenditure for the case where $p\alpha = 0.07$, and where the stressor does not modify the death rate. The line represents conditions for which the expected growth rates are the same so both strategies coexist. b) The line of coexistence for the two strategies is shown as $p\alpha$, the product of the frequency of stress and the stressor strength is increased. c, d) Similar plots are shown for the case where the stressor is a pure biocidal.

(Figure 5.2). I first consider what happens under realistic parameter values. Suppose we have a relatively strong stressor ($\alpha = 0.7$) that is present around 10% of the time, while the other 90% of the time the organism grows unimpeded ($p = 0.1$) (Figure 5.2a). Under these conditions, we can see there are rather strict limits in terms of the energy fraction ϕ that can be allocated to stress responses. When $\phi > 0.075$, the stress response is unfavorable regardless of how much resistance to the stressor is gained from the stressor. Under smaller energy fractions allocated to the stress response, the strategy with the active stress response is viable, but typically only under relatively strong resistance β.

Next, I explore how this boundary between when each stress response is favorable changes depending on the stressor strength and frequency. The dependency is entirely in terms of the product $p\alpha$ (Figure 5.2b). I find that it is indeed possible to construct situations in which the stress response will be favorable even at relatively low acquired resistance ($\beta \approx 0.2$) under reasonable energy fractions ϕ. However, to do this, the stressor needs to be both affect growth very strongly and arise frequently.

For a purely biocidal stressor (i.e. a stressor that only affects the death rate), we have $\alpha, \beta = 0$ (since these parameters represent the effect of the stressor in the growth rate and the resistance the stress response grants to this effect). Then the stress response is favorable when

$$\theta > \phi \frac{1 + p\rho}{p\rho}$$

If we take the same values for ρ, θ (the parameters involved in the effect in the death rate and resistance) as we did before for α, β, we find that the energy fraction that can be allocated for a stress response has a nearly identical behavior as that of the biostatic case (Figure 5.2c). This figure corresponds to $\rho = 0.7$, which corresponds to 1.7 times the death rate when compared to unstressed conditions. However, there is an important difference between the biostatic and biocidal cases. For biostatic stressors the stressor strength $\alpha \in [0, 1]$ is

constrained to the unit interval because $\alpha = 1$ when the growth rate is reduced completely and the living organism is non-growing. In contrast, ρ does not have the same upper limit. A value of $\rho = 1$ corresponds to a stressor that results in twice the death rate compared to the unstressed case. However, stressors that increase the death rate far beyond this are possible. We indicate this in Figure 5.2d by extending the range of $p\rho$ explored to $p\rho = 0.5$ (which could, for example, correspond to a stressor present 10% of the time that increases the death rate by a factor of six).

As such, the model presented here predicts that a greater energy fraction can be allocated to stress responses that deal with biocidal stressors compared to biostatic stressors, provided that the biocidal stressor increases the death rate by more than twice its baseline value in the absence of stress. As such, the evolution of stress responses to highly biocidal stressors is predicted to be more favorable compared to highly biostatic stressors.

5.4 Stochastic simulations

Here, I explore some stochastic trajectories of a more complex case and compare them to the deterministic approximation. For this case, we consider three different stressors s that arise with rate λ_s. We assume the population consists of four strategies, detailed in Table 5.2. These consist of one specialist stress response for each stressor present and a general stress response that provides (weaker) resistance to all three stresses simultaneously. For the sake of this simulation, I only consider strategies with individual stress responses active rather than combinations of multiple stress responses. The parameter values used are shown in Table 5.3.

The population dynamics parameters were chosen to be reasonable for bacteria, while the stochastic stress parameters correspond to relatively strong stressors present frequently (about 25% of the time), with some stressors being more common than others. The system was started in the unstressed state and the continuous time Markov chain corresponding to

k	Stress response type	β_{k1}	β_{k2}	β_{k3}
0	no stress response	0	0	0
1	specialist	β_s	0	0
2	specialist	0	β_s	0
3	specialist	0	0	β_s
4	generalist	β_g	β_g	β_g

Table 5.2: Strategies explored in the stochastic simulation. We took $\beta_s = 0.7$ and $\beta_g = 0.4$ for generating the stochastic trajectories below. For these simulations, we are only considering cases with a single stress response.

the stressor state was simulated for 1000 (model) hours. Population dynamics were then simulated using the generated stressor states with an initial population of 100 individuals per strategy and a carrying capacity of 10^5 individuals. One stochastic realization is shown on Figure 5.3.

One hundred such simulations were averaged and compared with the predictions of the deterministic approximation using the mean growth rate rather than the stochastic growth rate that depends on the environment (Figure 5.4). Under these conditions, the deterministic model seems to provide a reasonable approximation to the stochastic dynamics, although it tends to overestimate the no-stress-response strategy compared to the strategies with stress responses to common stressors. Under the simulated conditions, the generalist stress response seems to be the dominant strategy. However, this will depend on the parameters, particularly the energy fraction ϕ, and the values for β_g and β_s (the resistance granted by the generalist or specialist response).

Parameter	Value	Parameter	Value
λ_1	0.1	$r_{\max}$	2
λ_2	0.07	K	10^5
λ_3	0.05	$\delta_{\min}$	0.1
$\eta_1 = \eta_2 = \eta_3$	1	$\rho_1 = \rho_2 = \rho_3$	0
$\alpha_1 = \alpha_2 = \alpha_3$	0.7	$\theta_1 = \theta_2 = \theta_3$	0
$\phi_1 = \phi_2 = \phi_3 = \phi_4$	0.05	n_{k0}	10^2

Table 5.3: Parameter values for the stochastic simulations for a purely biostatic stressor. Rate constants are in units of hours^{-1}.

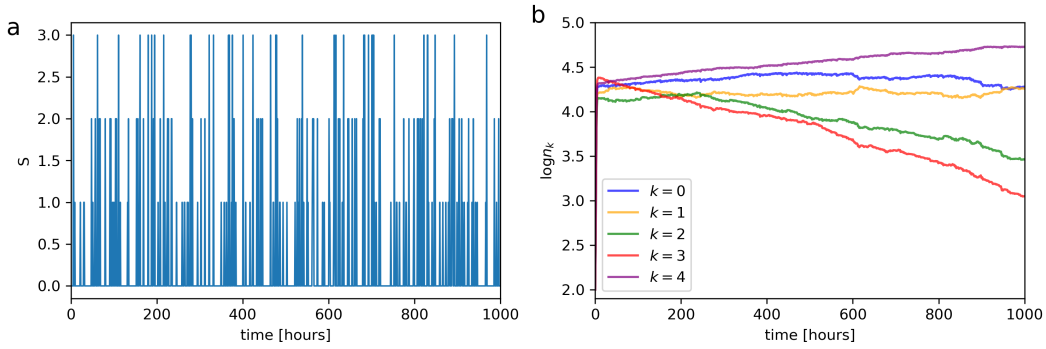

Figure 5.3: *An example stochastic trajectory.* a) A single generated stochastic trajectory for the environmental stress S_t is shown through time, where $S_t = 0$ corresponds to no stress and $S_t = s \neq 0$ to stressor s being present. b) The generated stochastic dynamics are shown, with an initial population $n_{k0} = 100$ for all strategies k. The five strategies correspond to a) $k = 0$, no stress response, b) $k \in \{1, 2, 3\}$ a single specific stress response to each stressor and c) $k = 4$ a generalist stress response.

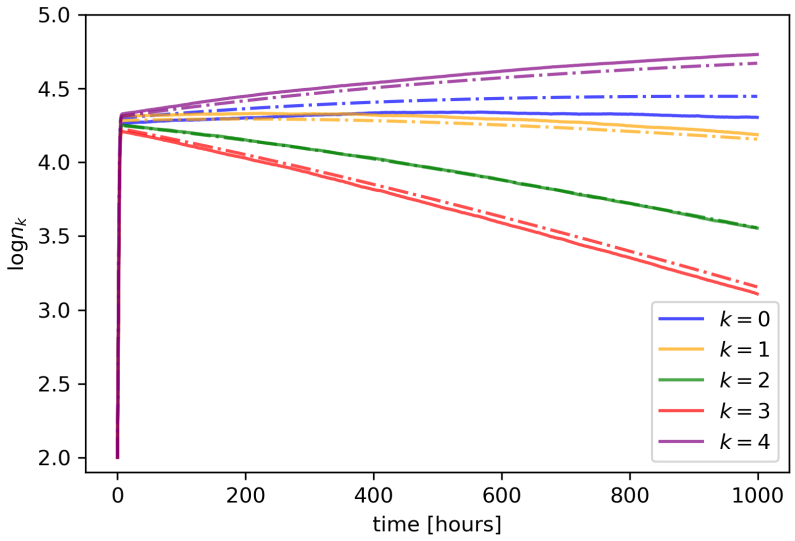

Figure 5.4: *Stochastic model compared to deterministic approximation.* The full line corresponds to the average of 100 stochastic trajectories of the model described above with the same parameter values. The dotted line corresponds to the predictions of the deterministic approximation using the mean growth and death rates.

5.5 Discussion

In this work we present a model for the evolution of stress responses based on evolutionary game theory. This model is based on a stochastic model for environmental stress which is coupled to a system of ordinary differential equations that describe the population growth of competing organisms that follow different strategies for survival, in the form of having different combinations of stress responses. Stress responses are assumed to increase the fitness of the organisms in the presence of some subset of the stressors at the cost of reducing their fitness in unstressed conditions.

Based on a deterministic approximation of the model, we found that the energy fraction ϕ_k that a stress response takes away from reproduction strongly constrains the feasible stress responses, especially for biostatic stressors. This energy fraction needs to be small in order for a stress response to be advantageous, and extremely small for a stress response with only weak resistance to stress to be advantageous. In contrast, much larger energy fractions can be allocated to stressors that are highly biocidal. These results suggest that strategies that possess stress responses that confer resistance to highly biocidal stressors will be more advantageous than stress responses that help with resisting biostatic stressors.

These conclusions are based on the single stressor case. When multiple stressors are involved, a generalist stress response can be advantageous compared to specialist stress responses as shown with the stochastic simulations despite providing weaker resistance to individual stressors. The robustness of these conclusions needs to be evaluated in future work by considering cases with multiple stressors, and with generalist and specialist stress responses.

Rather than a complete exploration, the work here is meant as a proof of concept and a starting point to illustrate the possibilities that this model provides in modeling the tradeoffs in the ways living organisms respond to stressors. This model will be used to study the evolutionary tradeoffs involved in choosing between specialist and generalist stress responses,

and how these tradeoffs depend on whether stressors are biocidal or biostatic more completely in future work.

CHAPTER 6

Discussion and future directions

Understanding how multiple stressors interact in affecting the growth of a living organism and how evolution of resistance to one stressor affects resistance to other stressors are fundamental questions in ecology in particular, and biology in general. In this work, I follow a few different approaches to try to understand these processes.

In the Bliss interaction framework that is used in Chapter 2, interactions between stressors are defined by the direction in which the observed growth deviates from a null model that assumes independent effects on growth. Because of the simplicity of this model, it may be surprising that so much information can be inferred from networks of interactions. The results of the work in Chapter 2 indicate that stressor interaction networks can reveal groups of stressors that have overlap in terms of their mechanism of damage to the bacteria. Moreover, this overlap seems to influence the acquired antibiotic cross-resistance or cross-sensitivity in bacteria evolved at high temperatures. Thus, it seems that a greater focus in the physiological overlap of stressors, rather than the identity of the stressor, may be helpful in understanding the relationship between stressor interactions and the evolution of cross-resistance. Importantly, no aspect of this methodology is specific to antibiotics and temperature since it is based only in comparing the observed and expected growth when stressors are present simultaneously. As such, similarity in the interaction profile of stressors could potentially be used in future work to evaluate the similarity among any combination of physical, chemical, and/or biological stressors that affect organismic growth.

The Bliss independence interaction framework used in Chapter 2 is descriptive rather

than mechanistic. It has the advantage of generality, since it can be applied to any situation where the growth of an organism is impaired. Mechanistic models are in some sense at the other extreme compared to descriptive models. They are much more detailed and specific to the phenomenon that is being modeled, at the cost of reduced generality and more modeling effort. However, they often enable a deeper understanding the modeled phenomenon than descriptive approaches and can generate quantitative predictions under various hypothetical scenarios. I believe there is room for both kinds of approaches in the study of biological systems.

The third and fourth chapters are closely related. In the Chapter 3, the focus is on developing a flexible model for describing temperature responses by modifying an existing model, and in Chapter 4, on applying it to infer the temperature response curves of bacteria under the presence of antibiotics. Parameter inference was done through a Bayesian approach, which I have come to prefer due to its ability to propagate uncertainty in measurements to uncertainty in model parameters and its flexibility in being able to incorporate prior information about the parameters from previous experiments. This is especially useful when the parameters are meaningful in a biological or physical sense. In this case, we can come up with informative prior distributions that make sense given the known biology of the phenomenon to aid parameter inference. I tried to follow this approach in the work here, by reparametrizing the temperature response model into a form where meaningful prior distributions can be formulated for many parameters based on known biology and information about the experimental setup.

The work in Chapter 4 also follows up on the results of Chapter 2. We find that the antibiotic-temperature groups found previously seem to explain the direction of antibiotic-induced shifts in the optimal temperature for growth. Our results provide insights into the interactions between temperature and other stressors. Particularly, we show that stressors can modify the temperature response curves of a living organism and that these changes can be predicted from the way the stressor harms its physiology.

Based on our results from Chapter 4, we propose a shared-damage hypothesis, mainly that when the physiological damage that is caused by two different stressors overlaps, this will result on a synergistic effect that will reduce growth more sharply than when there is no overlap. An exciting potential application of the shared-damage hypothesis is in predicting the effect of other stressors on the thermal optima of living organisms. To do this, further work could evaluate the extent to which the physiological damage caused by other environmental stressors—such as pressure and pH—is similar to either temperature stress or antibiotics. This can be done by comparing either the gene-expression profile or the interaction profile (i.e., synergies and antagonisms with other stressors) of the environmental stressor of interest with those of extreme temperatures and/or antibiotics. Our hypothesis would then predict that stressors that induce similar damage as high temperature will result in left shifts in the optimal temperature (and vice versa). Moreover, the direction of the shift induced by a stressor should be the same as that of other stressors (e.g., antibiotics) that cause similar physiological damage. For example, beta-lactam antibiotics compromise the integrity of the bacterial cell wall, so we speculate that the induced damage to the cell could have certain similarities to osmotic shock. If this were true, it seems possible that osmotic shock might change the temperature responses in a similar way as beta-lactams.

Finally, in Chapter 5 we introduce a mathematical model of the evolution of stress responses based on evolutionary game theory and some results relating to the differences between biostatic stressors (that reduce the growth rate) and biocidal stressors (that increase the death rate). Unlike the other chapters of this dissertation, this is purely a modeling project that is not based on experimental data. I believe that a framework for explaining the evolution of these stress responses will be helpful for exploring the evolutionary tradeoffs inherent to stress responses. The tradeoffs in the evolution of specialist and generalist stress responses are of special interest to me due to their connections with the work in Chapter 2, where our results suggest that stress responses may often be co-opted to deal with different stressors that cause similar physiological damage.

Future work in this project will involve working out the parameter regimes (energy fractions and resistance) for which a generalist stress response will outperform individual specialist stress responses, for both biocidal and biostatic stressors. Also, many of the preliminary results presented in Chapter 5 rely on a deterministic approximation to the stochastic system that is not rigorously justified with a mathematical argument. Additional work could also focus on finding a more rigorous approximation to the stochastic system, and/or to find the conditions under which the approximation will work or not through either analytical work or simulations. It may also be possible to obtain some analytic results using the full stochastic version of the model.

Modifications to the stochastic stress model would also be of interest. In particular, the recent presence of a stressor may make it more likely for the same stressor to appear in the near future. This could be included in the model while keeping the Markovian property by the inclusion of additional "stressor-specific" unstressed states that need to be visited before returning to the main unstressed state. Another idea could be to extend the model to multiple stressors to explore if the tradeoffs in evolving a stress response against synergistic or antagonistic stressors differ. To do this, a stressor interaction framework (such as Bliss independence, the framework used in Chapter 2) could be introduced as part of the model.

In the longer term, it may also be possible to incorporate mutation between different stress response strategies and model the ensuing populations. This would enable modeling the dynamics of the evolution of the stress responses, starting from a population consisting of only the baseline condition without stress responses.

In conclusion, the work in this dissertation explores how multiple stressors interact in affecting the population growth of living organisms through various approaches that combine theoretical tools with experimental data. The experimental system used in this work, involving the choice of antibiotics and temperature as stressors, and the bacterium *E. coli* as the living organism, is valuable due to its experimental tractability and clinical relevance.

The results of this work improve our understanding of how the overlap in the physio-

logical effects of stressors influences the evolution of cross-resistance or cross-sensitivity. In particular, from the results of Chapter 2 it seems that cross-resistance is more likely to arise when there is overlap in the mechanisms by which the stressors damage the physiology of a living organism. We also make progress in understanding the joint effects of stressors in the growth of living organisms, mainly through the proposed shared-damage hypothesis in Chapter 4. Moreover, the mathematical framework presented in Chapter 5 will be helpful to learn more about the constraints in the evolution of stress responses, and the conditions in which generalist stress responses, which deal with multiple stressors, are a favorable evolutionary strategy compared to specialist stress responses. A better understanding of stressor interactions and the evolutionary tradeoffs in the evolution of stress responses may improve our ability to make rational choices when using antibiotics and other antimicrobial compounds in clinical settings and help delay or prevent the emergence of antibiotic resistance.

REFERENCES

[ABG06] Michael J. Angilletta, Albert F. Bennett, Helga Guderley, Carlos A. Navas, Frank Seebacher, and Robbie S. Wilson. "Coadaptation: a unifying principle in evolutionary thermal biology." *Physiological and biochemical zoology: PBZ*, **79**(2):282–294, April 2006.

[ACU17] Matthew P. Adams, Catherine J. Collier, Sven Uthicke, Yan X. Ow, Lucas Langlois, and Katherine R. O'Brien. "Model fit versus biological relevance: Evaluating photosynthesis-temperature models for three tropical seagrass species." *Scientific Reports*, **7**:39930, January 2017.

[Ali70] R. M. Ali. "The influence of suspension density and temperature on the filtration rate of Hiatella arctica." *Marine Biology*, **6**(4):291–302, August 1970.

[Ang09] Michael J. Angilletta Jr. *Thermal Adaptation: A Theoretical and Empirical Synthesis*. Oxford University Press, Oxford, 2009.

[AS12] Priyanga Amarasekare and Van Savage. "A framework for elucidating the temperature dependence of fitness." *The American Naturalist*, **179**(2):178–191, February 2012.

[ASC19] Jani V. Anttila, Mikhail Shubin, Johannes Cairns, Florian Borse, Qingli Guo, Tommi Mononen, Ignacio Vázquez-García, Otto Pulkkinen, and Ville Mustonen. "Contrasting the impact of cytotoxic and cytostatic drug therapies on tumour progression." *PLOS Computational Biology*, **15**(11):e1007493, November 2019. Publisher: Public Library of Science.

[BB16] Karen Bush and Patricia A. Bradford. "-Lactams and -Lactamase Inhibitors: An Overview." *Cold Spring Harbor Perspectives in Medicine*, **6**(8):a025247, August 2016.

[BBL18] Aura M. Barria, Leonardo D. Bacigalupe, Nelson A. Lagos, and Marco A. Lardies. "Thermal physiological traits and plasticity of metabolism are sensitive to biogeographic breaks in a rock-pool marine shrimp." *Journal of Experimental Biology*, **221**(19):jeb181008, October 2018.

[BC15] Georgina Brennan and Sinéad Collins. "Growth responses of a green alga to multiple environmental drivers." *Nature Climate Change*, **5**(9), September 2015.

[Ben80] Albert F. Bennett. "The thermal dependence of lizard behaviour." *Animal Behaviour*, **28**(3):752–762, August 1980.

[BH16] Lauren B. Buckley and Raymond B. Huey. "How Extreme Temperatures Impact Organisms and the Evolution of their Thermal Tolerance." *Integrative and Comparative Biology*, **56**(1):98–109, July 2016.

[BKS99] A. R. Bhatti, K. Kumar, C. Stobo, G. R. Chaudhry, and J. M. Ingram. "High temperature induced antibiotic sensitivity changes in Pseudomonas aeruginosa." *Microbios*, **97**(387):103–115, 1999.

[BL02] Jeffrey L. Bada and Antonio Lazcano. "Origin of life. Some like it hot, but not the first biomolecules." *Science (New York, N.Y.)*, **296**(5575):1982–1983, June 2002.

[BL04] Dieter Braun and Albert Libchaber. "Thermal force approach to molecular evolution." *Physical Biology*, **1**(1-2):P1–8, June 2004.

[Bli39] C. I. Bliss. "The Toxicity of Poisons Applied Jointly." *Annals of Applied Biology*, **26**(3):585–615, 1939. _eprint: https://onlinelibrary.wiley.com/doi/pdf/10.1111/j.1744-7348.1939.tb06990.x.

[BMG11] Aurelia Battesti, Nadim Majdalani, and Susan Gottesman. "The RpoS-mediated general stress response in Escherichia coli." *Annual Review of Microbiology*, **65**:189–213, 2011.

[BN14] Kalpna Bhandari and Harsh Nayyar. "Low Temperature Stress in Plants: An Overview of Roles of Cryoprotectants in Defense." In Parvaiz Ahmad and Mohd Rafiq Wani, editors, *Physiological Mechanisms and Adaptation Strategies in Plants Under Changing Environment: Volume 1*, pp. 193–265. Springer, New York, NY, 2014.

[Boo06] Kathryn J. Boor. "Bacterial Stress Responses: What Doesn't Kill Them Can Make Them Stronger." *PLOS Biology*, **4**(1):e23, January 2006. Publisher: Public Library of Science.

[BPL99] Jean-Francois Briere, Pascale Pracros, Alain-Yves Le Roux, and Jean-Sebastien Pierre. "A Novel Rate Model of Temperature-Dependent Development for Arthropods." *Environmental Entomology*, **28**(1):22–29, February 1999.

[BRI02] Grégory Beaugrand, Philip C. Reid, Frédéric Ibañez, J. Alistair Lindley, and Martin Edwards. "Reorganization of North Atlantic marine copepod biodiversity and climate." *Science (New York, N.Y.)*, **296**(5573):1692–1694, May 2002.

[BSP13] Silvie Bernatová, Ota Samek, Zdeněk Pilát, Mojmír Šerý, Jan Ježek, Petr Jákl, Martin Šiler, Vladislav Krzyžánek, Pavel Zemánek, Veronika Holá, Milada Dvořáčková, and Filip Růžička. "Following the Mechanisms of Bacteriostatic versus Bactericidal Action Using Raman Spectroscopy." *Molecules*, **18**(11):13188–13199, October 2013.

[BW06] Sanela Begic and Elizabeth A. Worobec. "Regulation of Serratia marcescens ompF and ompC porin genes in response to osmotic stress, salicylate, temperature and pH." *Microbiology*, **152**(2):485–491, 2006. Publisher: Microbiology Society,.

[BYH16] Desiree Y. Baeder, Guozhi Yu, Nathanaël Hozé, Jens Rolff, and Roland R. Regoes. "Antimicrobial combinations: Bliss independence and Loewe additivity derived from mechanistic multi-hit models." *Philosophical Transactions of the Royal Society B: Biological Sciences*, **371**(1695):20150294, May 2016.

[CFM18] Zhongqi Chen, Anthony P. Farrell, Amanda Matala, and Shawn R. Narum. "Mechanisms of thermal adaptation and evolutionary potential of conspecific populations to changing environments." *Molecular Ecology*, **27**(3):659–674, February 2018.

[CGW10] Karen Cardoso, Rinaldo Ferreira Gandra, Edirlene Sara Wisniewski, Clarice Aoki Osaku, Marina Kimiko Kadowaki, Vicente Felipach-Neto, Leandro Fávero Aby-Azar Haus, and Rita de Cássia Garcia Simão. "DnaK and GroEL are induced in response to antibiotic and heat shock in Acinetobacter baumannii." *Journal of Medical Microbiology*, **59**(Pt 9):1061–1068, September 2010.

[CH91] L. N. Csonka and A. D. Hanson. "Prokaryotic osmoregulation: genetics and physiology." *Annual Review of Microbiology*, **45**:569–606, 1991.

[CHK20] Scott D. Cinel, Daniel A. Hahn, and Akito Y. Kawahara. "Predator-induced stress responses in insects: A review." *Journal of Insect Physiology*, **122**:104039, April 2020.

[CKL19] Mauricio Cruz-Loya, Tina Manzhu Kang, Natalie Ann Lozano, Rina Watanabe, Elif Tekin, Robert Damoiseaux, Van M. Savage, and Pamela J. Yeh. "Stressor interaction networks suggest antibiotic resistance co-opted from stress responses to temperature." *The ISME journal*, **13**(1):12–23, January 2019.

[COB97] H. G. Cuppers, S. Oomes, and S. Brul. "A model for the combined effects of temperature and salt concentration on growth rate of food spoilage molds." *Applied and Environmental Microbiology*, **63**(10):3764–3769, October 1997.

[CR54] L. E. Chadwick and H. Rahn. "Temperature dependence of rattling frequency in the rattlesnake, Crotalus v. viridis." *Science (New York, N.Y.)*, **119**(3092):442–443, April 1954.

[CR01] Ian Chopra and Marilyn Roberts. "Tetracycline Antibiotics: Mode of Action, Applications, Molecular Biology, and Epidemiology of Bacterial Resistance." *Microbiology and Molecular Biology Reviews*, June 2001. Publisher: American Society for Microbiology.

[CTK21a] Mauricio Cruz-Loya, Elif Tekin, Tina Manzhu Kang, Natalya Cardona, Natalie Lozano-Huntelman, Alejandra Rodriguez-Verdugo, Van M. Savage, and Pamela J. Yeh. "Antibiotics Shift the Temperature Response Curve of Escherichia coli Growth." *mSystems*, July 2021. Publisher: American Society for Microbiology 1752 N St., N.W., Washington, DC.

[CTK21b] Mauricio Cruz-Loya, Elif Tekin, Tina Manzhu Kang, Natalya Cardona, Natalie Lozano-Huntelman, Alejandra Rodríguez-Verdugo, Van Savage, and Pamela Yeh. "Data from: Antibiotics shift the temperature response curve of Escherichia coli growth.", 2021. Artwork Size: 151284 bytes Pages: 151284 bytes Version Number: 4 Type: dataset.

[CUB14] Hongbaek Cho, Tsuyoshi Uehara, and Thomas G. Bernhardt. "Beta-Lactam Antibiotics Induce a Lethal Malfunctioning of the Bacterial Cell Wall Synthesis Machinery." *Cell*, **159**(6):1300–1311, December 2014. Publisher: Elsevier.

[CZJ20] Ya-Nan Chang, Chen Zhu, Jing Jiang, Huiming Zhang, Jian-Kang Zhu, and Cheng-Guo Duan. "Epigenetic regulation in plant abiotic stress responses." *Journal of Integrative Plant Biology*, **62**(5):563–580, 2020. _eprint: https://onlinelibrary.wiley.com/doi/pdf/10.1111/jipb.12901.

[DBM19] David Demory, Anne-Claire Baudoux, Adam Monier, Nathalie Simon, Christophe Six, Pei Ge, Fabienne Rigaut-Jalabert, Dominique Marie, Antoine Sciandra, Olivier Bernard, and Sophie Rabouille. "Picoeukaryotes of the Micromonas genus: sentinels of a warming ocean." *The ISME journal*, **13**(1):132–146, January 2019.

[De 99] A. De Maio. "Heat shock proteins: facts, thoughts, and dreams." *Shock (Augusta, Ga.)*, **11**(1):1–12, January 1999.

[DKK11] Vanessa M. D'Costa, Christine E. King, Lindsay Kalan, Mariya Morar, Wilson W. L. Sung, Carsten Schwarz, Duane Froese, Grant Zazula, Fabrice Calmels, Regis Debruyne, G. Brian Golding, Hendrik N. Poinar, and Gerard D. Wright. "Antibiotic resistance is ancient." *Nature*, **477**(7365), September 2011.

[DMQ13] Martin Dragosits, Vadim Mozhayskiy, Semarhy Quinones-Soto, Jiyeon Park, and Ilias Tagkopoulos. "Evolutionary potential, cross-stress behavior and the genetic basis of acquired stress resistance in Escherichia coli." *Molecular Systems Biology*, **9**:643, 2013.

[DOW06] Isabelle Daniel, Philippe Oger, and Roland Winter. "Origins of life and biochemistry under high-pressure conditions." *Chemical Society Reviews*, **35**(10):858–875, September 2006. Publisher: The Royal Society of Chemistry.

[DPS11] Anthony I. Dell, Samraat Pawar, and Van M. Savage. "Systematic variation in the temperature dependence of physiological and ecological traits." *Proceedings of the National Academy of Sciences of the United States of America*, **108**(26):10591–10596, June 2011.

[DTH08] Curtis A. Deutsch, Joshua J. Tewksbury, Raymond B. Huey, Kimberly S. Sheldon, Cameron K. Ghalambor, David C. Haak, and Paul R. Martin. "Impacts of climate warming on terrestrial ectotherms across latitude." *Proceedings of the National Academy of Sciences of the United States of America*, **105**(18):6668–6672, May 2008.

[DTP08] Lars E. P. Dietrich, Tracy K. Teal, Alexa Price-Whelan, and Dianne K. Newman. "Redox-active antibiotics control gene expression and community behavior in divergent bacteria." *Science (New York, N.Y.)*, **321**(5893):1203–1206, August 2008.

[DW00] K. A. Datsenko and B. L. Wanner. "One-step inactivation of chromosomal genes in Escherichia coli K-12 using PCR products." *Proceedings of the National Academy of Sciences of the United States of America*, **97**(12):6640–6645, June 2000.

[FDF10] Klaus Fischer, Anneke Dierks, Kristin Franke, Thorin L. Geister, Magdalena Liszka, Sarah Winter, and Claudia Pflicke. "Environmental effects on temperature stress resistance in the tropical butterfly Bicyclus anynana." *PloS One*, **5**(12):e15284, December 2010.

[FGS97] Jacques Fargues, Mark Goettel, Nathalie Smits, Adaman Ouedraogo, and M. Rougier. "Effect of Temperature on Vegetative Growth of Beauveria bassiana Isolates from Different Origins." *Mycologia*, **89**:383, May 1997.

[FSS16] Phillip B. Fenberg, Angela Self, John R. Stewart, Rebecca J. Wilson, and Stephen J. Brooks. "Exploring the universal ecological responses to climate change in a univoltine butterfly." *The Journal of Animal Ecology*, **85**(3):739–748, May 2016.

[FT17] Masami Fujiwara and Takenori Takada. "Environmental Stochasticity." In *eLS*, pp. 1–8. John Wiley & Sons, Ltd, 2017. _eprint: https://onlinelibrary.wiley.com/doi/pdf/10.1002/9780470015902.a0021220.pub2.

[GBL13] Juan Diego Gaitán-Espitia, María Belén Arias, Marco A. Lardies, and Roberto F. Nespolo. "Variation in thermal sensitivity and thermal tolerances in an invasive species across a climatic gradient: lessons from the land snail Cornu aspersum." *PloS One*, **8**(8):e70662, 2013.

[GBN11] Raju Gautam, Majid Bani-Yaghoub, William H. Neill, Dörte Döpfer, Charles Kaspar, and Renata Ivanek. "Modeling the effect of seasonal variation in ambient temperature on the transmission dynamics of a pathogen with a free-living stage: example of Escherichia coli O157:H7 in a dairy herd." *Preventive Veterinary Medicine*, **102**(1):10–21, October 2011.

[GBP95] W. R. Greco, G. Bravo, and J. C. Parsons. "The search for synergy: a critical review from a response surface perspective." *Pharmacological Reviews*, **47**(2):331–385, June 1995.

[GD84] E. Goldstein and K. Drlica. "Regulation of bacterial DNA supercoiling: plasmid linking numbers vary with growth temperature." *Proceedings of the National Academy of Sciences*, **81**(13):4046–4050, July 1984. Publisher: National Academy of Sciences Section: Research Article.

[Gel06] Andrew Gelman. "Prior distributions for variance parameters in hierarchical models (comment on article by Browne and Draper)." *Bayesian Analysis*, **1**(3):515–534, September 2006. Publisher: International Society for Bayesian Analysis.

[GG03] Tanja M. Gruber and Carol A. Gross. "Multiple sigma subunits and the partitioning of bacterial transcription space." *Annual Review of Microbiology*, **57**:441–466, 2003.

[GGB13] Lise Goltermann, Liam Good, and Thomas Bentin. "Chaperonins Fight Aminoglycoside-induced Protein Misfolding and Promote Short-term Tolerance in Escherichia coli." *Journal of Biological Chemistry*, **288**(15):10483–10489, April 2013. Publisher: Elsevier.

[Gil95] George W. Gilchrist. "Specialists and Generalists in Changing Environments. I. Fitness Landscapes of Thermal Sensitivity." *The American Naturalist*, **146**(2):252–270, August 1995. Publisher: The University of Chicago Press.

[GSE15] Philip Greulich, Matthew Scott, Martin R. Evans, and Rosalind J. Allen. "Growth-dependent bacterial susceptibility to ribosome-targeting antibiotics." *Molecular Systems Biology*, **11**(3):796, March 2015.

[GYK18] Lorenzo Galluzzi, Takahiro Yamazaki, and Guido Kroemer. "Linking cellular stress responses to systemic homeostasis." *Nature Reviews Molecular Cell Biology*, **19**(11):731–745, November 2018. Number: 11 Publisher: Nature Publishing Group.

[HBB02] Robert M. Hazen, Nabil Boctor, Jay A. Brandes, George D. Cody, Russell J. Hemley, Anurag Sharma, and Hatten S. Yoder. "High pressure and the origin of life." *Journal of Physics: Condensed Matter*, **14**(44):11489–11494, October 2002. Publisher: IOP Publishing.

[HCB12] Sarah Hofmann, Valeria Cherkasova, Peter Bankhead, Bernd Bukau, and Georg Stoecklin. "Translation suppression promotes stress granule formation and cell survival in response to cold shock." *Molecular Biology of the Cell*, **23**(19):3786–3800, October 2012.

[HH00] Ary A. Hoffmann and Miriam J. Hercus. "Environmental Stress as an Evolutionary Force." *BioScience*, **50**(3):217–226, March 2000.

[HK89] R. B. Huey and J. G. Kingsolver. "Evolution of thermal sensitivity of ectotherm performance." *Trends in Ecology & Evolution*, **4**(5):131–135, May 1989.

[HK11] Raymond B. Huey and Joel G. Kingsolver. "Variation in universal temperature dependence of biological rates." *Proceedings of the National Academy of Sciences of the United States of America*, **108**(26):10377–10378, June 2011.

[HMW02] C. Drew Harvell, Charles E. Mitchell, Jessica R. Ward, Sonia Altizer, Andrew P. Dobson, Richard S. Ostfeld, and Michael D. Samuel. "Climate warming and disease risks for terrestrial and marine biota." *Science (New York, N.Y.)*, **296**(5576):2158–2162, June 2002.

[HP93] Ary A. Hoffmann and Peter A. Parsons. *Evolutionary Genetics and Environmental Stress*. Oxford University Press, Oxford, August 1993.

[HTW19] Matthew I Hutchings, Andrew W Truman, and Barrie Wilkinson. "Antibiotics: past, present and future." *Current Opinion in Microbiology*, **51**:72–80, October 2019.

[JI94] P. G. Jones and M. Inouye. "The cold-shock response–a hot topic." *Mol Microbiol*, **11**(5):811–818, Mar 1994.

[KDH07] Michael A. Kohanski, Daniel J. Dwyer, Boris Hayete, Carolyn A. Lawrence, and James J. Collins. "A common mechanism of cellular death induced by bactericidal antibiotics." *Cell*, **130**(5):797–810, September 2007.

[KK93] A. S. Kaprelyants and D. B. Kell. "Dormancy in Stationary-Phase Cultures of Micrococcus luteus: Flow Cytometric Analysis of Starvation and Resuscitation." *Applied and Environmental Microbiology*, **59**(10):3187–3196, October 1993.

[KKB05] Edo Kussell, Roy Kishony, Nathalie Q Balaban, and Stanislas Leibler. "Bacterial Persistence: A Model of Survival in Changing Environments." *Genetics*, **169**(4):1807–1814, April 2005.

[KL03] Roy Kishony and Stanislas Leibler. "Environmental stresses can alleviate the average deleterious effect of mutations." *Journal of Biology*, **2**(2):14, May 2003.

[KZE96] K. Kovárová, A. J. Zehnder, and T. Egli. "Temperature-dependent growth kinetics of Escherichia coli ML 30 in glucose-limited continuous culture." *Journal of Bacteriology*, **178**(15):4530–4539, August 1996.

[LDH18] Simone Lederer, Tjeerd M. H. Dijkstra, and Tom Heskes. "Additive Dose Response Models: Explicit Formulation and the Loewe Additivity Consistency Condition." *Frontiers in Pharmacology*, **9**, 2018.

[LeB88] M. LeBel. "Ciprofloxacin: chemistry, mechanism of action, resistance, antimicrobial spectrum, pharmacokinetics, clinical trials, and adverse reactions." *Pharmacotherapy*, **8**(1):3–33, 1988.

[Lev92] S. B. Levy. "Active efflux mechanisms for antimicrobial resistance." *Antimicrobial Agents and Chemotherapy*, **36**(4):695–703, April 1992.

[Lew07] Kim Lewis. "Persister cells, dormancy and infectious disease." *Nature Reviews. Microbiology*, **5**(1):48–56, January 2007.

[LG87] Michael Lynch and Wilfried Gabriel. "Environmental Tolerance." *The American Naturalist*, **129**(2):283–303, February 1987. Publisher: The University of Chicago Press.

[LHJ95] Derek J. Lactin, N. J. Holliday, D. L. Johnson, and R. Craigen. "Improved Rate Model of Temperature-Dependent Development by Arthropods." *Environmental Entomology*, **24**(1):68–75, February 1995.

[LHK16] Kathleen Loughman, Jesse Hall, Samantha Knowlton, Devin Sindeldecker, Tricia Gilson, Deanna M. Schmitt, James W.-M. Birch, Tara Gajtka, Brianna N. Kobe, Aleksandr Florjanczyk, Jenna Ingram, Chandra S. Bakshi, and Joseph Horzempa. "Temperature-Dependent Gentamicin Resistance of Francisella tularensis is Mediated by Uptake Modulation." *Frontiers in Microbiology*, **7**:37, 2016.

[Lin86] S. Lindquist. "The heat-shock response." *Annual Review of Biochemistry*, **55**:1151–1191, 1986.

[LM26] S. Loewe and H. Muischnek. "Über Kombinationswirkungen." *Naunyn-Schmiedebergs Archiv für experimentelle Pathologie und Pharmakologie*, **114**(5):313–326, July 1926.

[LMH86] H. Liao, T. McKenzie, and R. Hageman. "Isolation of a thermostable enzyme variant by cloning and selection in a thermophile." *Proceedings of the National Academy of Sciences of the United States of America*, **83**(3):576–580, February 1986.

[LPB21] Maryl Lambros, Ximo Pechuan-Jorge, Daniel Biro, Kenny Ye, and Aviv Bergman. "Emerging Adaptive Strategies Under Temperature Fluctuations in a Laboratory Evolution Experiment of Escherichia Coli." *Frontiers in Microbiology*, **12**, 2021.

[LW94] M. G. Lorenz and W. Wackernagel. "Bacterial gene transfer by natural genetic transformation in the environment." *Microbiological Reviews*, **58**(3):563–602, September 1994.

[LZS18] Jinzhong Lin, Dejian Zhou, Thomas A. Steitz, Yury S. Polikanov, and Matthieu G. Gagnon. "Ribosome-Targeting Antibiotics: Modes of Action, Mechanisms of Resistance, and Implications for Drug Design." *Annual Review of Biochemistry*, **87**:451–478, June 2018.

[Mar08] José L. Martínez. "Antibiotics and antibiotic resistance genes in natural environments." *Science (New York, N.Y.)*, **321**(5887):365–367, July 2008.

[MB02] Lauren Ancel Meyers and James J. Bull. "Fighting change with change: adaptive variation in an uncertain world." *Trends in Ecology & Evolution*, **17**(12):551–557, December 2002. Publisher: Elsevier.

[MB05] M. P. Mayer and B. Bukau. "Hsp70 chaperones: cellular functions and molecular mechanism." *Cellular and molecular life sciences: CMLS*, **62**(6):670–684, March 2005.

[MCA04] María C. Mansilla, Larisa E. Cybulski, Daniela Albanesi, and Diego de Mendoza. "Control of membrane lipid fluidity by molecular thermosensors." *Journal of Bacteriology*, **186**(20):6681–6688, October 2004.

[MCE17] Erin A. Mordecai, Jeremy M. Cohen, Michelle V. Evans, Prithvi Gudapati, Leah R. Johnson, Catherine A. Lippi, Kerri Miazgowicz, Courtney C. Murdock, Jason R. Rohr, and Sadie J. Ryan. "Detecting the impact of temperature on transmission of Zika, dengue, and chikungunya using mechanistic models." *PLoS neglected tropical diseases*, **11**(4):e0005568, 2017. Publisher: Public Library of Science San Francisco, CA USA.

[MGT99] Marie-Paule Mingeot-Leclercq, Youri Glupczynski, and Paul M. Tulkens. "Aminoglycosides: Activity and Resistance." *Antimicrobial Agents and Chemotherapy*, April 1999.

[MH08] Tara Laine Martin and Raymond B. Huey. "Why "suboptimal" is optimal: Jensen's inequality and ectotherm thermal preferences." *The American Naturalist*, **171**(3):E102–118, March 2008.

[MHK22] Luiza P. Morawska, Jhonatan A. Hernandez-Valdes, and Oscar P. Kuipers. "Diversity of bet-hedging strategies in microbial communities—Recent cases

and insights." *WIREs Mechanisms of Disease*, **14**(2):e1544, 2022. _eprint: https://onlinelibrary.wiley.com/doi/pdf/10.1002/wsbm.1544.

[MIS76] K. Maeda, Y. Imae, J. I. Shioi, and F. Oosawa. "Effect of temperature on motility and chemotaxis of Escherichia coli." *Journal of Bacteriology*, **127**(3):1039–1046, September 1976.

[MKH13] Péter K. Molnár, Susan J. Kutz, Bryanne M. Hoar, and Andrew P. Dobson. "Metabolic approaches to understanding climate change impacts on seasonal host-macroparasite dynamics." *Ecology Letters*, **16**(1):9–21, January 2013.

[MKO97] Tohru Mizushima, Kazuhiro Kataoka, Yasuyuki Ogata, Ryu-ichi Inoue, and Kazuhisa Sekimizu. "Increase in negative supercoiling of plasmid DNA in Escherichia coli exposed to cold shock." *Molecular Microbiology*, **23**(2):381–386, 1997. _eprint: https://onlinelibrary.wiley.com/doi/pdf/10.1046/j.1365-2958.1997.2181582.x.

[Mlo09] Christine Mlot. "Microbiology. Antibiotics in nature: beyond biological warfare." *Science (New York, N.Y.)*, **324**(5935):1637–1639, June 2009.

[MMF18] Derek R. MacFadden, Sarah F. McGough, David Fisman, Mauricio Santillana, and John S. Brownstein. "Antibiotic Resistance Increases with Local Temperature." *Nature Climate Change*, **8**(6):510–514, June 2018.

[MMP11] Leonard A. Mermel, Jason T. Machan, and Stephen Parenteau. "Seasonality of MRSA infections." *PloS One*, **6**(3):e17925, March 2011.

[MPR14] Surojit Mondal, Bani Kumar Pathak, Sutapa Ray, and Chandana Barat. "Impact of P-Site tRNA and Antibiotics on Ribosome Mediated Protein Folding: Studies Using the Escherichia coli Ribosome." *PLOS ONE*, **9**(7):e101293, July 2014. Publisher: Public Library of Science.

[MUT14] Shannon M. Mitchell, Jeffrey L. Ullman, Amy L. Teel, and Richard J. Watts. "pH and temperature effects on the hydrolysis of three -lactam antibiotics: ampicillin, cefalotin and cefoxitin." *The Science of the Total Environment*, **466-467**:547–555, January 2014.

[NLG06] Piye Niu, Lin Liu, Zhiyong Gong, Hao Tan, Feng Wang, Jing Yuan, Youmei Feng, Qingyi Wei, Robert M. Tanguay, and Tangchun Wu. "Overexpressed heat shock protein 70 protects cells against DNA damage caused by ultraviolet C in a dose-dependent manner." *Cell Stress & Chaperones*, **11**(2):162–169, 2006.

[NS04] Martin A. Nowak and Karl Sigmund. "Evolutionary Dynamics of Biological Games." *Science*, **303**(5659):793–799, February 2004. Publisher: American Association for the Advancement of Science.

[NTA10] Martin A. Nowak, Corina E. Tarnita, and Tibor Antal. "Evolutionary dynamics in structured populations." *Philosophical Transactions of the Royal Society B: Biological Sciences*, **365**(1537):19–30, January 2010. Publisher: Royal Society.

[OMS08] J. Ohlberger, T. Mehner, G. Staaks, and F. Hölker. "Temperature-related physiological adaptations promote ecological divergence in a sympatric species pair of temperate freshwater fish, Coregonus spp." *Functional Ecology*, **22**(3):501–508, 2008. _eprint: https://onlinelibrary.wiley.com/doi/pdf/10.1111/j.1365-2435.2008.01391.x.

[OVS15] Jordan G. Okie, David J. Van Horn, David Storch, John E. Barrett, Michael N. Gooseff, Lenka Kopsova, and Cristina D. Takacs-Vesbach. "Niche and metabolic principles explain patterns of diversity and distribution: theory and a case study with soil bacterial communities." *Proceedings. Biological Sciences*, **282**(1809):20142630, June 2015.

[PAI99] Sangita Phadtare, Janivette Alsina, and Masayori Inouye. "Cold-shock response and cold-shock proteins." *Current Opinion in Microbiology*, **2**(2):175–180, April 1999.

[Par06] Camille Parmesan. "Ecological and Evolutionary Responses to Recent Climate Change." *Annual Review of Ecology, Evolution, and Systematics*, **37**(1):637–669, 2006. _eprint: https://doi.org/10.1146/annurev.ecolsys.37.091305.110100.

[Phi08] Patrick C. Phillips. "Epistasis — the essential role of gene interactions in the structure and evolution of genetic systems." *Nature Reviews Genetics*, **9**(11):855–867, November 2008. Number: 11 Publisher: Nature Publishing Group.

[PI04] Sangita Phadtare and Masayori Inouye. "Genome-Wide Transcriptional Analysis of the Cold Shock Response in Wild-Type and Cold-Sensitive, Quadruple-csp-Deletion Strains of Escherichia coli." *Journal of Bacteriology*, **186**(20):7007–7014, October 2004. Publisher: American Society for Microbiology.

[PJZ17] Anja Paulick, Vladimir Jakovljevic, SiMing Zhang, Michael Erickstad, Alex Groisman, Yigal Meir, William S. Ryu, Ned S. Wingreen, and Victor Sourjik. "Mechanism of bidirectional thermotaxis in Escherichia coli." *eLife*, **6**:e26607, August 2017.

[PKM16] Karolina Pakos-Zebrucka, Izabela Koryga, Katarzyna Mnich, Mila Ljujic, Afshin Samali, and Adrienne M. Gorman. "The integrated stress response." *EMBO reports*, **17**(10):1374–1395, October 2016.

[PM04] R. Parra and N. Magan. "Modelling the effect of temperature and water activity on growth of Aspergillus niger strains and applications for food spoilage moulds." *Journal of Applied Microbiology*, **97**(2):429–438, 2004.

[Poo12a] Keith Poole. "Bacterial stress responses as determinants of antimicrobial resistance." *The Journal of Antimicrobial Chemotherapy*, **67**(9):2069–2089, September 2012.

[Poo12b] Keith Poole. "Stress responses as determinants of antimicrobial resistance in Gram-negative bacteria." *Trends in Microbiology*, **20**(5):227–234, May 2012. Publisher: Elsevier.

[PPC97] I. T. Paulsen, J. H. Park, P. S. Choi, and M. H. Saier. "A family of gram-negative bacterial outer membrane factors that function in the export of proteins, carbohydrates, drugs and heavy metals from gram-negative bacteria." *FEMS microbiology letters*, **156**(1):1–8, November 1997.

[PS04] G. A. Pankey and L. D. Sabath. "Clinical Relevance of Bacteriostatic versus Bactericidal Mechanisms of Action in the Treatment of Gram-Positive Bacterial Infections." *Clinical Infectious Diseases*, **38**(6):864–870, March 2004.

[PYB16] Daniel Padfield, Genevieve Yvon-Durocher, Angus Buckling, Simon Jennings, and Gabriel Yvon-Durocher. "Rapid evolution of metabolic traits explains thermal adaptation in phytoplankton." *Ecology Letters*, **19**(2):133–142, February 2016.

[RCC18] Jason R. Rohr, David J. Civitello, Jeremy M. Cohen, Elizabeth A. Roznik, Barry Sinervo, and Anthony I. Dell. "The complex drivers of thermal acclimation and breadth in ectotherms." *Ecology Letters*, **21**(9):1425–1439, September 2018.

[RGT13] Alejandra Rodríguez-Verdugo, Brandon S. Gaut, and Olivier Tenaillon. "Evolution of Escherichia coli rifampicin resistance in an antibiotic-free environment during thermal stress." *BMC evolutionary biology*, **13**:50, February 2013.

[RHB10] Klaus Richter, Martin Haslbeck, and Johannes Buchner. "The heat shock response: life on the verge of death." *Molecular Cell*, **40**(2):253–266, October 2010.

[RLB95] L. Rosso, J. R. Lobry, S. Bajard, and J. P. Flandrois. "Convenient Model To Describe the Combined Effects of Temperature and pH on Microbial Growth." *Applied and Environmental Microbiology*, **61**(2):610–616, February 1995.

[RLC20] Alejandra Rodríguez-Verdugo, Natalie Lozano-Huntelman, Mauricio Cruz-Loya, Van Savage, and Pamela Yeh. "Compounding Effects of Climate Warming and Antibiotic Resistance." *iScience*, **23**(4):101024, April 2020.

[RLH12] Vincent C. Reyes, Minghua Li, Eric M. V. Hoek, Shaily Mahendra, and Robert Damoiseaux. "Genome-Wide Assessment in Escherichia coli Reveals Time-Dependent Nanotoxicity Paradigms." *ACS Nano*, **6**(11):9402–9415, November 2012. Publisher: American Chemical Society.

[ROR05] David A. Ratkowsky, June Olley, and Tom Ross. "Unifying temperature effects on the growth rate of bacteria and the stability of globular proteins." *Journal of Theoretical Biology*, **233**(3):351–362, April 2005.

[RS80] N. J. Russell and S. P. Sandercock. "The regulation of bacterial membrane fluidity by modification of phospholipid fatty acyl chain length." In Morris Kates and Arnis Kuksis, editors, *Membrane Fluidity: Biophysical Techniques and Cellular Regulation*, Experimental Biology and Medicine, pp. 181–190. Humana Press, Totowa, NJ, 1980.

[RSW11] Thomas E. Reed, Daniel E. Schindler, and Robin S. Waples. "Interacting effects of phenotypic plasticity and evolution on population persistence in a changing climate." *Conservation Biology: The Journal of the Society for Conservation Biology*, **25**(1):56–63, February 2011.

[SAB16] Yinka Somorin, Florence Abram, Fiona Brennan, and Conor O'Byrne. "The General Stress Response Is Conserved in Long-Term Soil-Persistent Strains of Escherichia coli." *Applied and Environmental Microbiology*, May 2016. Publisher: American Society for Microbiology.

[SC10] Umender K. Sharma and Dipankar Chatterji. "Transcriptional switching in Escherichia coli during stress and starvation by modulation of 70 activity." *FEMS Microbiology Reviews*, **34**(5):646–657, September 2010.

[SD77] P. J. Sharpe and D. W. DeMichele. "Reaction kinetics of poikilotherm development." *Journal of Theoretical Biology*, **64**(4):649–670, February 1977.

[SDC05] Daniel Segrè, Alexander DeLuna, George M. Church, and Roy Kishony. "Modular epistasis in yeast metabolism." *Nature Genetics*, **37**(1), January 2005.

[SG10] Peijian Shi and Feng Ge. "A comparison of different thermal performance functions describing temperature-dependent development rates." *Journal of Thermal Biology - J THERM BIOL*, **35**:225–231, July 2010.

[SGB04] Van M. Savage, James F. Gilloly, James H. Brown, and Eric L. Charnov. "Effects of body size and temperature on population growth." *The American Naturalist*, **163**(3):429–441, March 2004.

[SGS11] Peijian Shi, Feng Ge, Yucheng Sun, and Chunli Chen. "A simple model for describing the effect of temperature on insect developmental rate." *Journal of Asia-Pacific Entomology*, **14**(1):15–20, March 2011.

[SL04] D. W. Schwartzman and C. H. Lineweaver. "The hyperthermophilic origin of life revisited." *Biochemical Society Transactions*, **32**(Pt 2):168–171, April 2004.

[Smi82] John Maynard Smith. *Evolution and the Theory of Games*. Cambridge University Press, Cambridge ; New York, 1st edition edition, December 1982.

[SN99] K. Sigmund and M. A. Nowak. "Evolutionary game theory." *Current biology: CB*, **9**(14):R503–505, July 1999.

[Som10] G. N. Somero. "The physiology of climate change: how potentials for acclimatization and genetic adaptation will determine 'winners' and 'losers'." *The Journal of Experimental Biology*, **213**(6):912–920, March 2010.

[SPK13] Anurag K. Sinha, Theetha L. Pavankumar, Srinivasulu Kamisetty, Pragya Mittal, and Malay K. Ray. "Replication arrest is a major threat to growth at low temperature in Antarctic Pseudomonas syringaeLz4W." *Molecular Microbiology*, **89**(4):792–810, August 2013.

[SSM81] R. M. Schoolfield, P. J. Sharpe, and C. E. Magnuson. "Non-linear regression of biological temperature-dependent rate models based on absolute reaction-rate theory." *Journal of Theoretical Biology*, **88**(4):719–731, February 1981.

[Ste06] Karl O Stetter. "Hyperthermophiles in the history of life." *Philosophical Transactions of the Royal Society B: Biological Sciences*, **361**(1474):1837–1843, October 2006. Publisher: Royal Society.

[SWF16] John Salvatier, Thomas V. Wiecki, and Christopher Fonnesbeck. "Probabilistic programming in Python using PyMC3." *PeerJ Computer Science*, **2**:e55, April 2016. Publisher: PeerJ Inc.

[TAK17] Mridul K. Thomas, María Aranguren-Gassis, Colin T. Kremer, Marilyn R. Gould, Krista Anderson, Christopher A. Klausmeier, and Elena Litchman. "Temperature-nutrient interactions exacerbate sensitivity to warming in phytoplankton." *Global Change Biology*, **23**(8):3269–3280, August 2017.

[TRC18] Natasha Tajuddin, Mohammed Rizman-Idid, Peter Convey, and Siti Aisyah Alias. "Thermal adaptation in a marine-derived tropical strain of Fusarium equiseti and polar strains of Pseudogymnoascus spp. under different nutrient sources." *Botanica Marina*, **61**(1):9–20, February 2018. Publisher: De Gruyter.

[TTC04] Hideto Takami, Yoshihiro Takaki, Gab-Joo Chee, Shinro Nishi, Shigeru Shimamura, Hiroko Suzuki, Satomi Matsui, and Ikuo Uchiyama. "Thermoadaptation trait revealed by the genome sequence of thermophilic Geobacillus kaustophilus." *Nucleic Acids Research*, **32**(21):6292–6303, 2004.

[Ven15] C. L. Ventola. "The antibiotic resistance crisis: part 1: causes and threats." *Pharmacy and Therapeutics*, **40**(4):277–283, Apr 2015.

[VMS92] U. Völker, H. Mach, R. Schmid, and M. Hecker. "Stress proteins and cross-protection by heat shock and salt stress in Bacillus subtilis." *Journal of General Microbiology*, **138**(10):2125–2135, October 1992.

[VN90] R. A. VanBogelen and F. C. Neidhardt. "Ribosomes as sensors of heat and cold shock in Escherichia coli." *Proceedings of the National Academy of Sciences of the United States of America*, **87**(15):5589–5593, August 1990.

[VRH10] R. Martin Vabulas, Swasti Raychaudhuri, Manajit Hayer-Hartl, and F. Ulrich Hartl. "Protein folding in the cytoplasm and the heat shock response." *Cold Spring Harbor Perspectives in Biology*, **2**(12):a004390, December 2010.

[Wen97] S. E. Wendelaar Bonga. "The stress response in fish." *Physiological Reviews*, **77**(3):591–625, July 1997. Publisher: American Physiological Society.

[WWL11] Timothy R. Walsh, Janis Weeks, David M. Livermore, and Mark A. Toleman. "Dissemination of NDM-1 positive bacteria in the New Delhi environment and its implications for human health: an environmental point prevalence study." *The Lancet. Infectious Diseases*, **11**(5):355–362, May 2011.

[WYI99] N. Wang, K. Yamanaka, and M. Inouye. "CspI, the ninth member of the CspA family of Escherichia coli, is induced upon cold shock." *Journal of Bacteriology*, **181**(5):1603–1609, March 1999.

[Yam99] K. Yamanaka. "Cold shock response in Escherichia coli." *Journal of Molecular Microbiology and Biotechnology*, **1**(2):193–202, November 1999.

[YKM95] Xinyou Yin, Martin J. Kropff, Graham McLaren, and Romeo M. Visperas. "A nonlinear model for crop development as a function of temperature." *Agricultural and Forest Meteorology*, **77**(1):1–16, November 1995.

[YTK06] Pamela Yeh, Ariane I. Tschumi, and Roy Kishony. "Functional classification of drugs by properties of their pairwise interactions." *Nature Genetics*, **38**(4):489–494, April 2006.

[ZBR06] Alon Zaslaver, Anat Bren, Michal Ronen, Shalev Itzkovitz, Ilya Kikoin, Seagull Shavit, Wolfram Liebermeister, Michael G. Surette, and Uri Alon. "A comprehensive library of fluorescent transcriptional reporters for Escherichia coli." *Nature Methods*, **3**(8), August 2006.

[S10] Malin Åkerfelt, Richard I. Morimoto, and Lea Sistonen. "Heat shock factors: integrators of cell stress, development and lifespan." *Nature Reviews Molecular Cell Biology*, **11**(8), August 2010.

[Św16] Agata Świeciło. "Cross-stress resistance in Saccharomyces cerevisiae yeast—new insight into an old phenomenon." *Cell Stress and Chaperones*, **21**(2):187–200, March 2016.